Supporting Information

Effects of Substituents on Photophysical and CO-Photoreleasing Properties of 2,6-Substituted *meso*-Carboxy BODIPY Derivatives

Esther M. Sanchez-Carnerero,[1] Marina Russo,[1] Andreas Jakob,[1] Lucie Muchová,[2] Libor Vítek,[2,3] Petr Klán[1,*]

[1] Department of Chemistry and RECETOX, Faculty of Science, Masaryk University, Kamenice 5, 625 00 Brno, Czech Republic; emmarque@ucm.es (E. M. S.-C.); russomarina.mr@gmail.com (M. R.); Jakob.Andreas@gmx.de (A. J.)

[2] Institute of Medical Biochemistry and Laboratory Diagnostics, General University Hospital and 1st Faculty of Medicine, Charles University, Kateřinská 32, 121 08 Praha 2, Czech Republic; lucie.muchova@lf1.cuni.cz (L. M.)

[3] 4th Department of Internal Medicine, General University Hospital, and 1st Faculty of Medicine, Charles University, Kateřinská 32, 121 08 Praha 2, Czech Republic; vitek@cesnet.cz (L. V.)

* Correspondence: klan@sci.muni.cz

Table of Content

NMR Spectra

Figure S1: ^{1}H NMR (300 MHz, $CDCl_3$): **11**

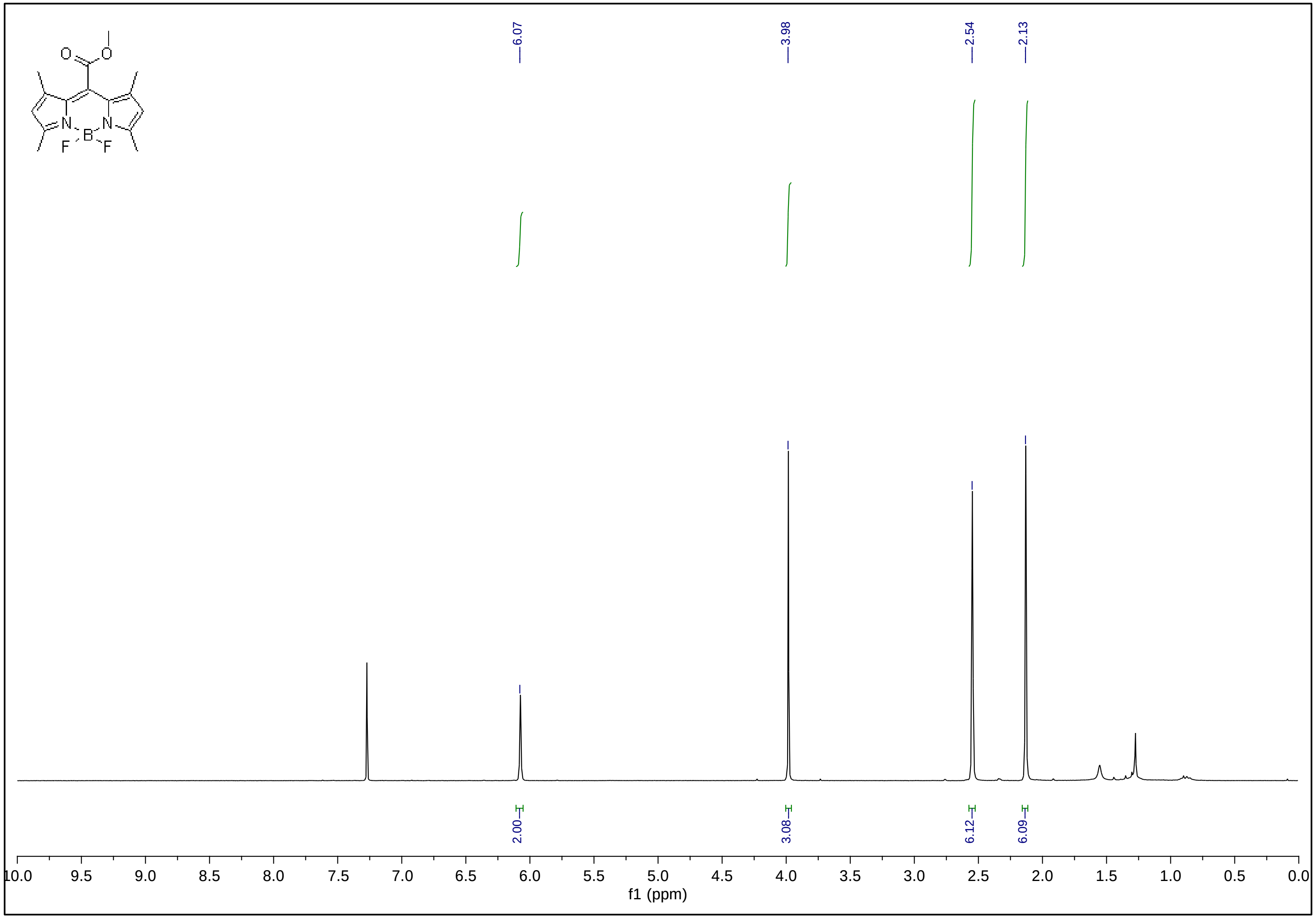

Figure S2: ^{1}H NMR (300 MHz, $CDCl_3$): **12**

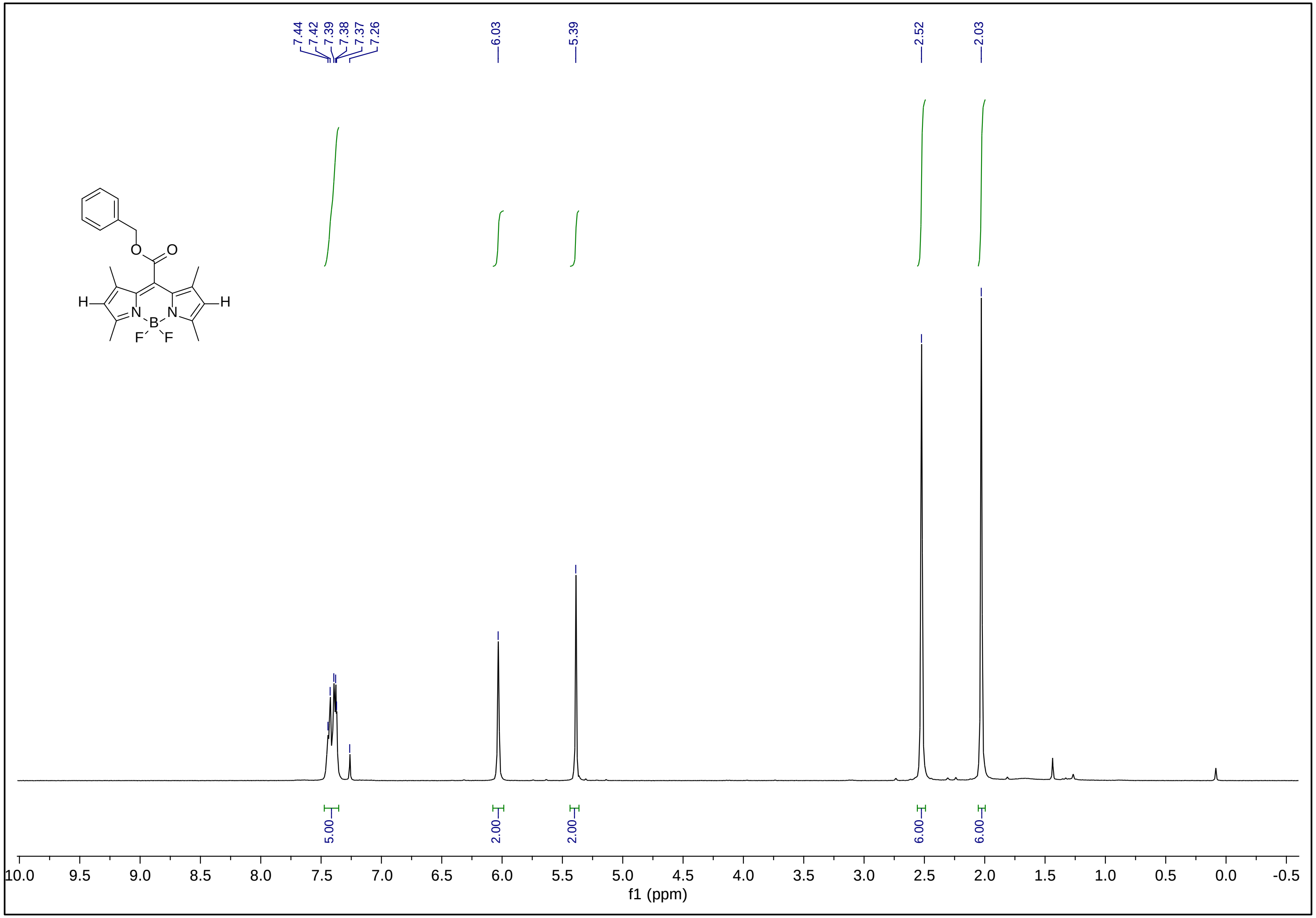

Figure S3: ^{1}H NMR (300 MHz, CD_3OD): **13**

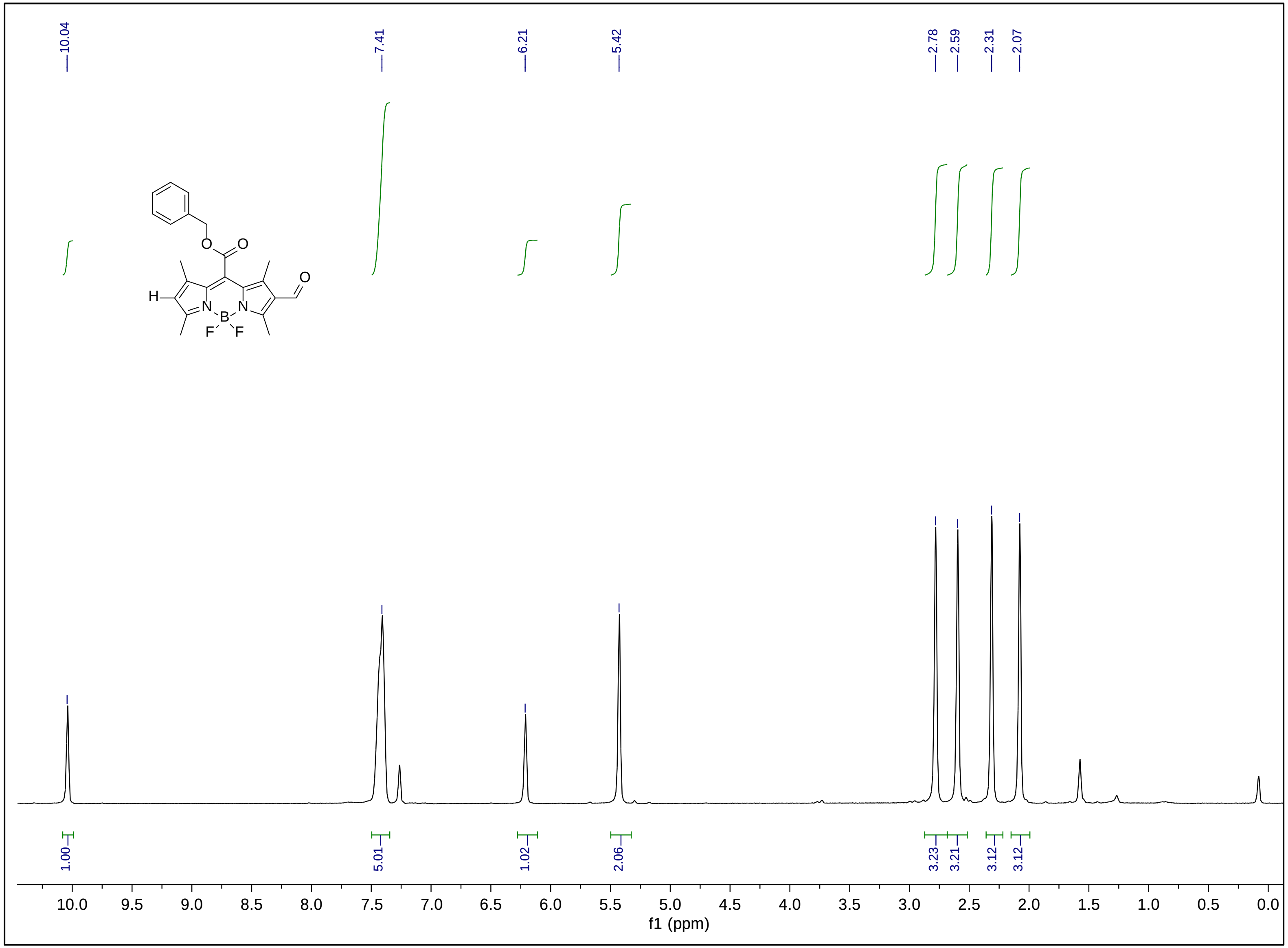

Figure S4: ^{1}H NMR (300 MHz, DMSO-d5): **14**

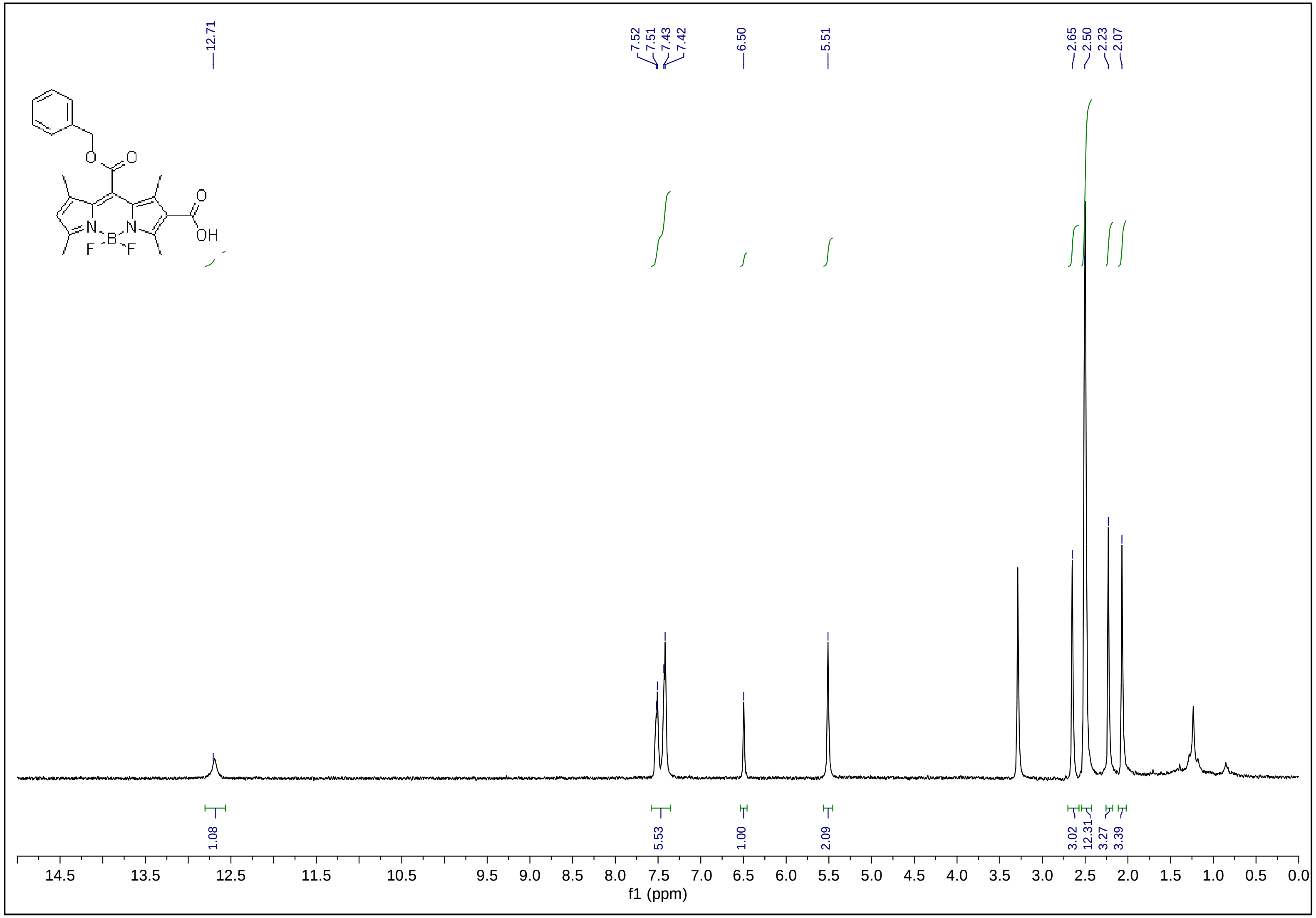

Figure S5: ^{1}H NMR (300 MHz, $CDCl_3$): **15**

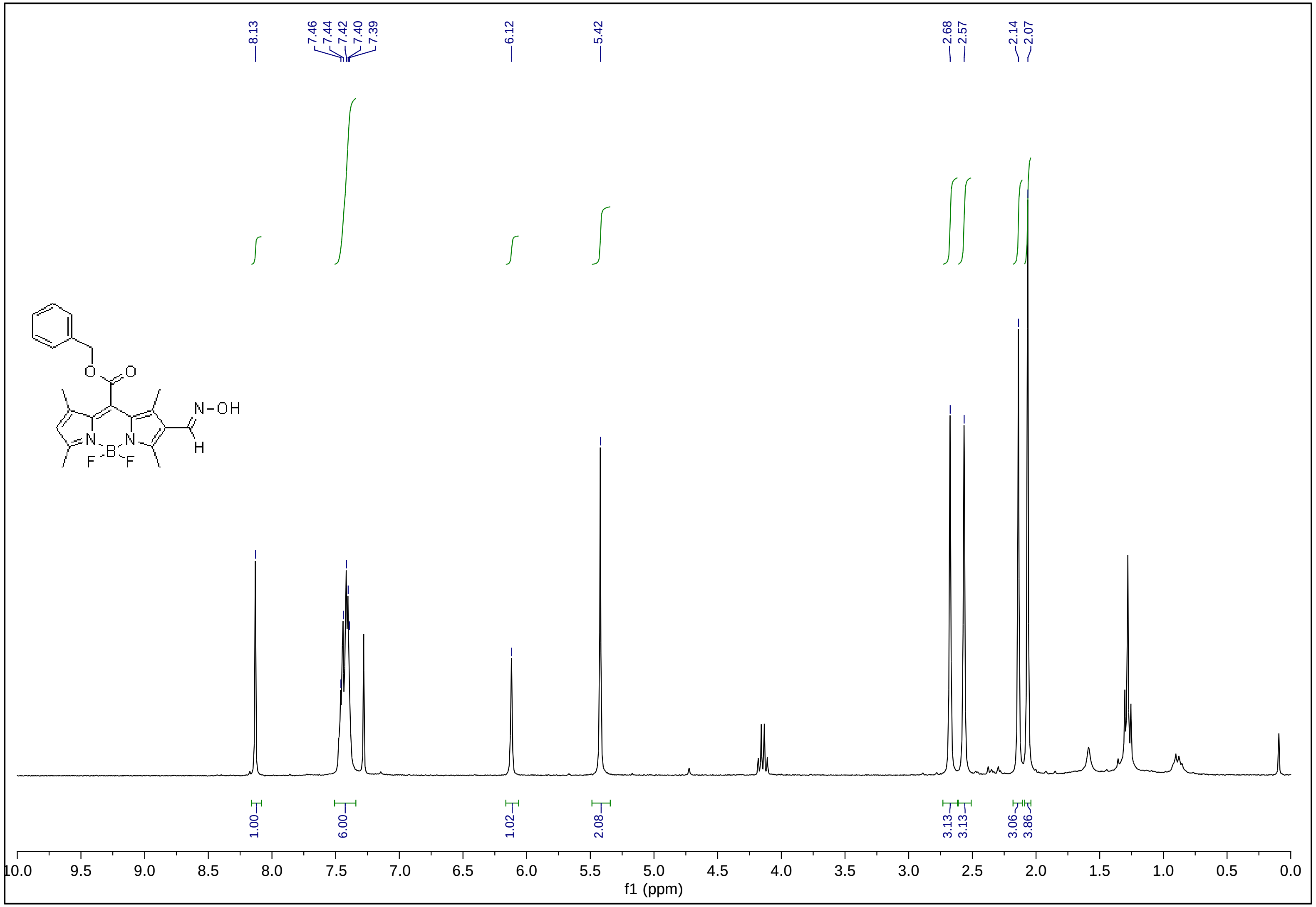

Figure S6: ^{1}H NMR (300 MHz, $CDCl_3$): **16**

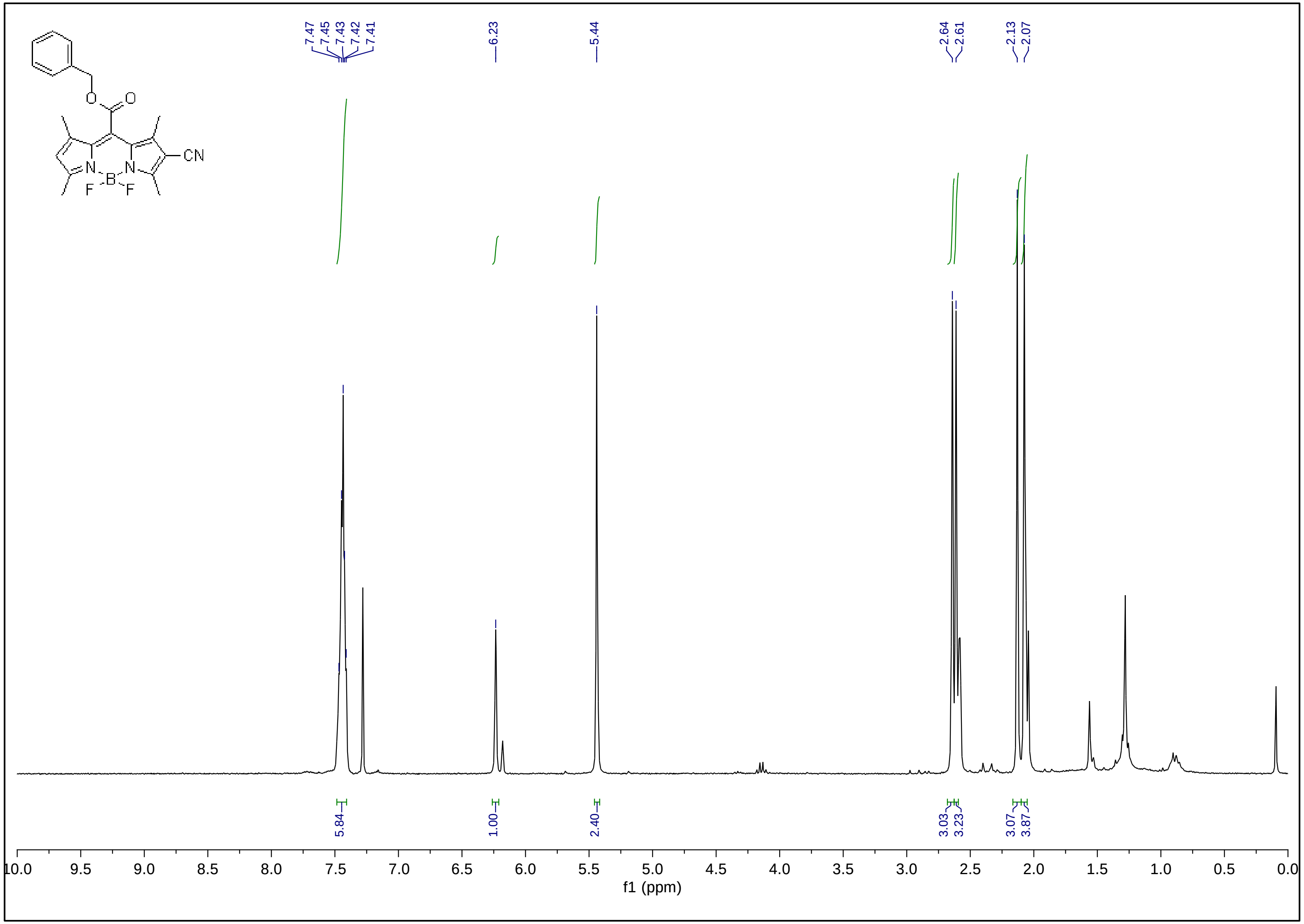

Figure S7: ^{1}H NMR (300 MHz, $CDCl_3$): **17**

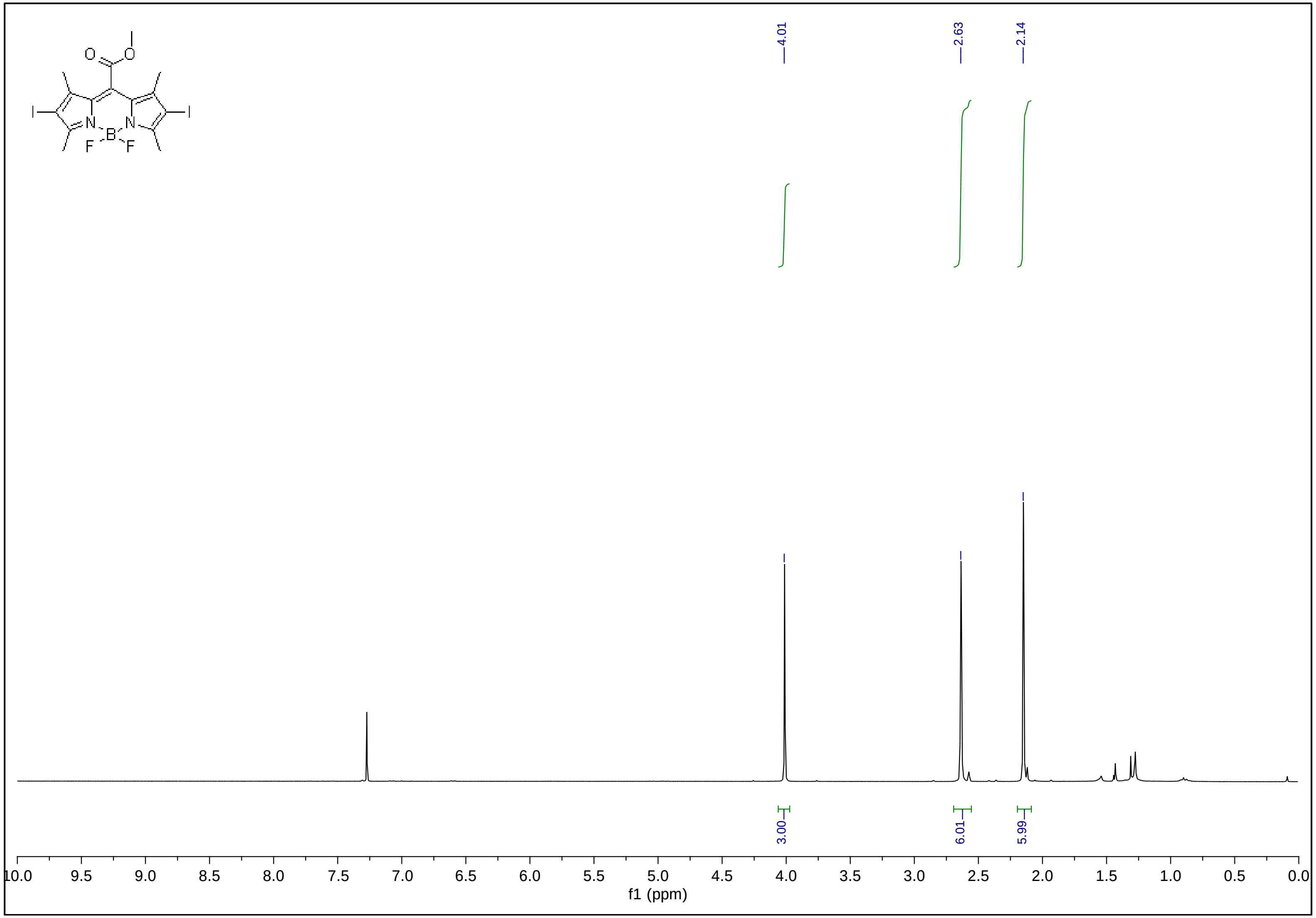

Figure S8: ^{1}H NMR (300 MHz, $CDCl_3$): **18**

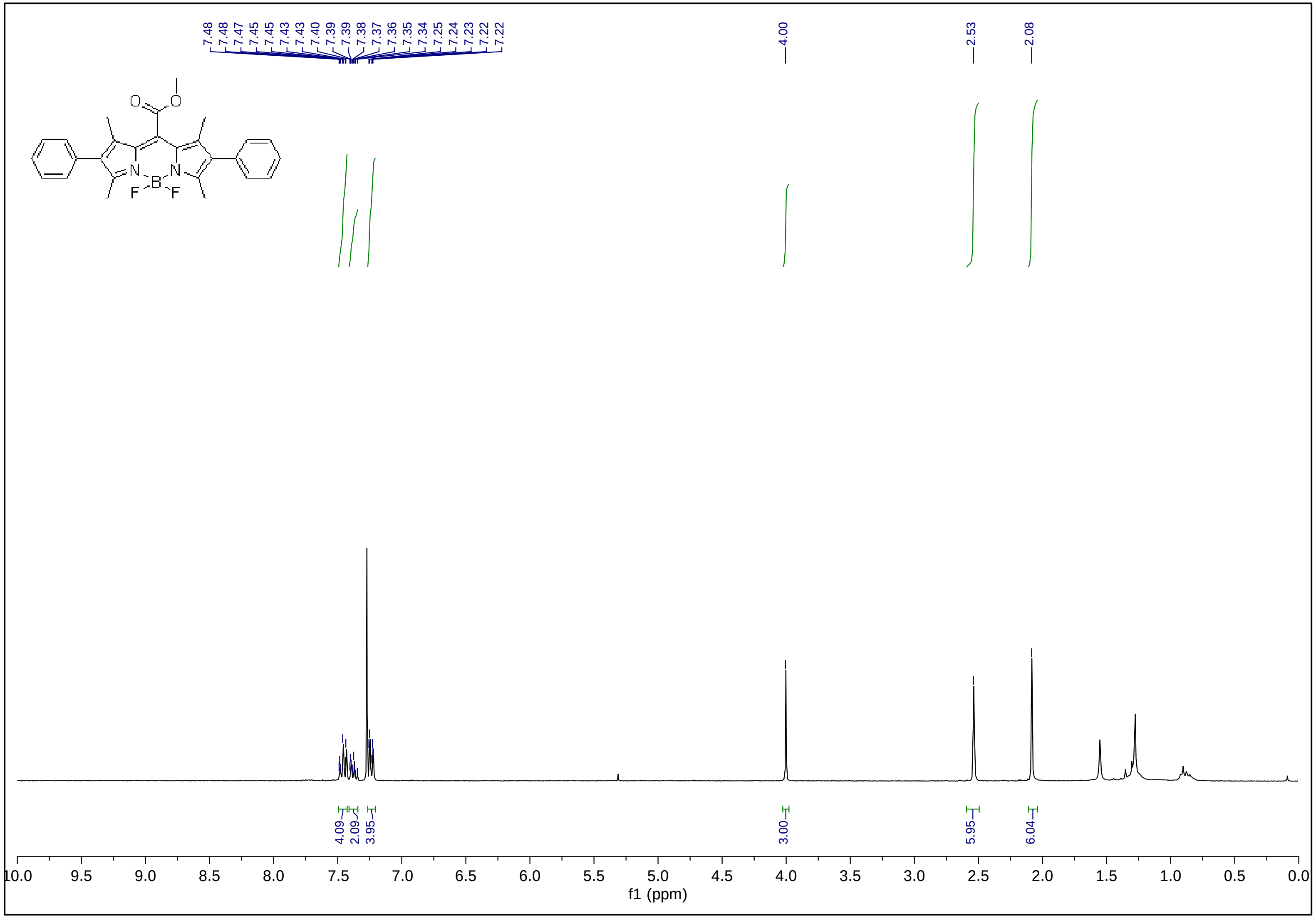

Figure S9: ^{1}H NMR (300 MHz, $CDCl_3$): **19**

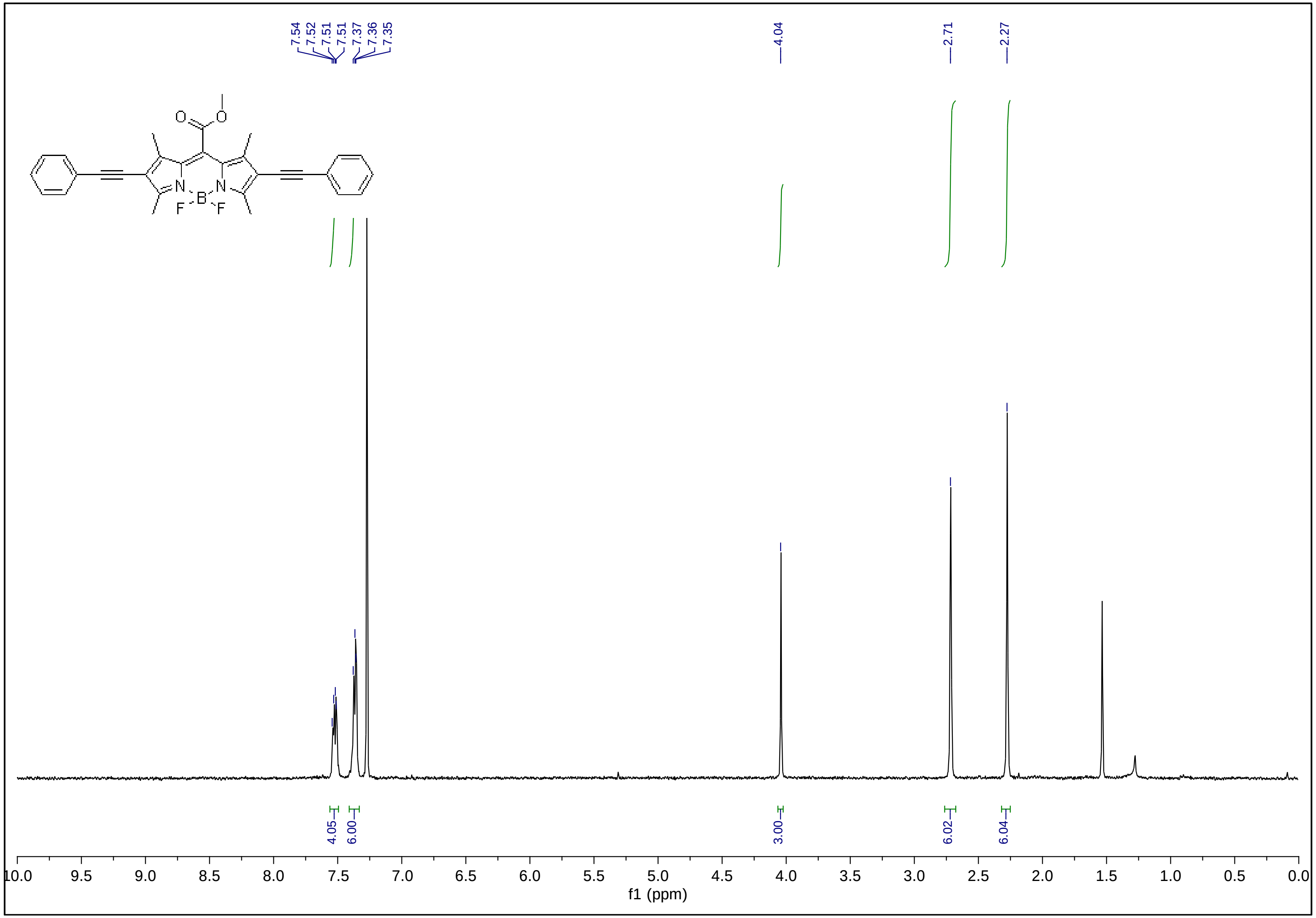

Figure S10: ^{1}H NMR (300 MHz, $CDCl_3$): **20**

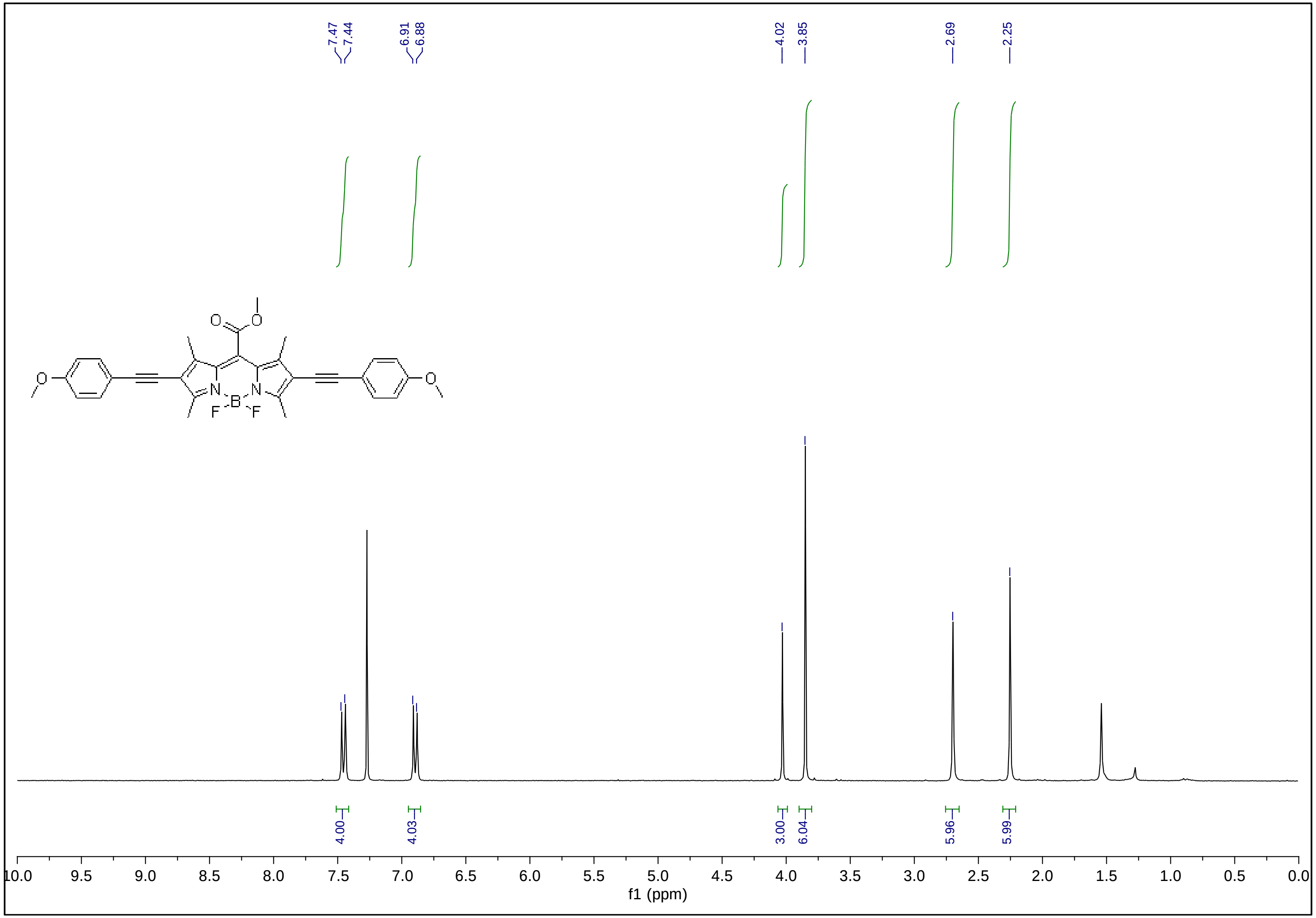

Figure S11: ^{1}H NMR (300 MHz, CD_2Cl_2): **21**

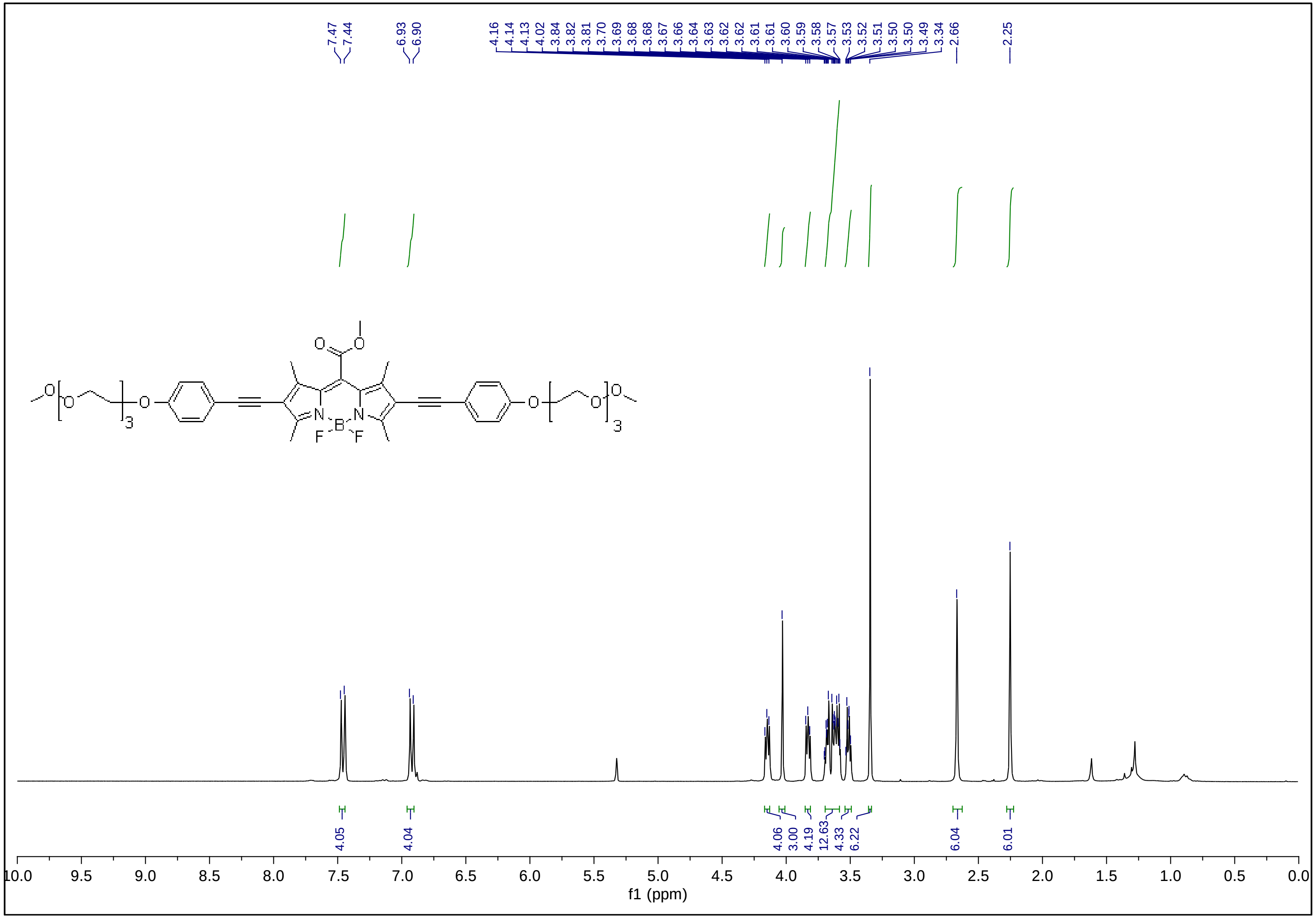

Figure S12: ^{1}H NMR (300 MHz, CD_3OD): **2**

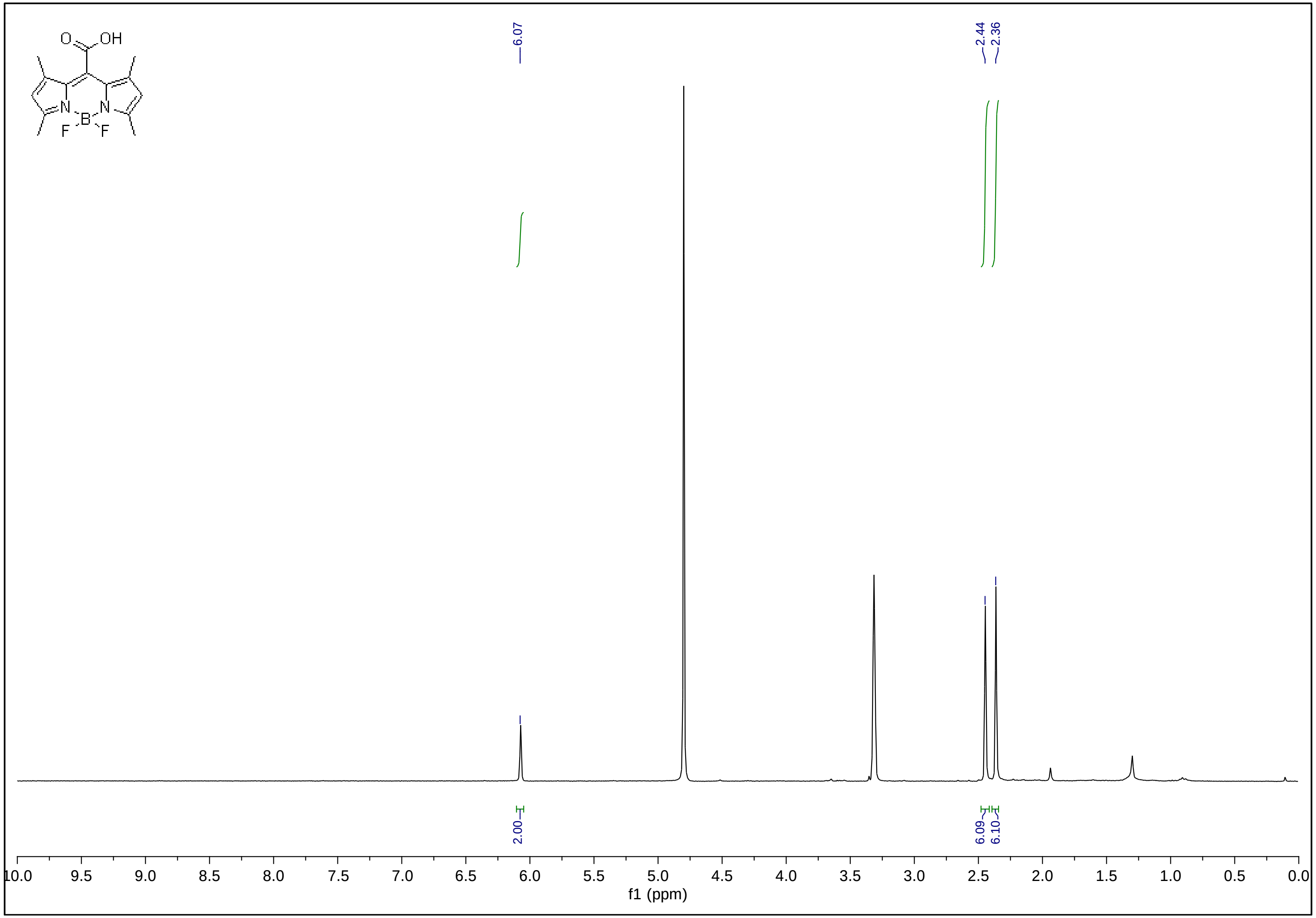

Figure S13: ^{1}H NMR (300 MHz, CD_3OD): **3**

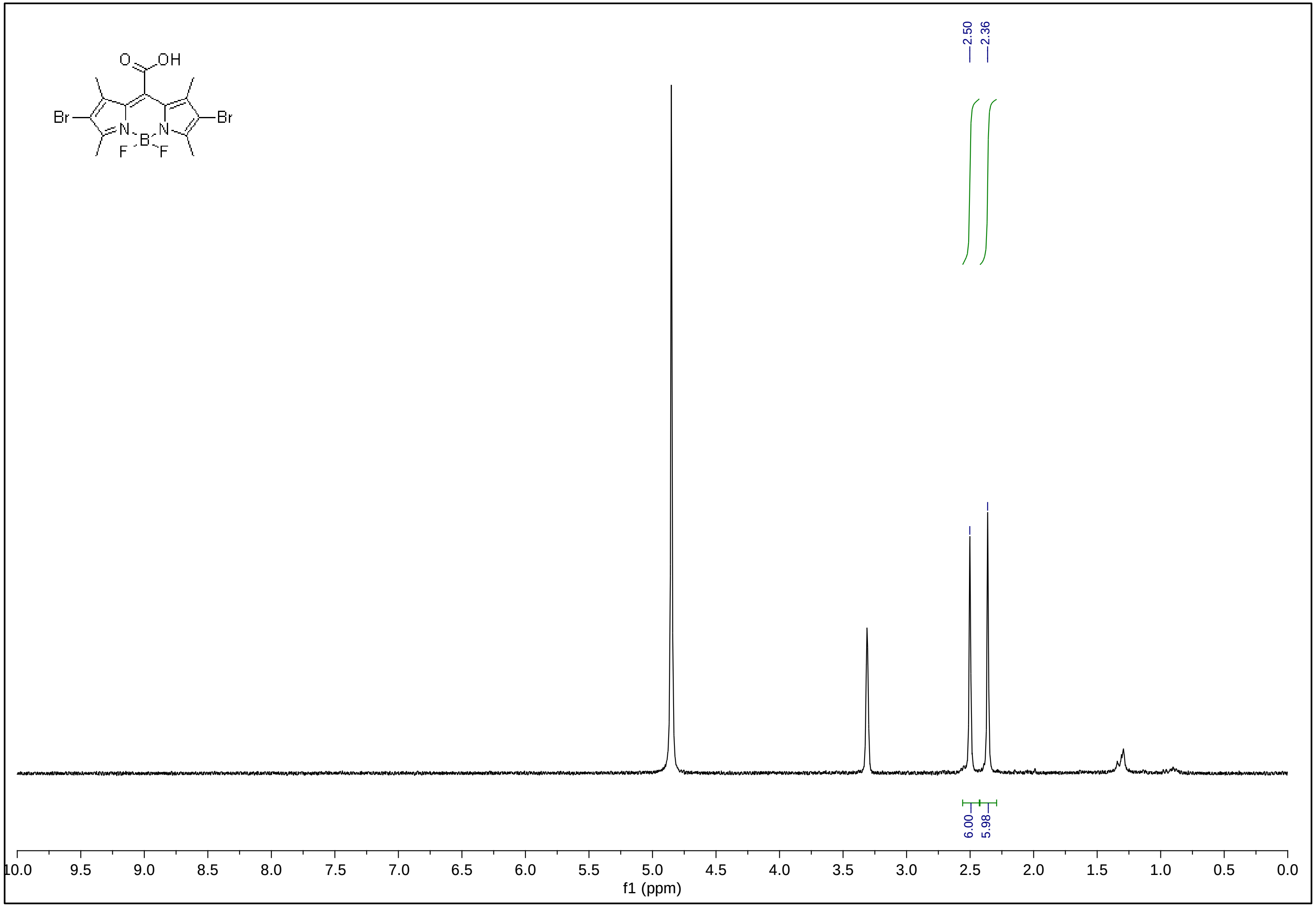

Figure S14: ^{1}H NMR (300 MHz, CD_3OD): **4**

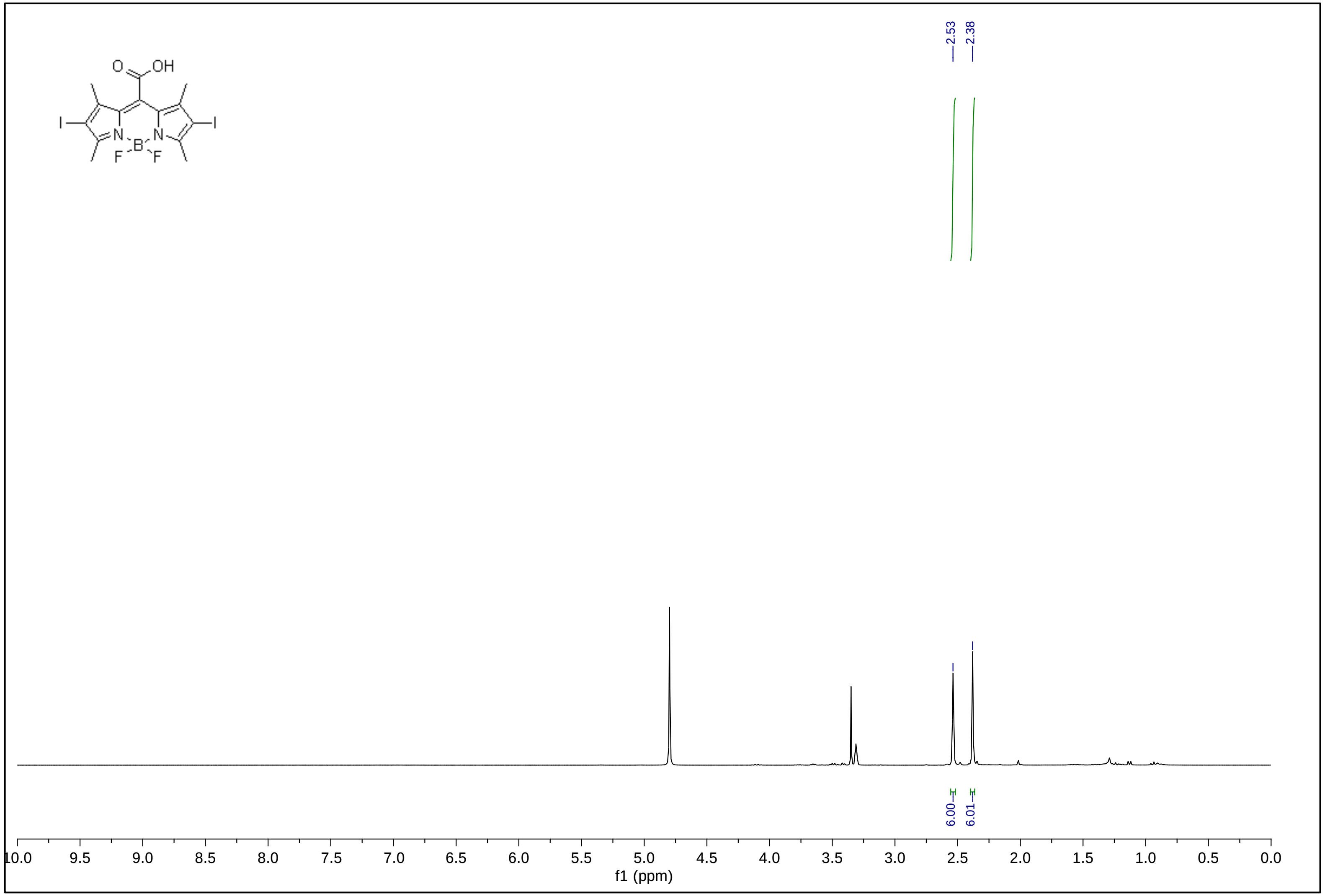

Figure S15: ^{1}H NMR (300 MHz, CD_3OD): **5**

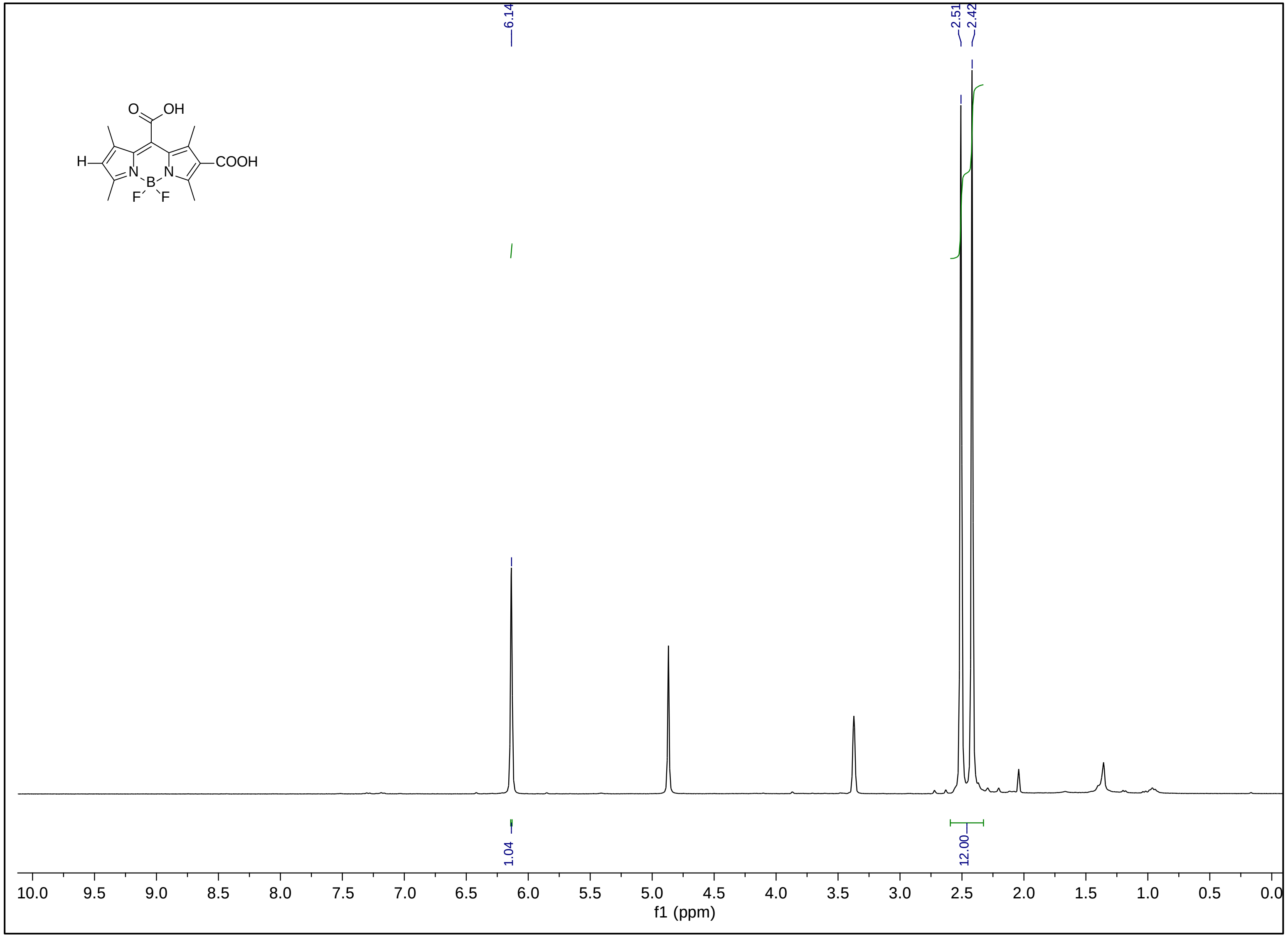

Figure S16: ^{1}H NMR (300 MHz, CD_3OD): **6**

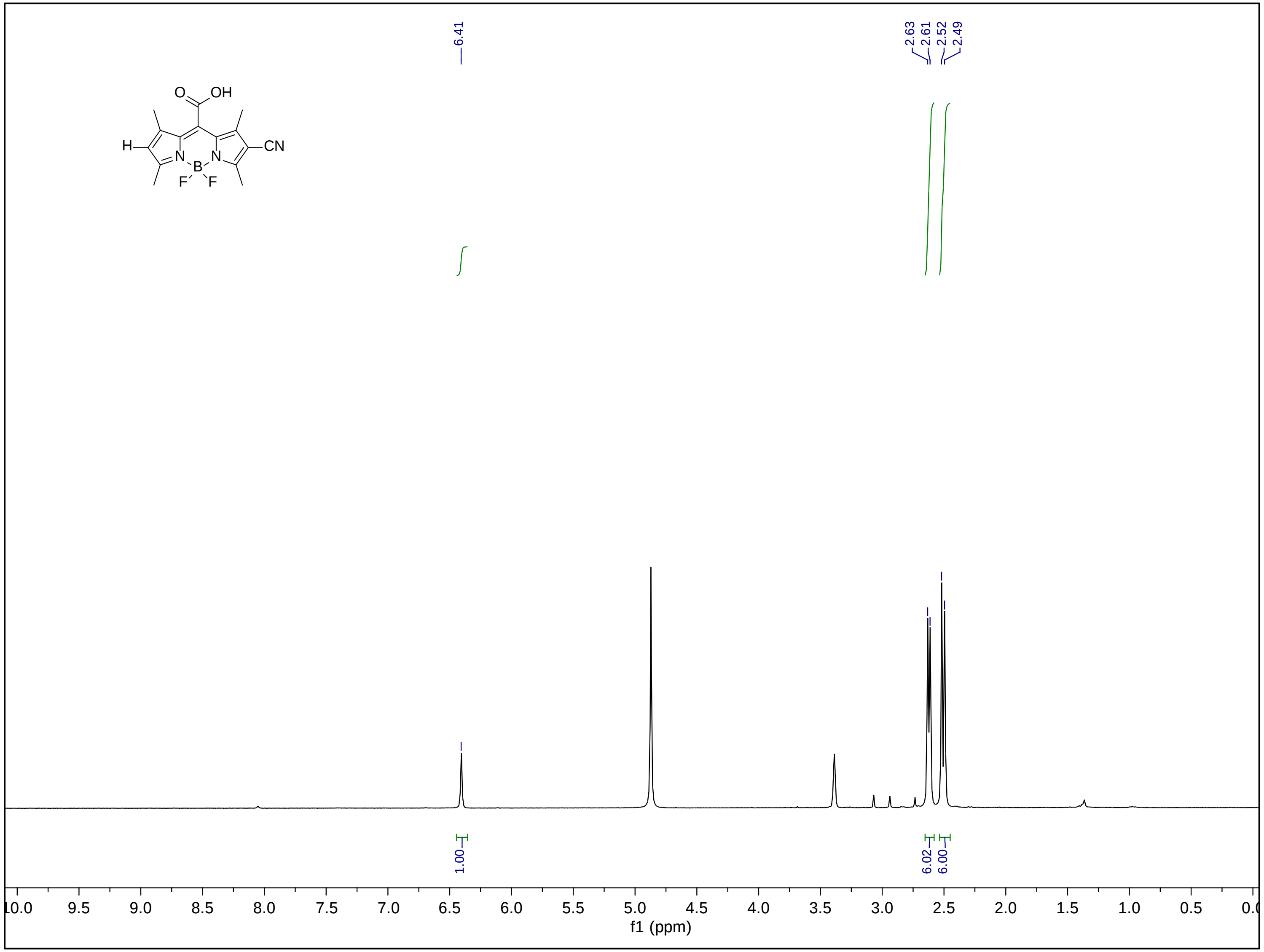

Figure S17: ^{1}H NMR (300 MHz, CD_3OD): **7**

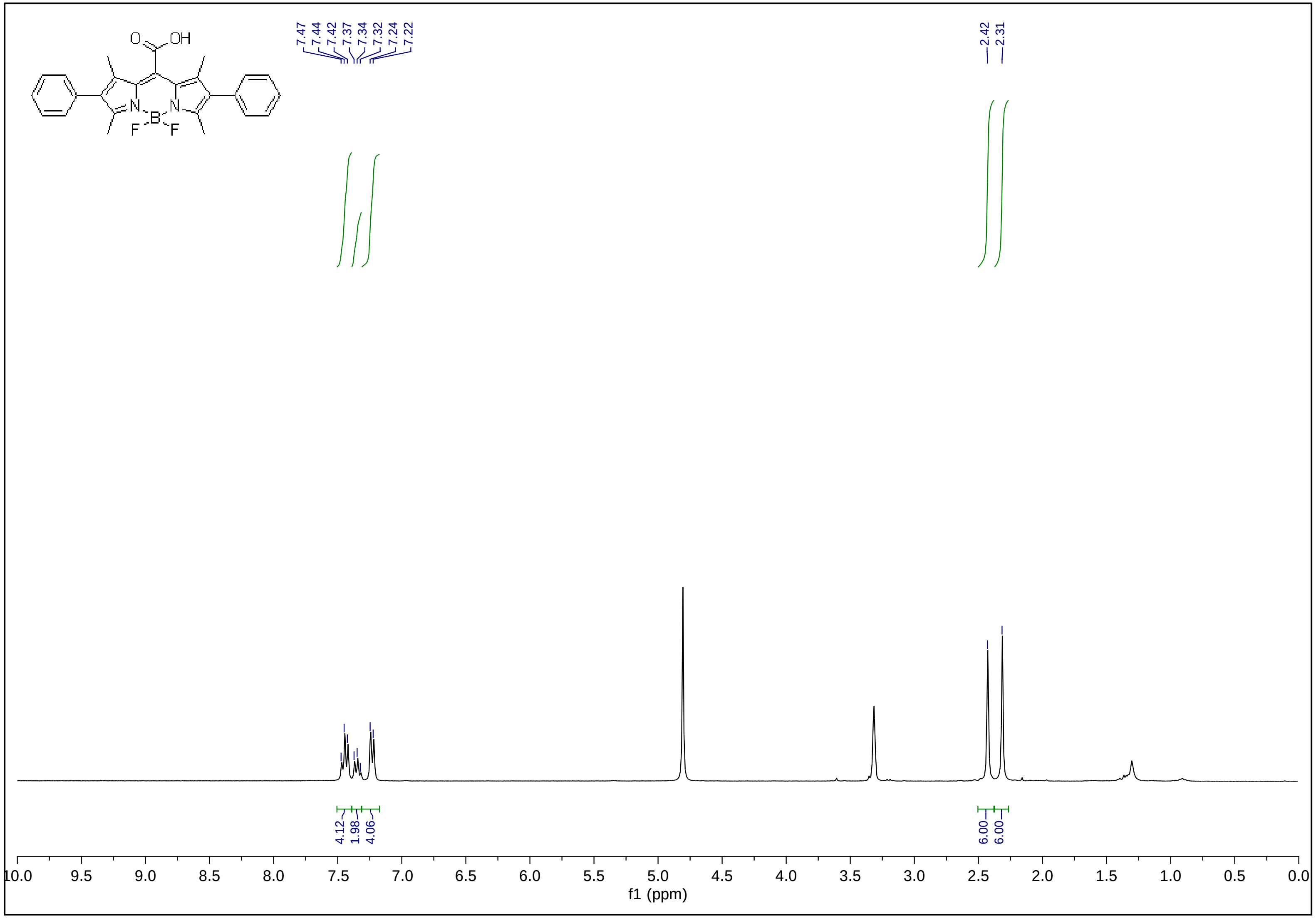

Figure S18: ^{1}H NMR (300 MHz, CD_3OD): **8**

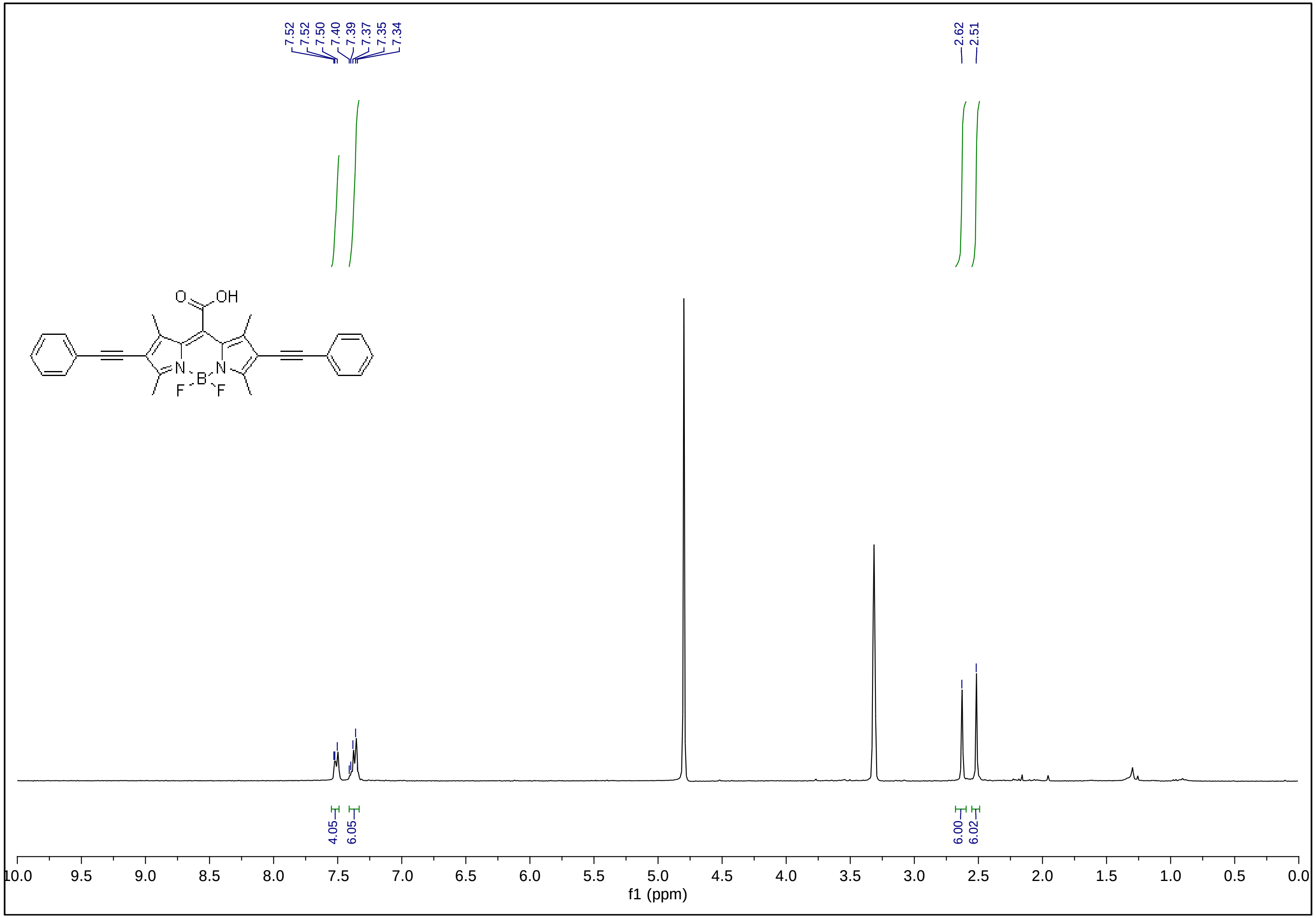

Figure S19: ^{1}H NMR (300 MHz, CD_3OD): **9**

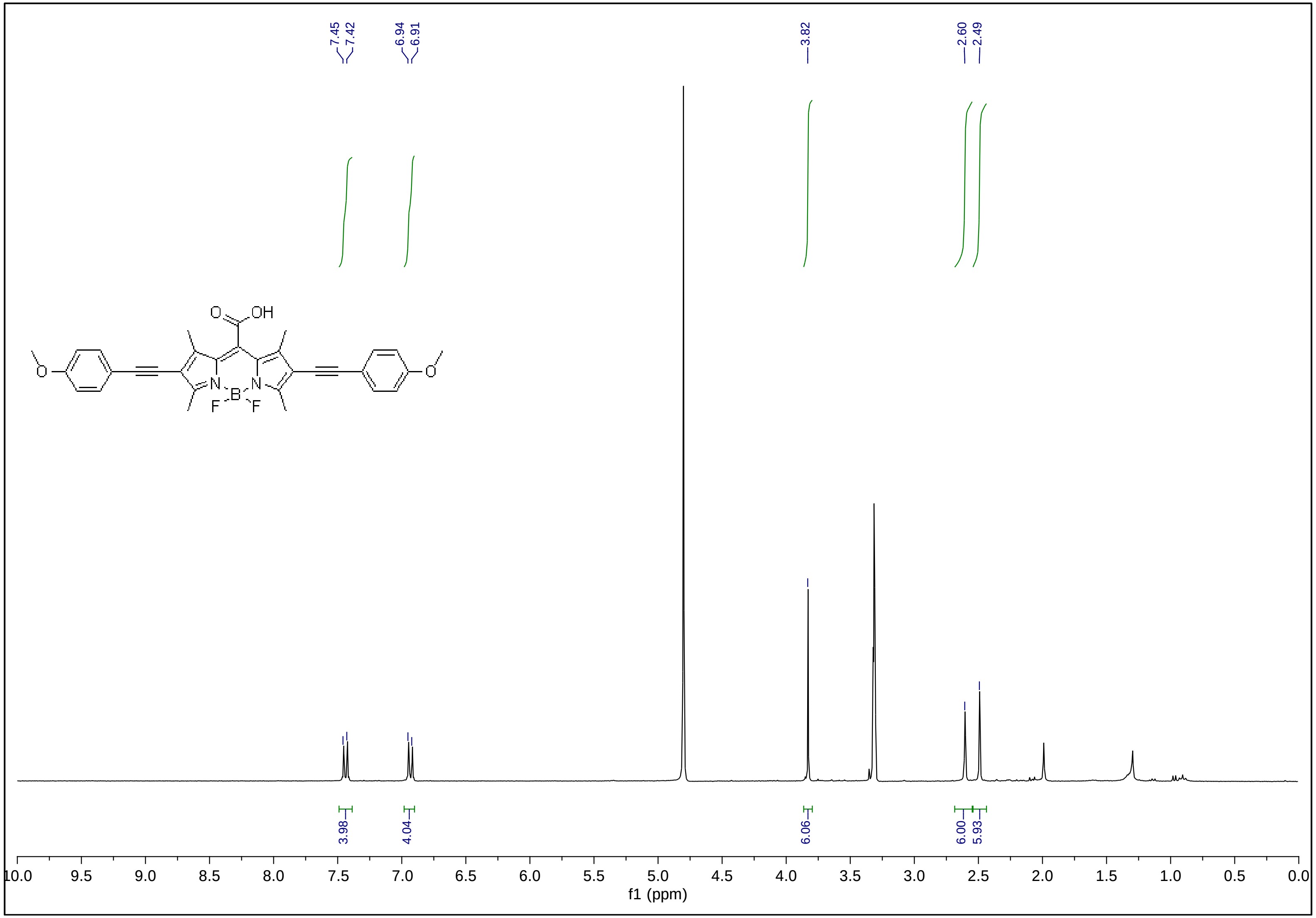

Figure S20: ^{1}H NMR (300 MHz, CD_3OD): **10**

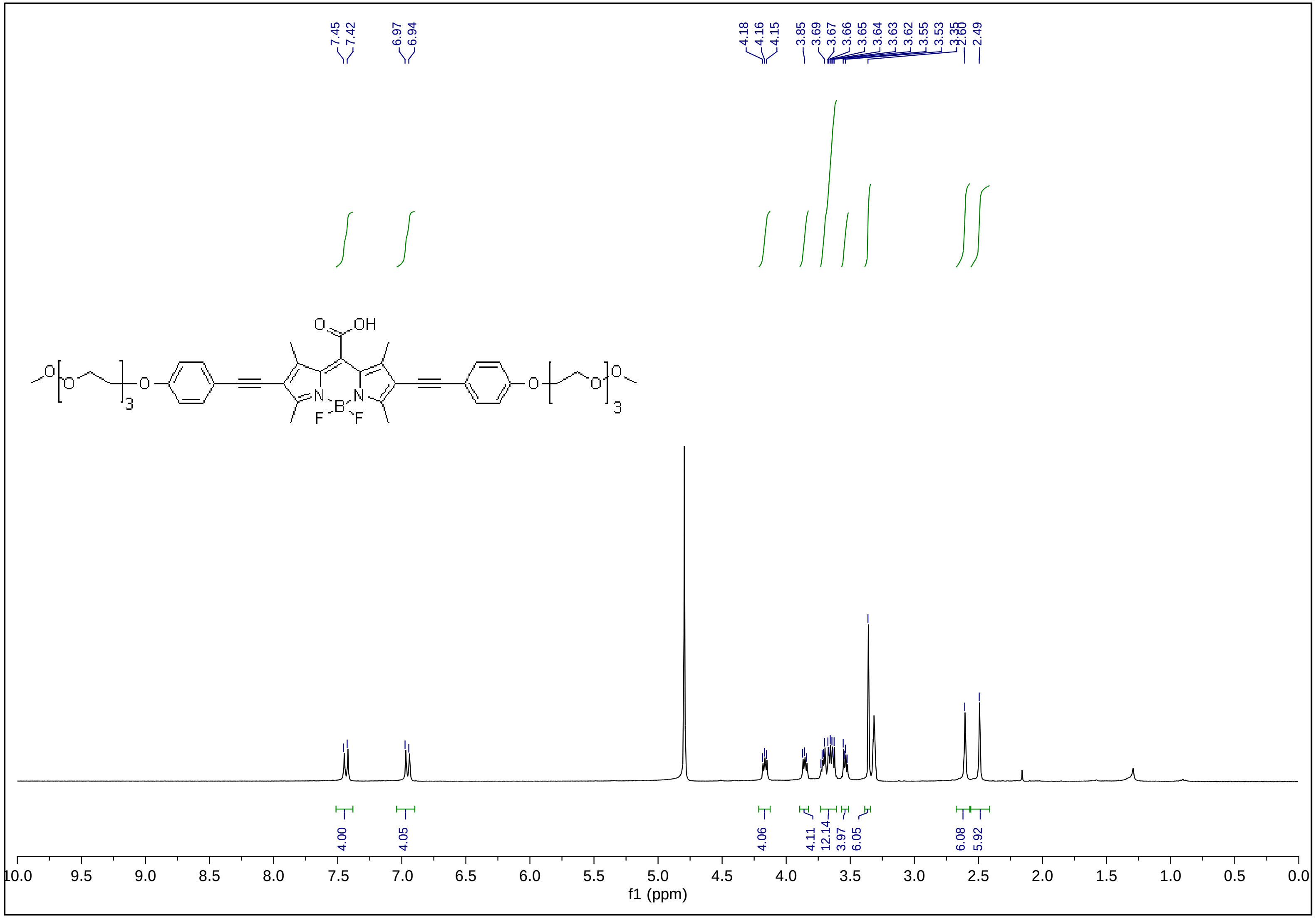

Figure S21: ^{13}C NMR (75 MHz, $CDCl_3$): **11**

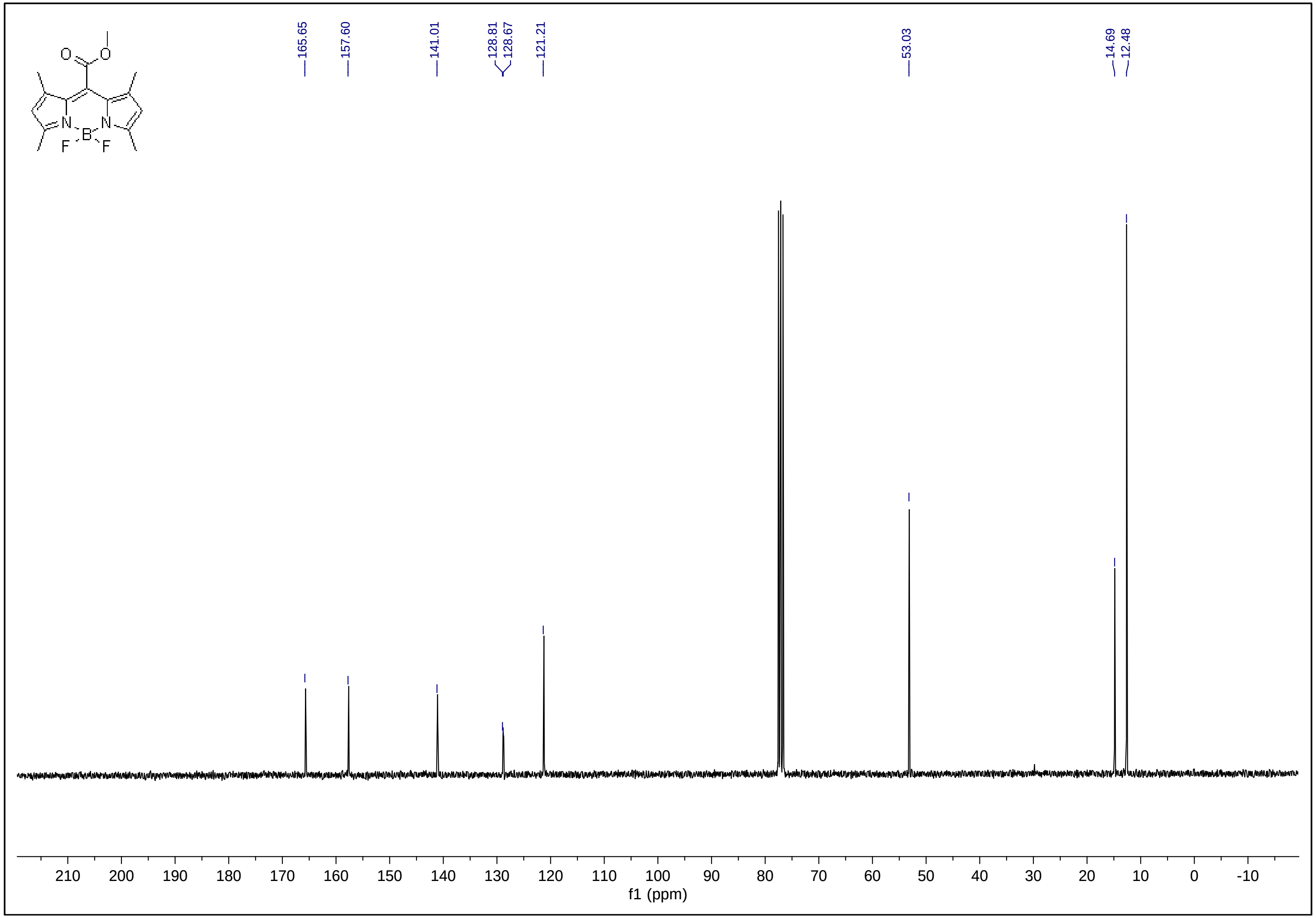

Figure S22: ^{13}C NMR (75 MHz, $CDCl_3$): **12**

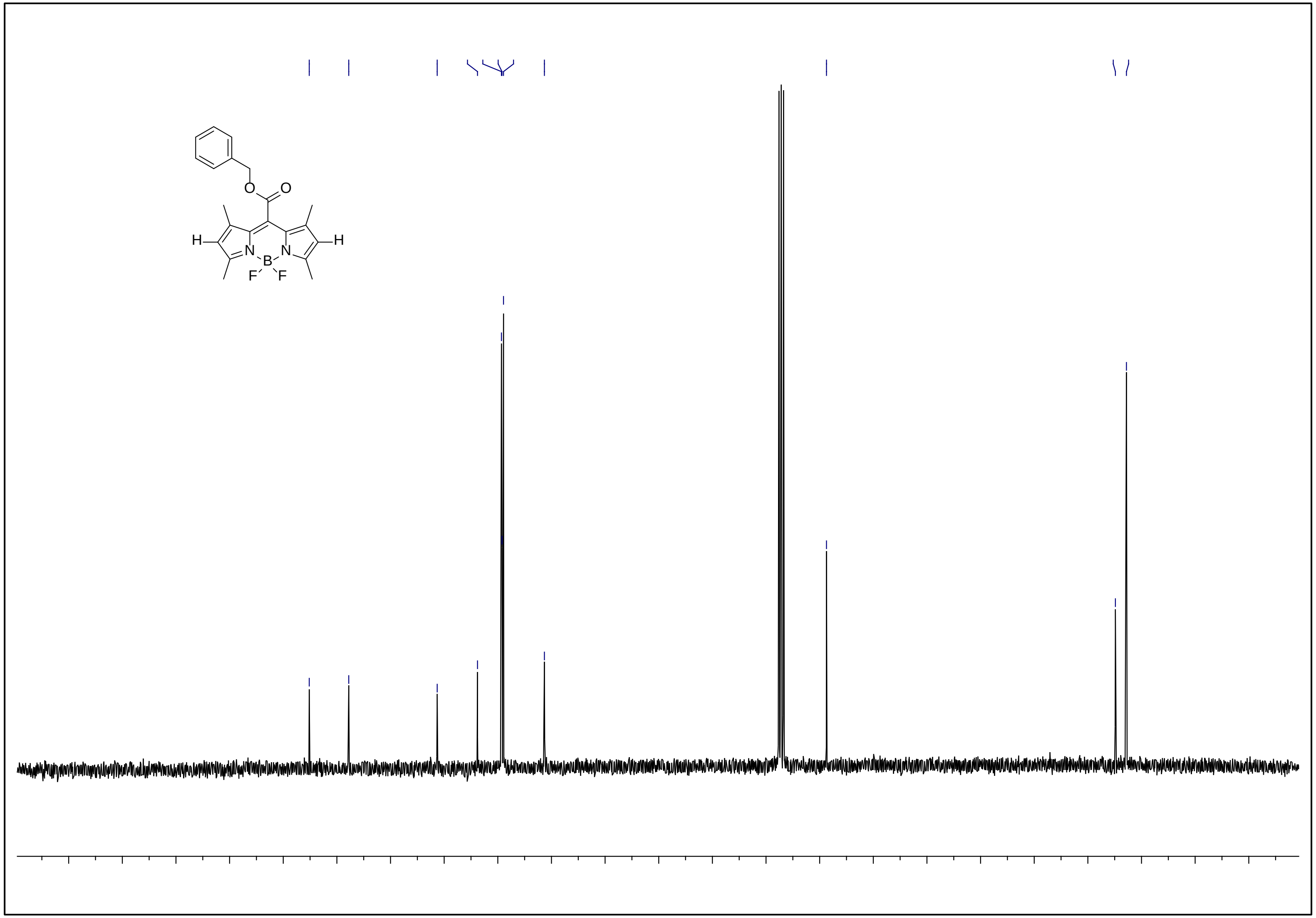

Figure S23: ^{13}C NMR (125 MHz, $CDCl_3$): **13**

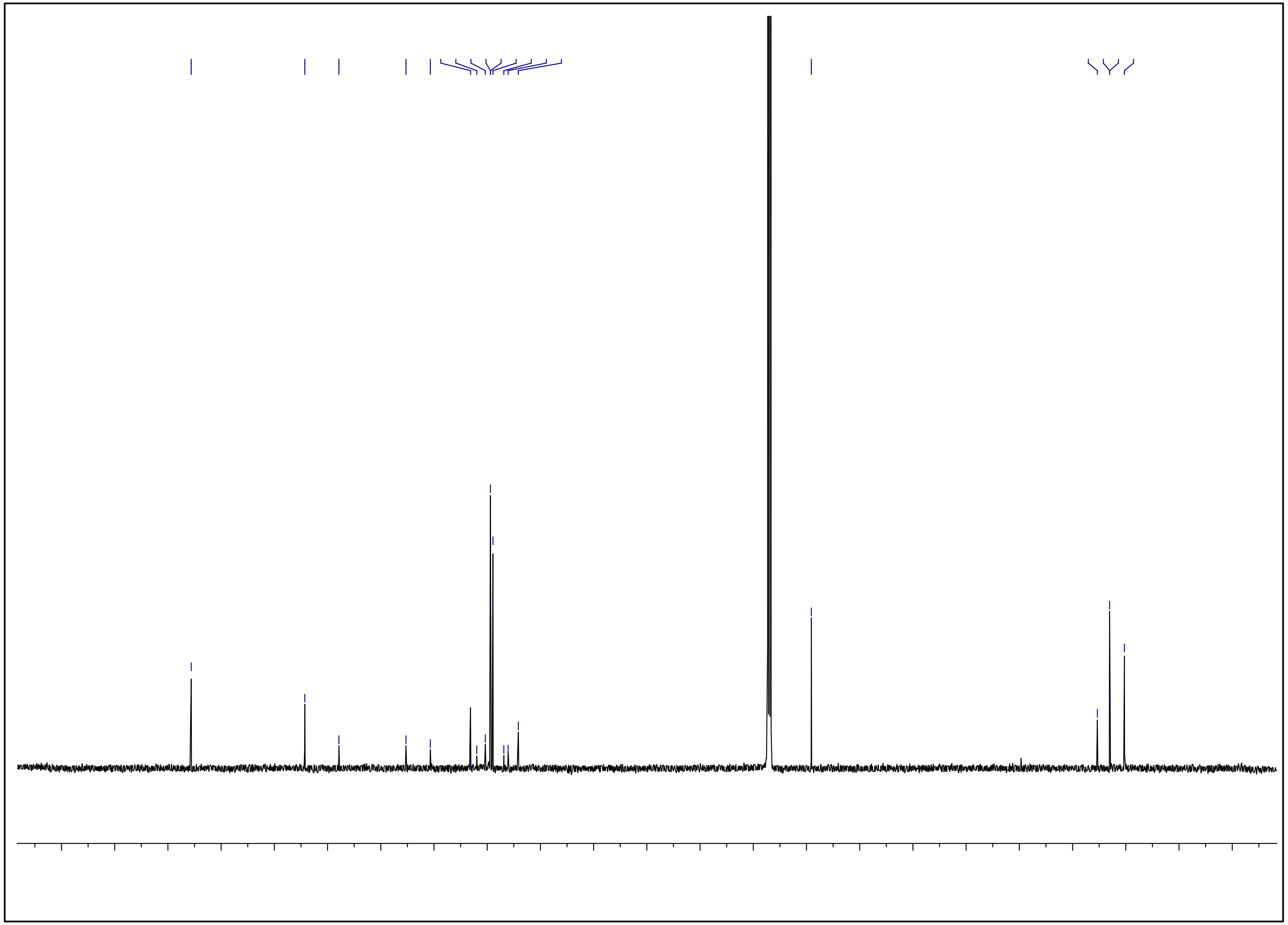

Figure S24: ^{13}C NMR (125 MHz, DMSO-d5): **14**

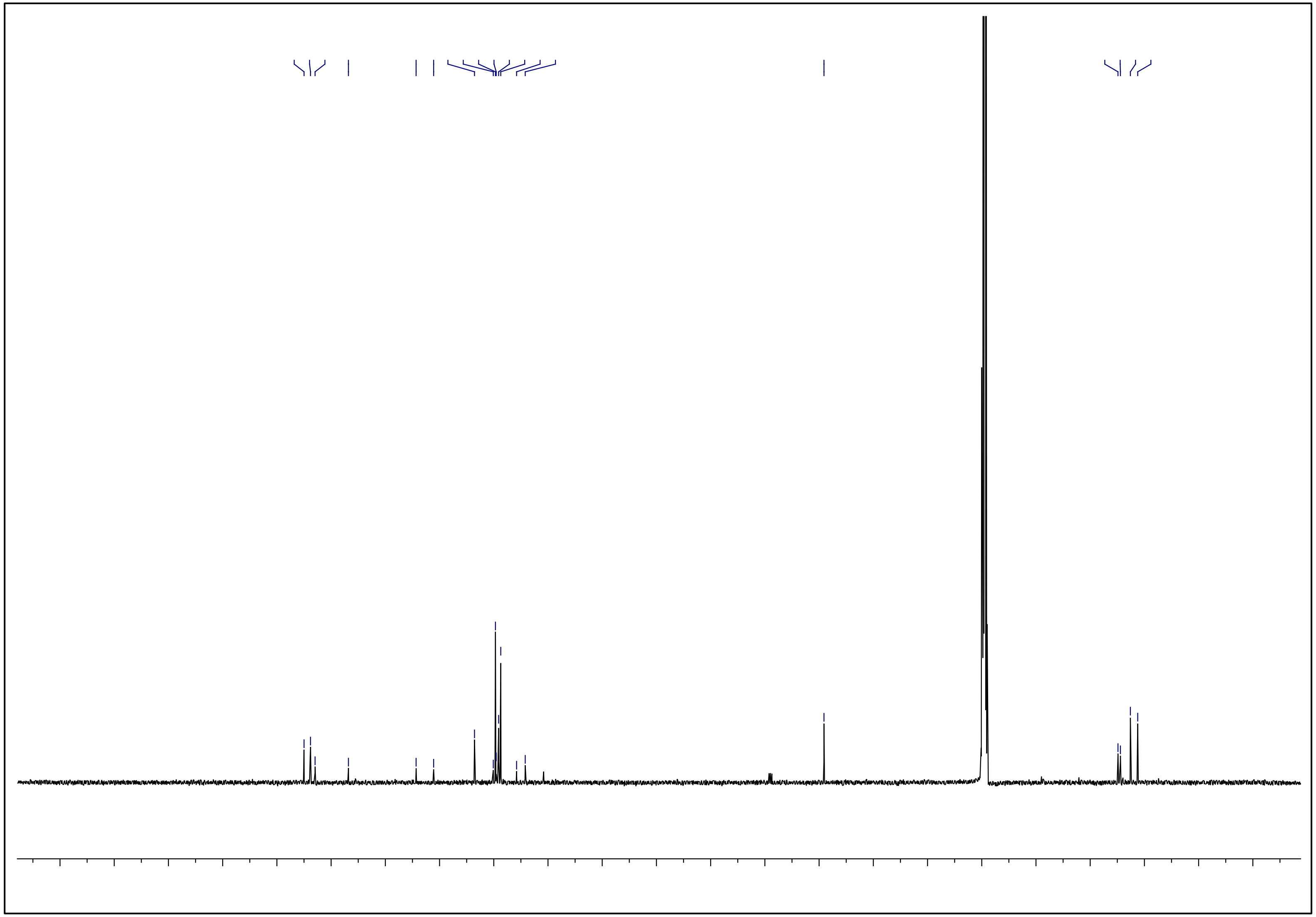

Figure S25: ^{13}C NMR (75 MHz, $CDCl_3$): **17** (a signal at ~30 ppm is acetone)

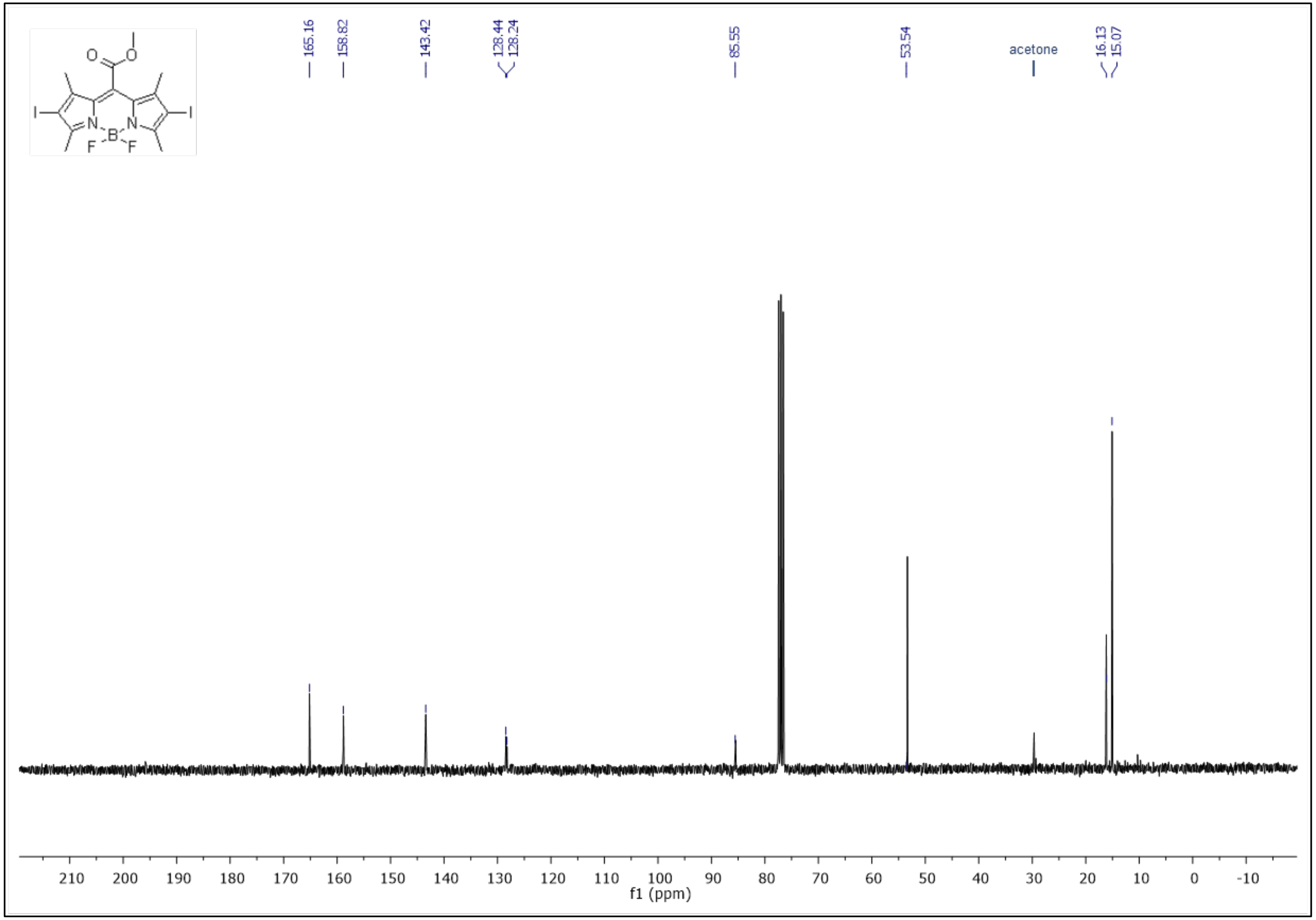

Figure S26: ^{13}C NMR (75 MHz, $CDCl_3$): **18** (a signal at ~30 ppm is acetone)

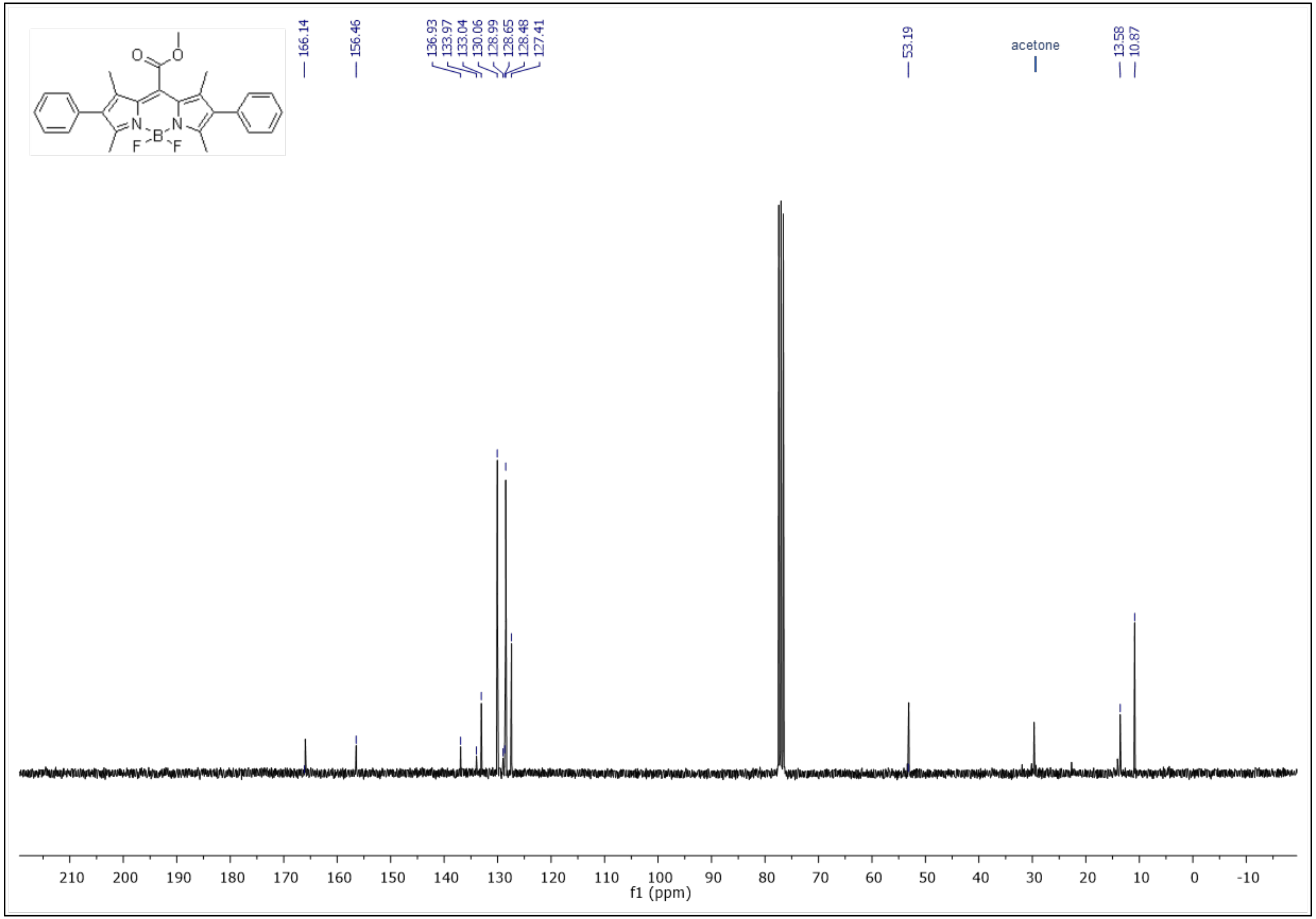

Figure S27: ^{13}C NMR (75 MHz, $CDCl_3$): **19**

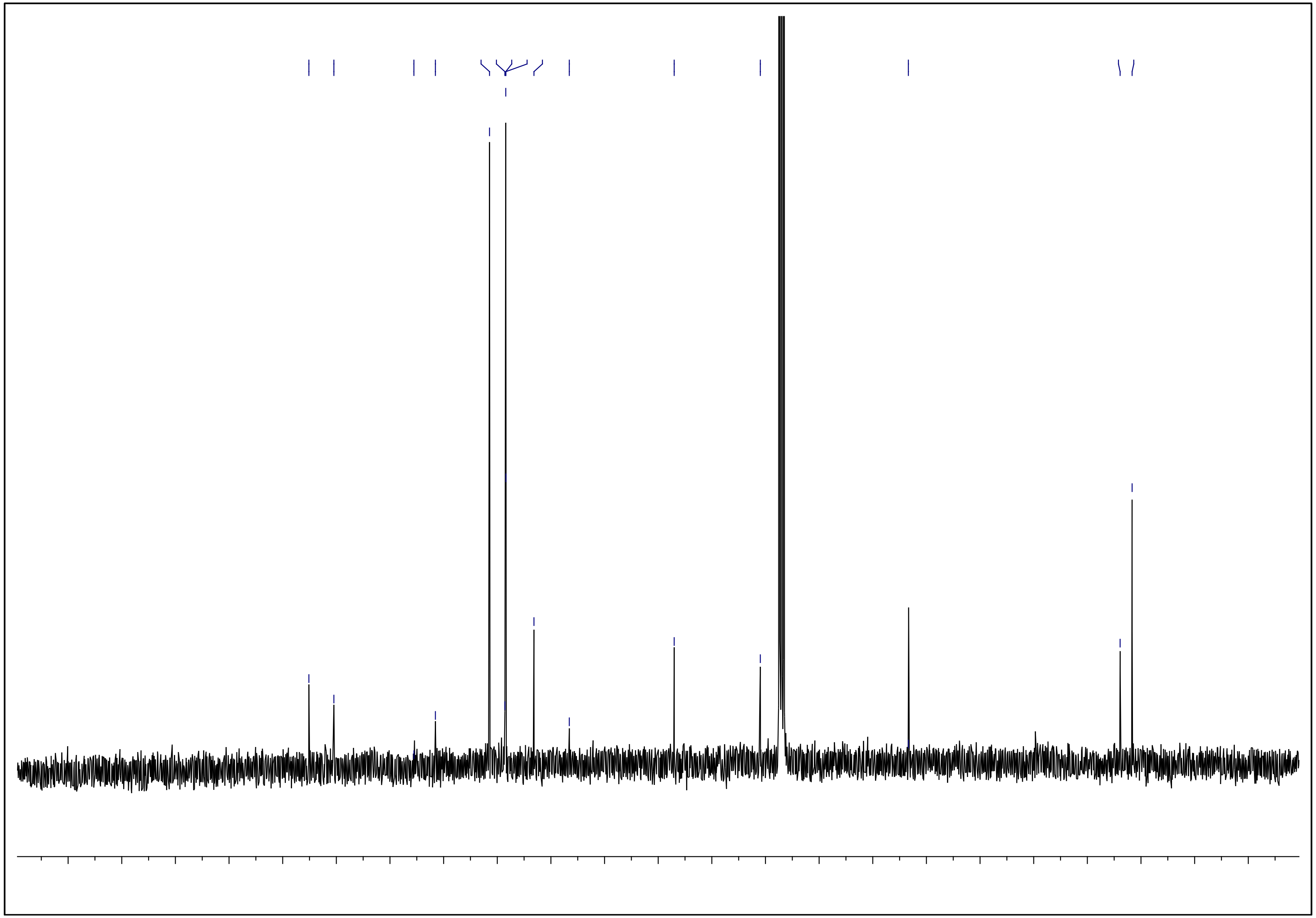

Figure S28: ^{13}C NMR (75 MHz, $CDCl_3$): **20**

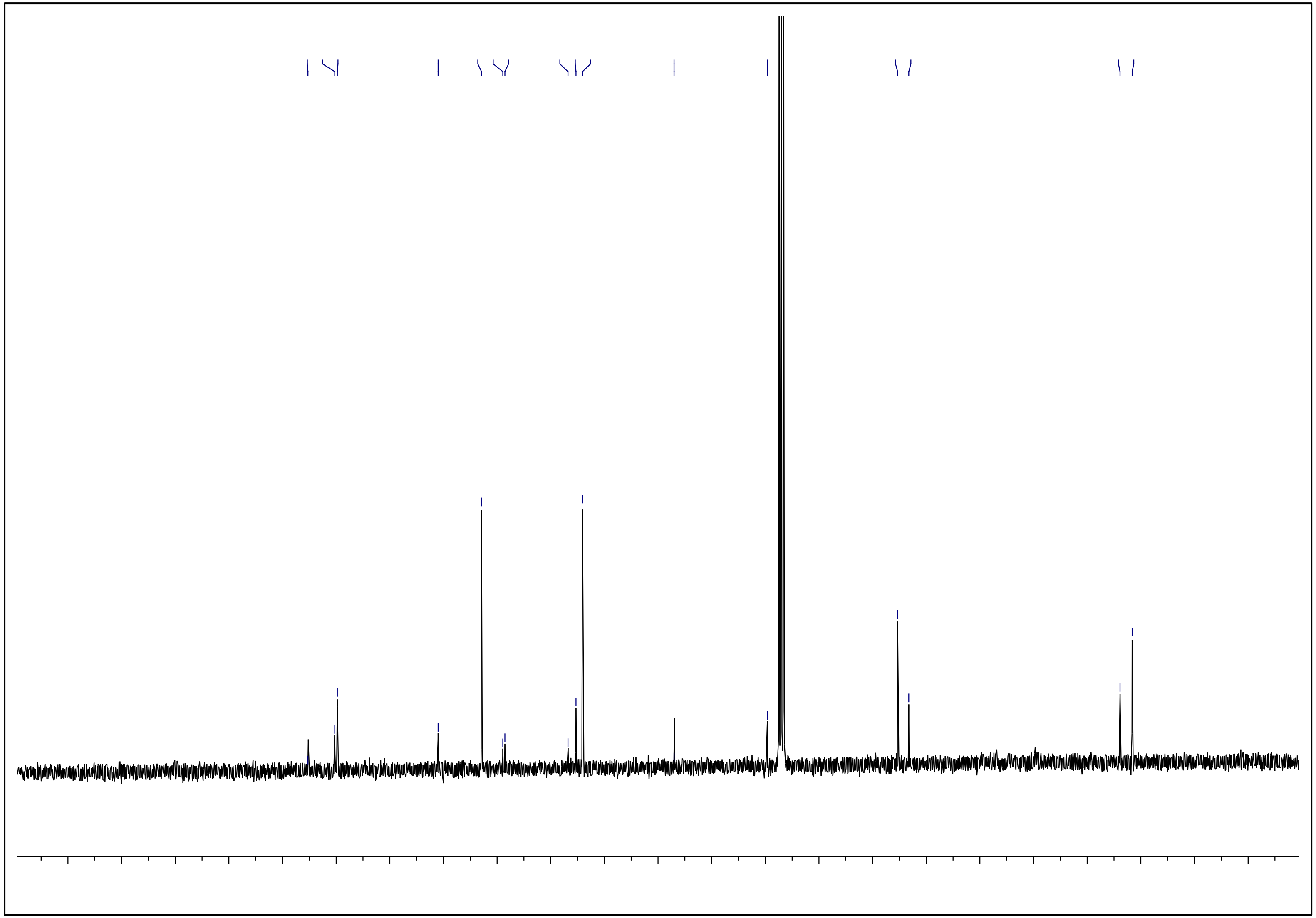

Figure S29: ^{13}C NMR (75 MHz, CD_2Cl_2): **21**

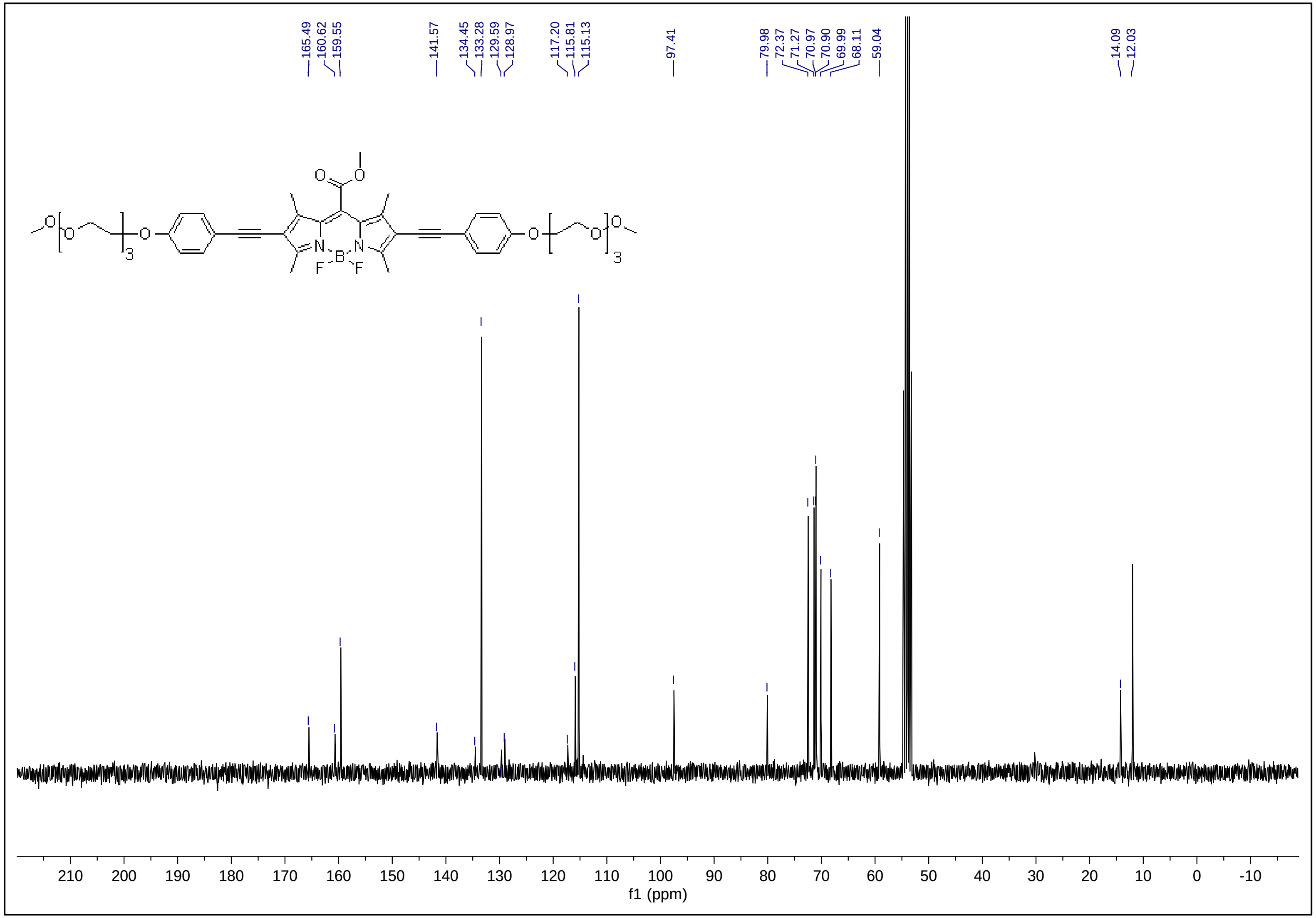

Figure S30: ^{13}C NMR (75 MHz, CD_3OD): **2**

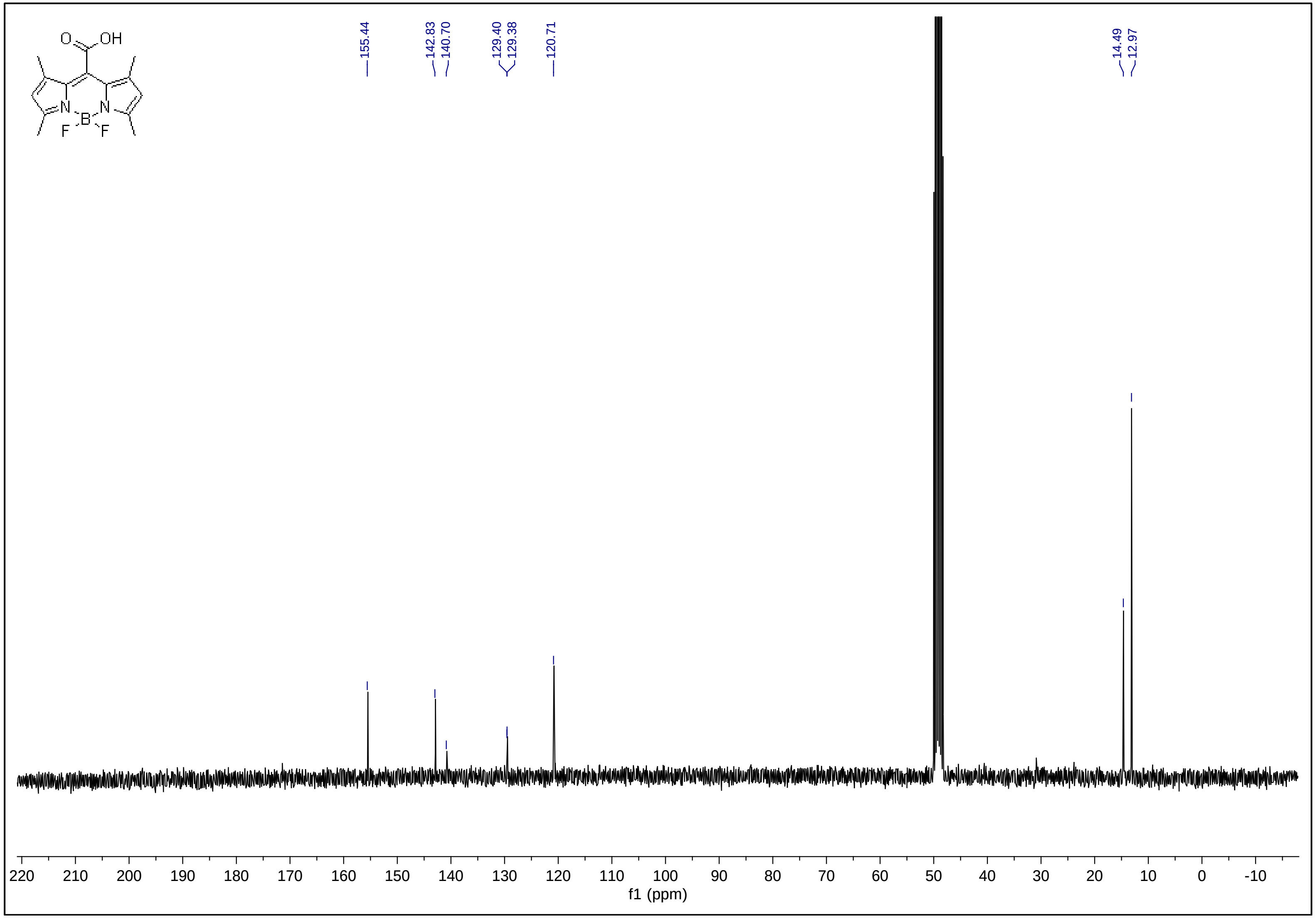

Figure S31: ^{13}C NMR (125 MHz, CD_3OD): **3**

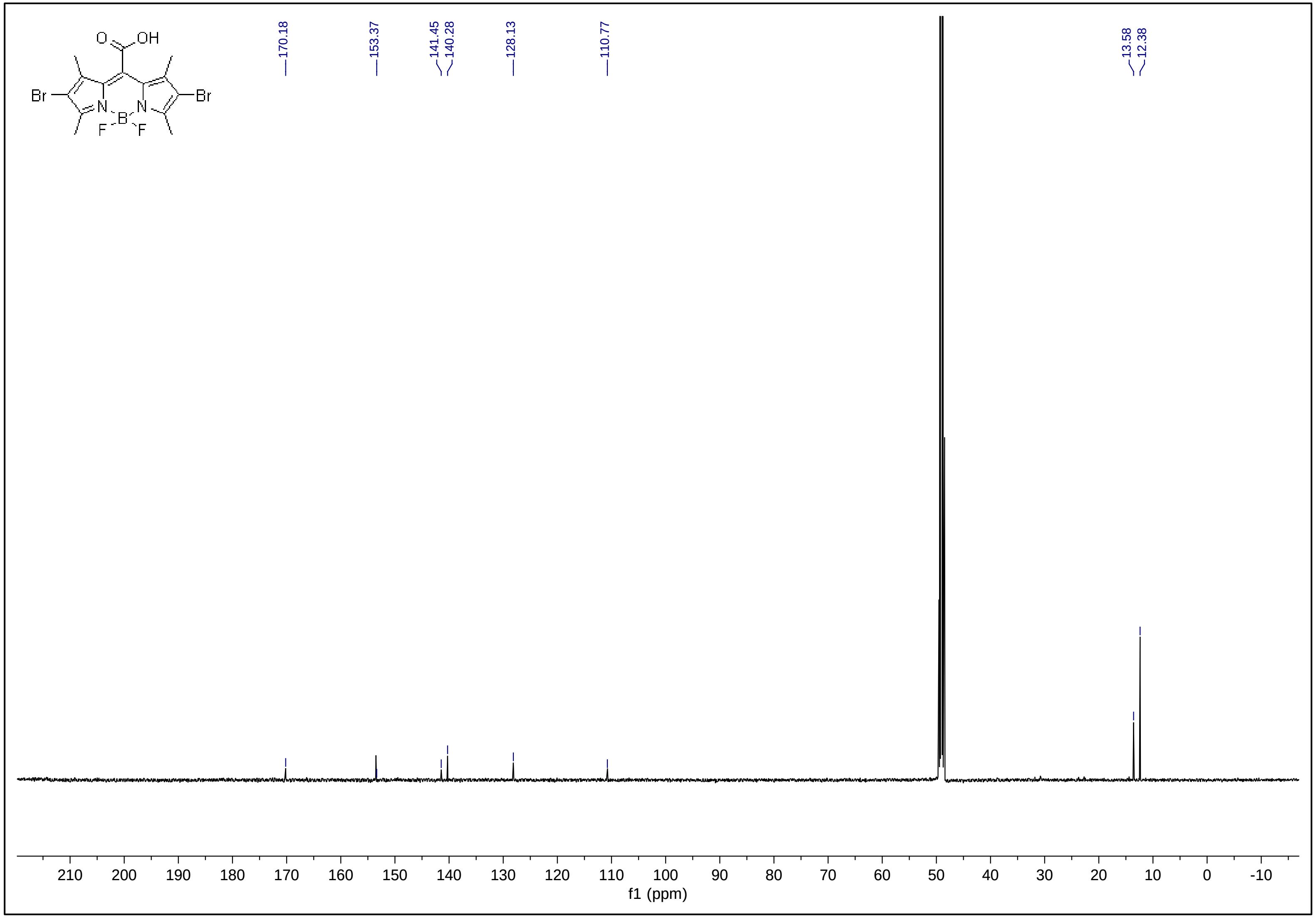

Figure S32: ^{13}C NMR (125 MHz, CD_3OD): **4**

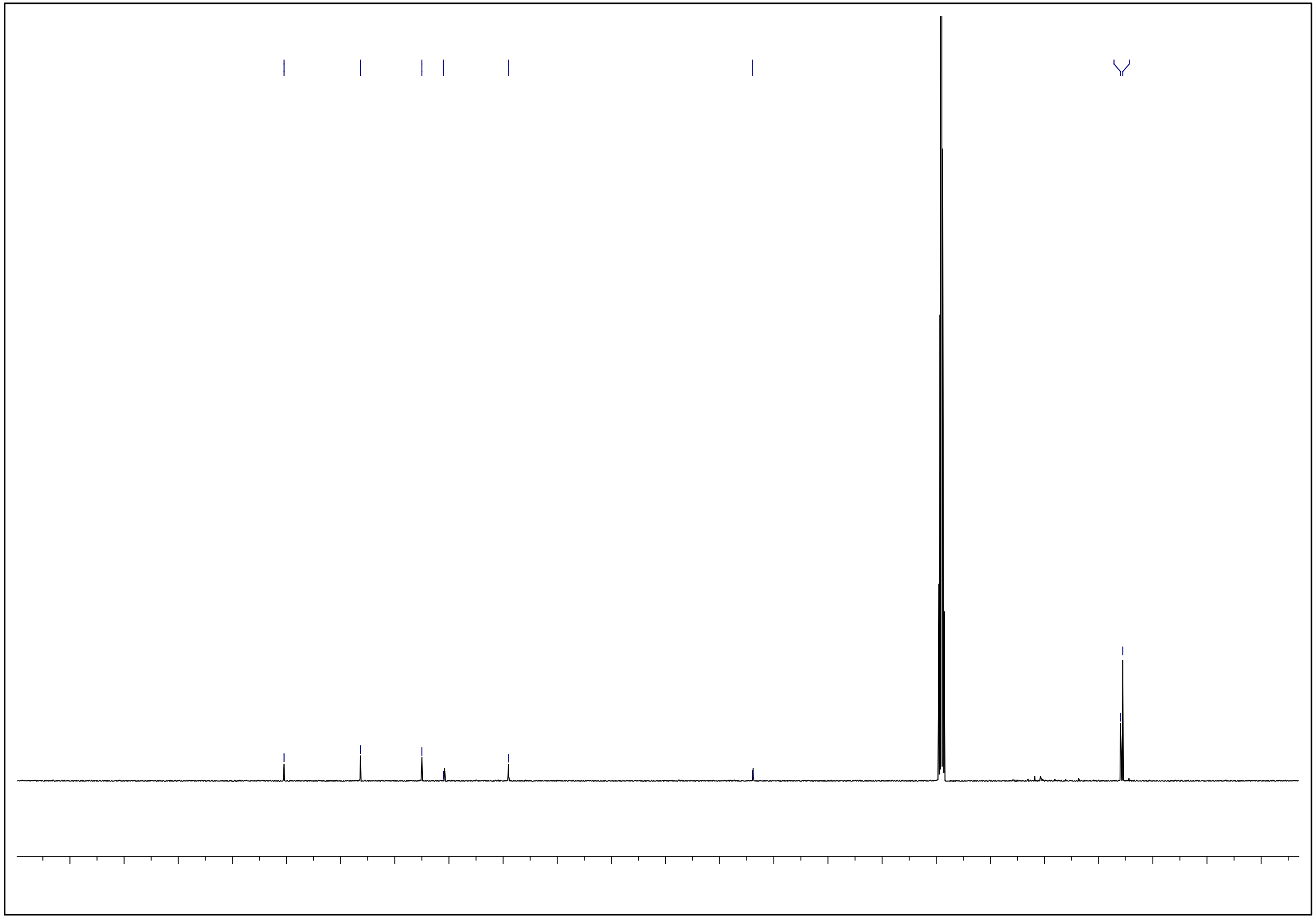

Figure S33: ^{13}C NMR (75 MHz, CD_3OD): **5**

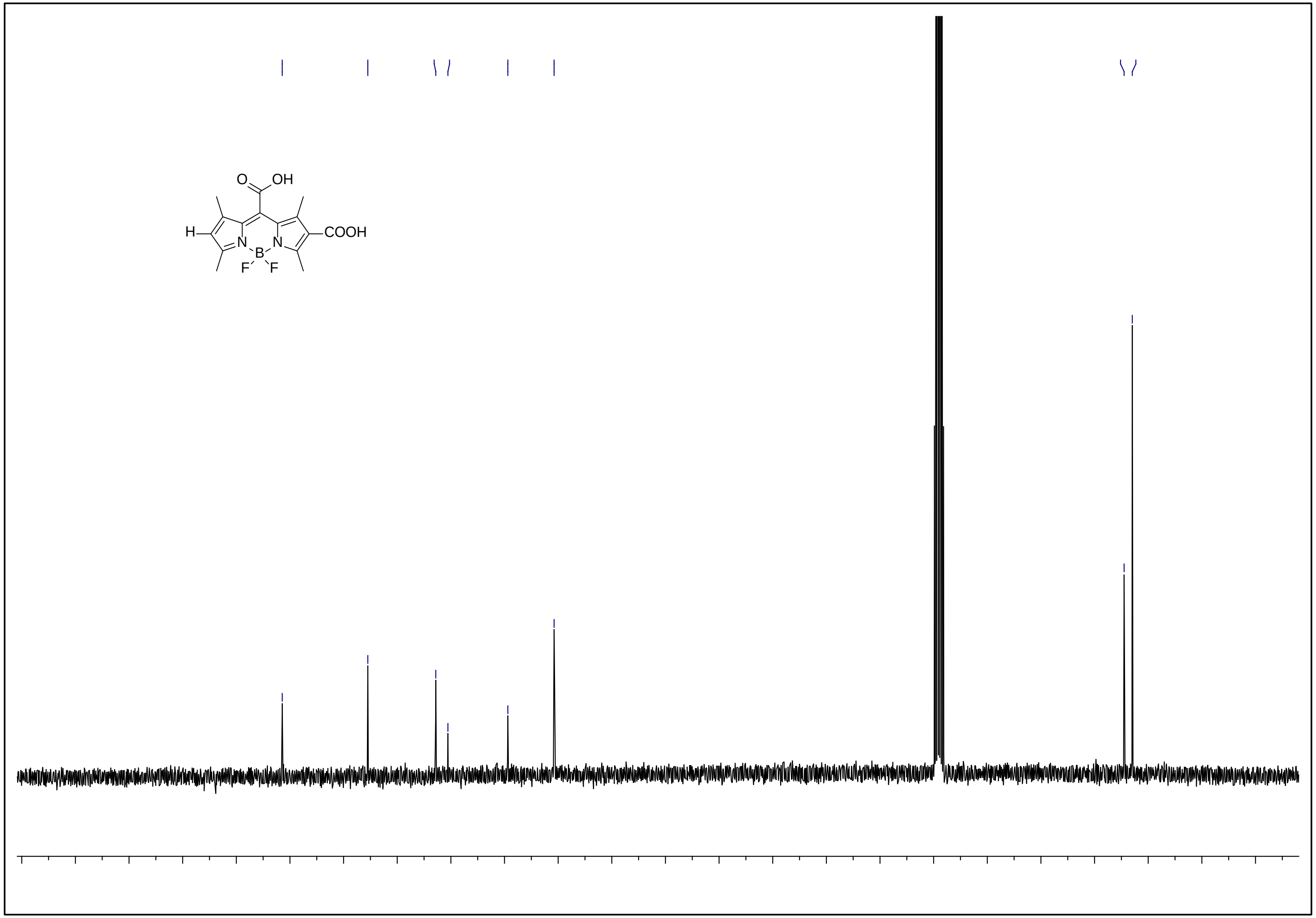

Figure S34: ^{13}C NMR (75 MHz, CD_3OD): **6**

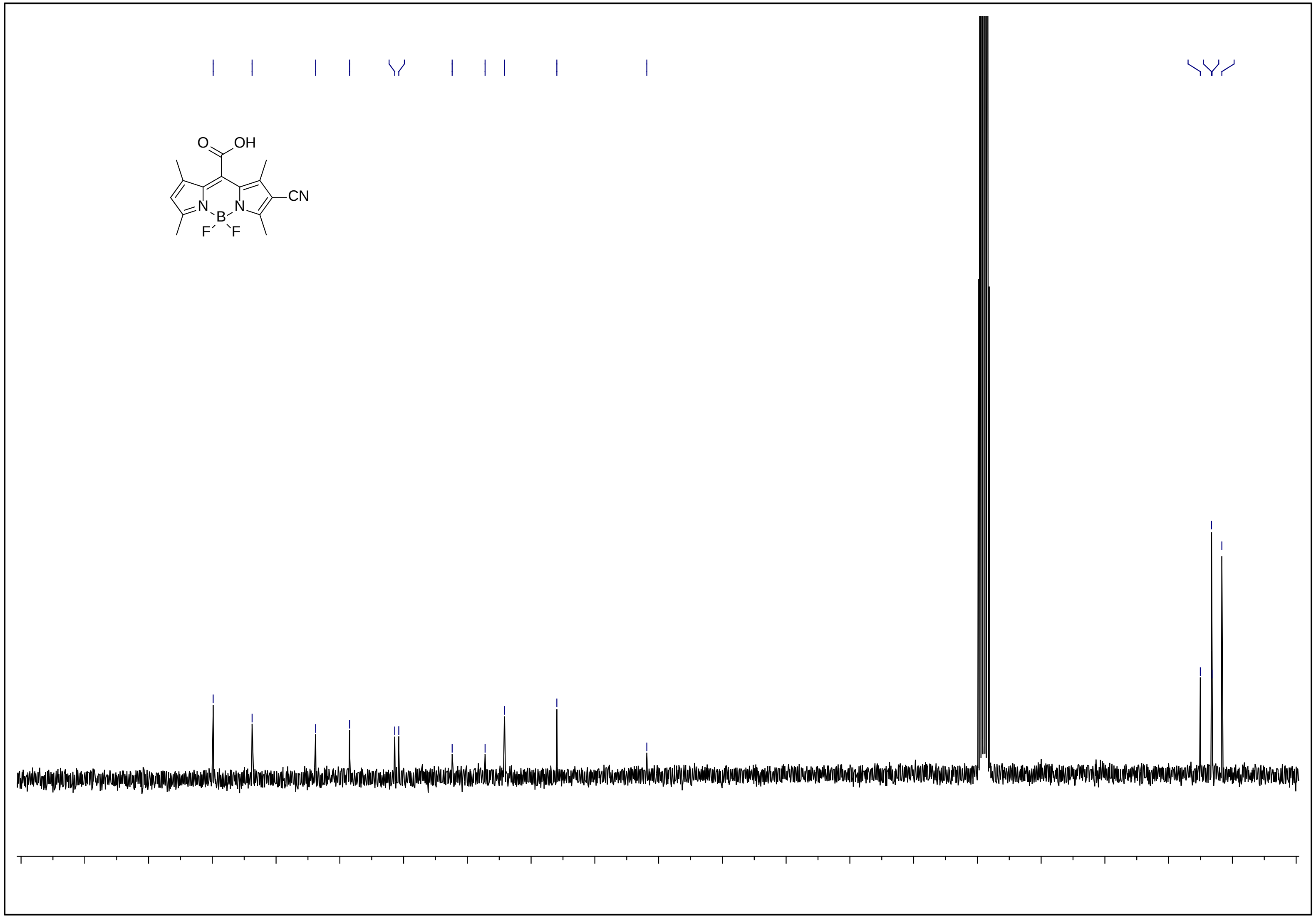

Figure S35: ^{13}C NMR (75 MHz, CD_3OD): **7**

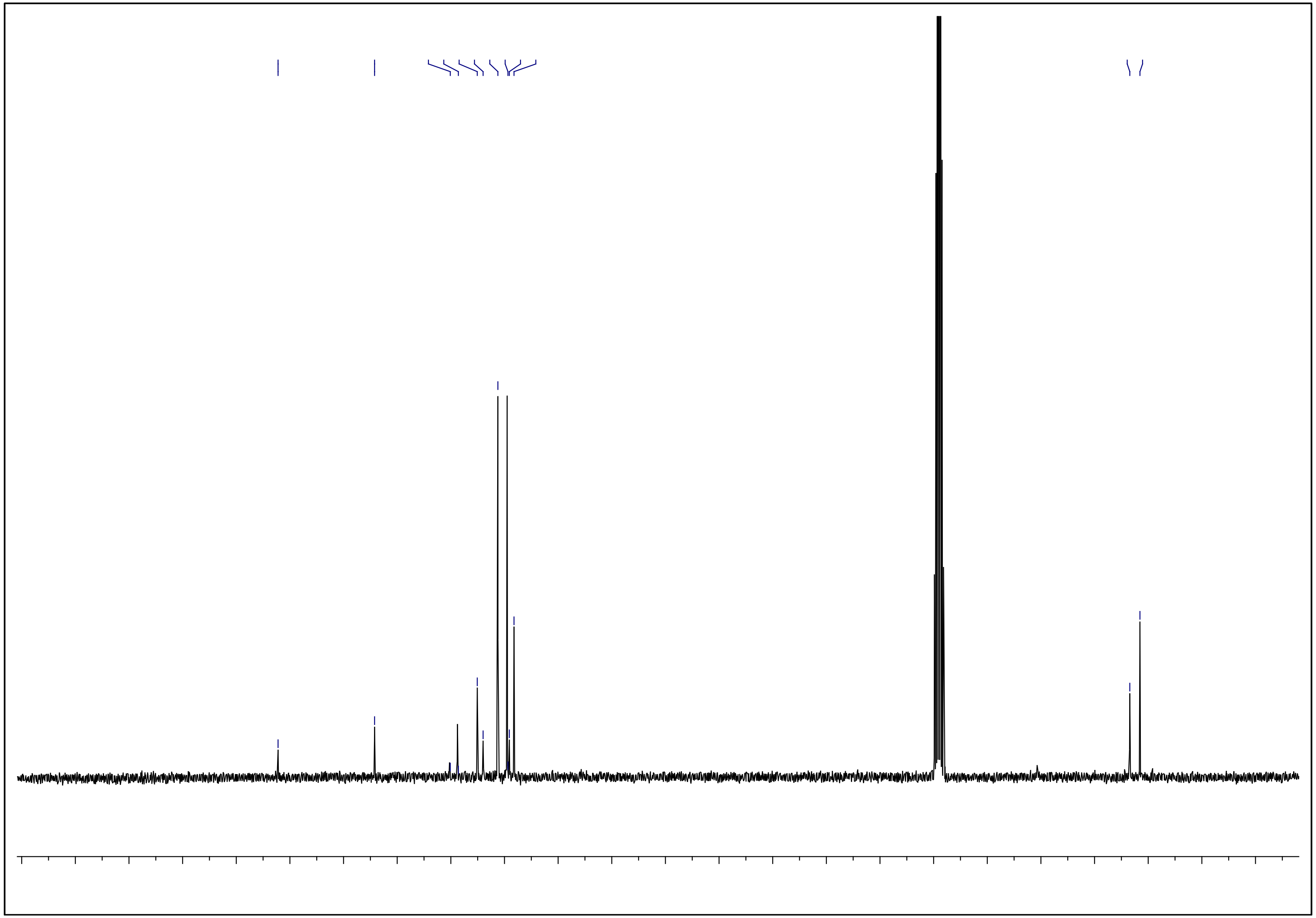

Figure S36: ^{13}C NMR (75 MHz, CD_3OD): **8**

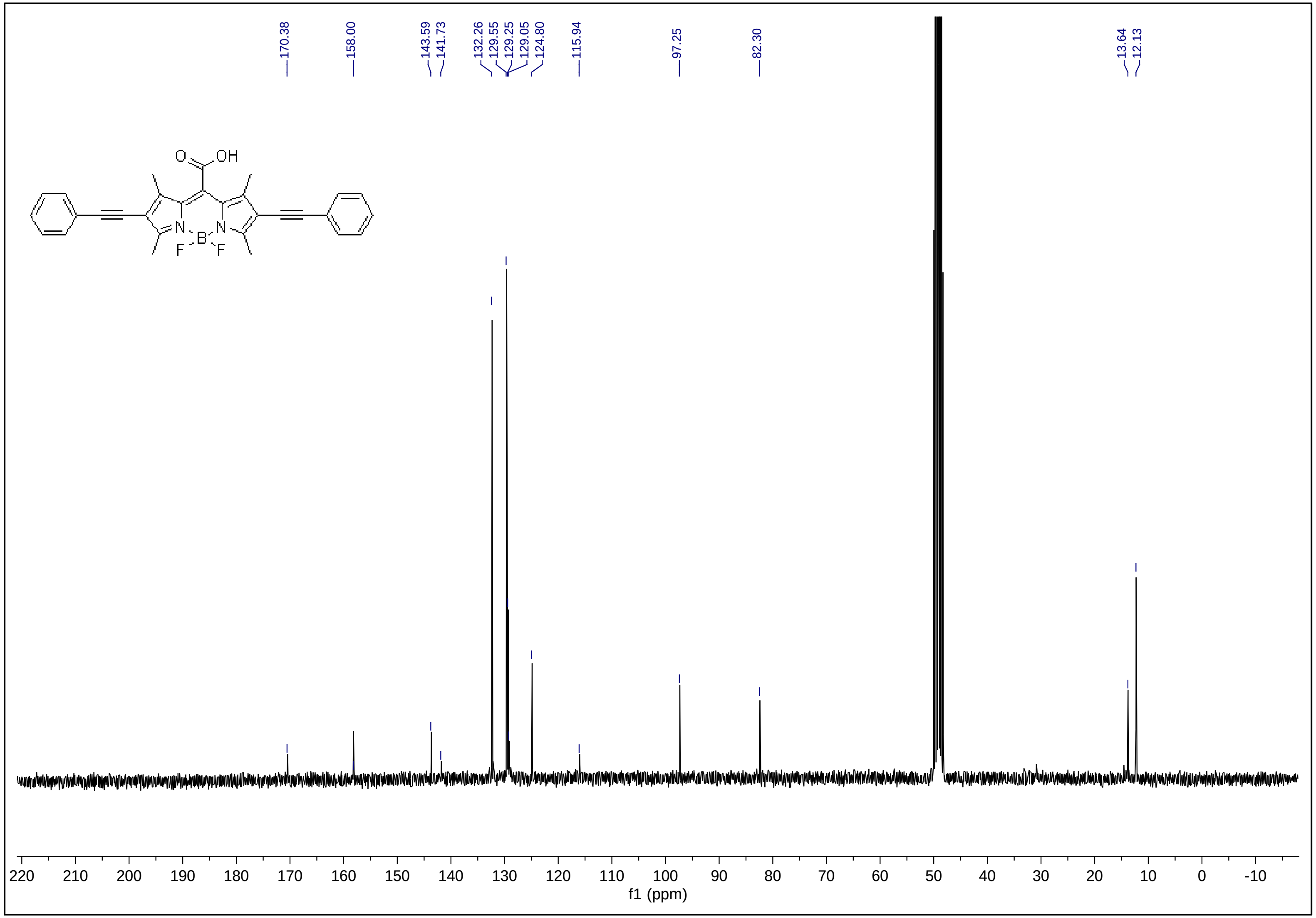

Figure S37: ^{13}C NMR (125 MHz, CD_3OD): **9**

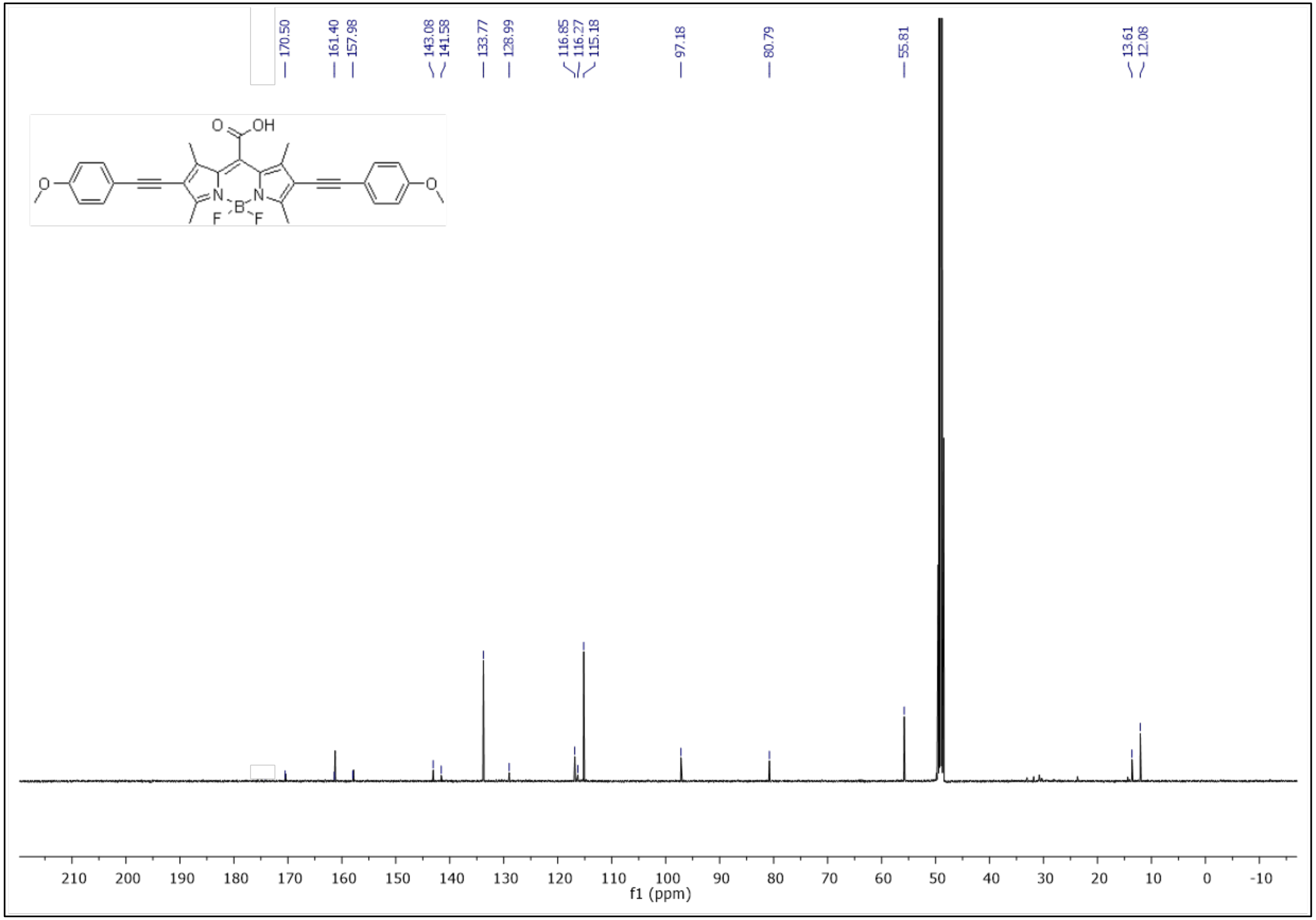

Figure S38: ^{13}C NMR (75 MHz, CD_3OD): **10**

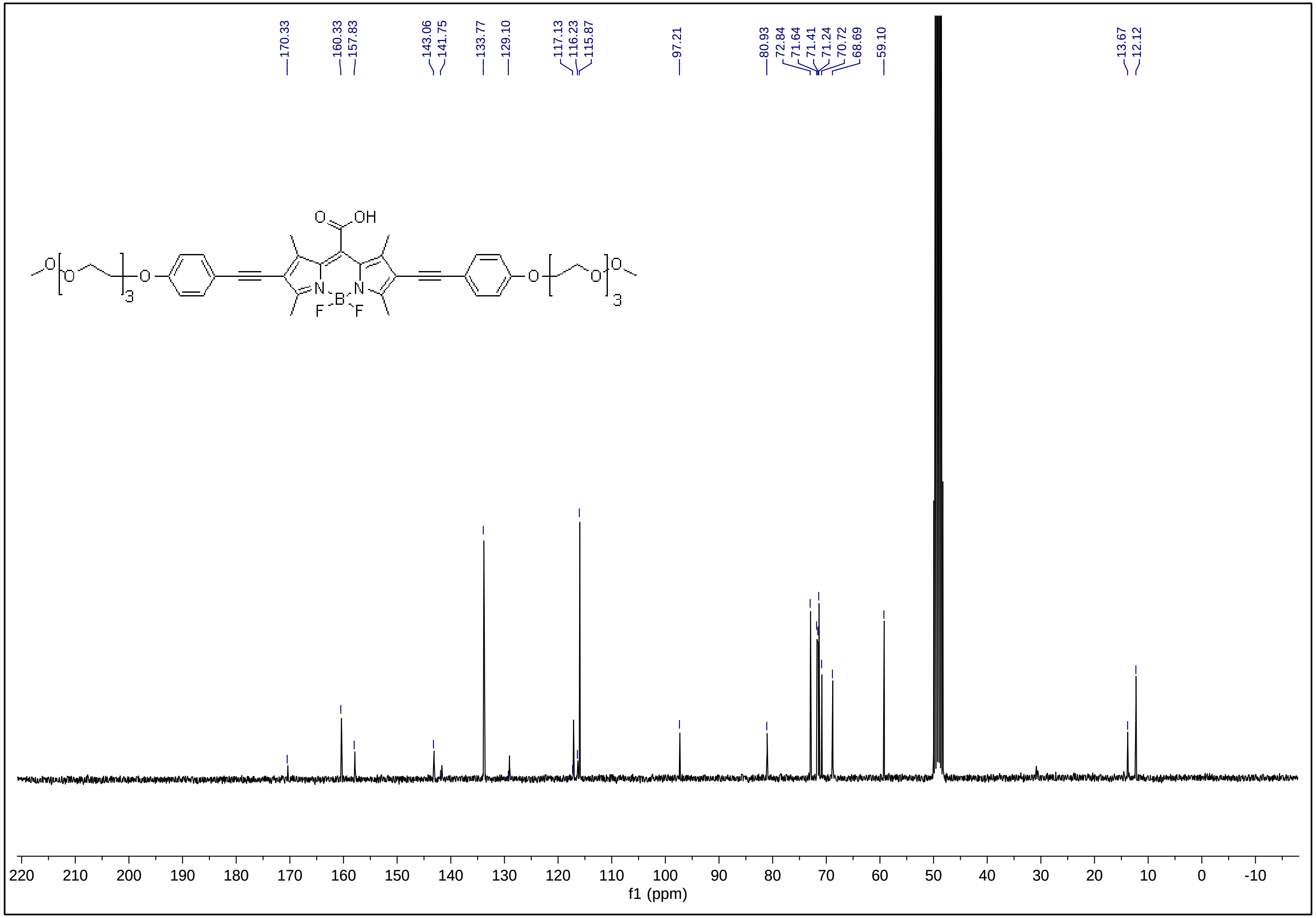

MS Spectra

Figure S39: HRMS (APCI+): **11**

APCI+ (MMI)
nitrogen flow 5 L/min, gas temperature 325°C, nebulizer 45 psi, skimmer 65 V, vaporizer 200°C, fragmentor 20 V, dissolved in CH_2Cl_2

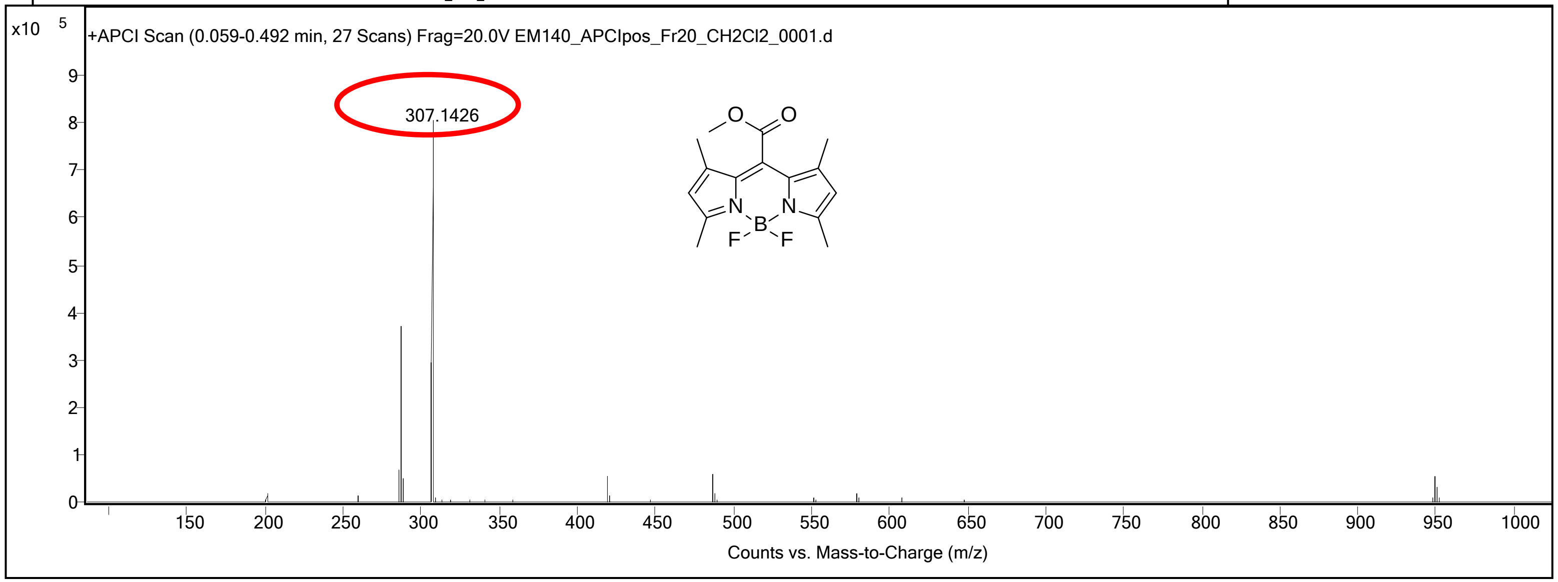

Figure S40: HRMS (APCI+): **12**

APCI - (MMI)
nitrogen flow 5 L/min, gas temperature 325°C, nebulizer 45 psig, skimmer -65 V, vaporizer 200°C, fragmentor -30 V, dissolved in methanol

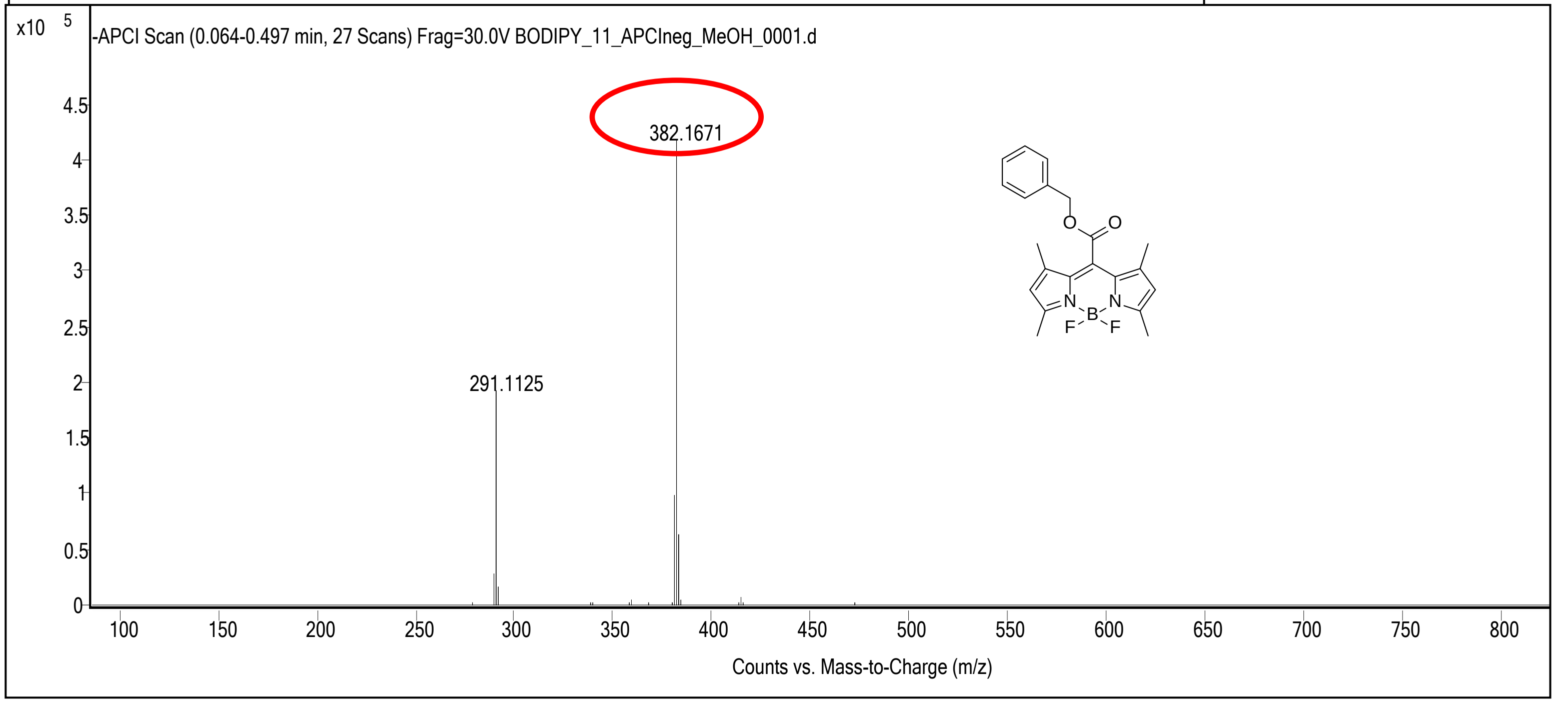

Figure S41: HRMS (APCI-): **13**

APCI - (MMI)
nitrogen flow 5 L/min, gas temperature 325°C, nebulizer 45 psig, skimmer -65 V, vaporizer 200°C, fragmentor -40 V, dissolved in chloroform

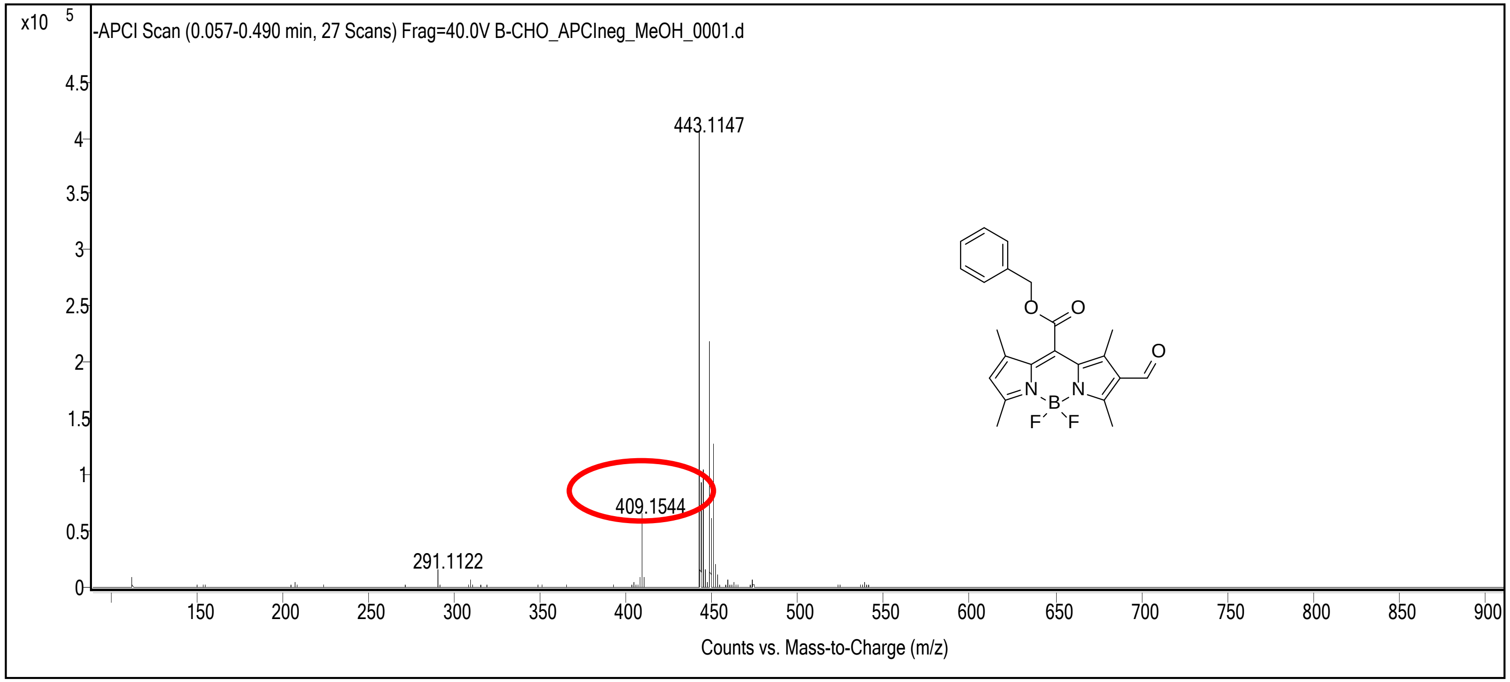

Figure S42: HRMS (APCI+): **14**

APCI - (MMI)
nitrogen flow 5 L/min, gas temperature 325°C, nebulizer 45 psig, skimmer -65 V, vaporizer 200°C, fragmentor -30 V, dissolved in methanol

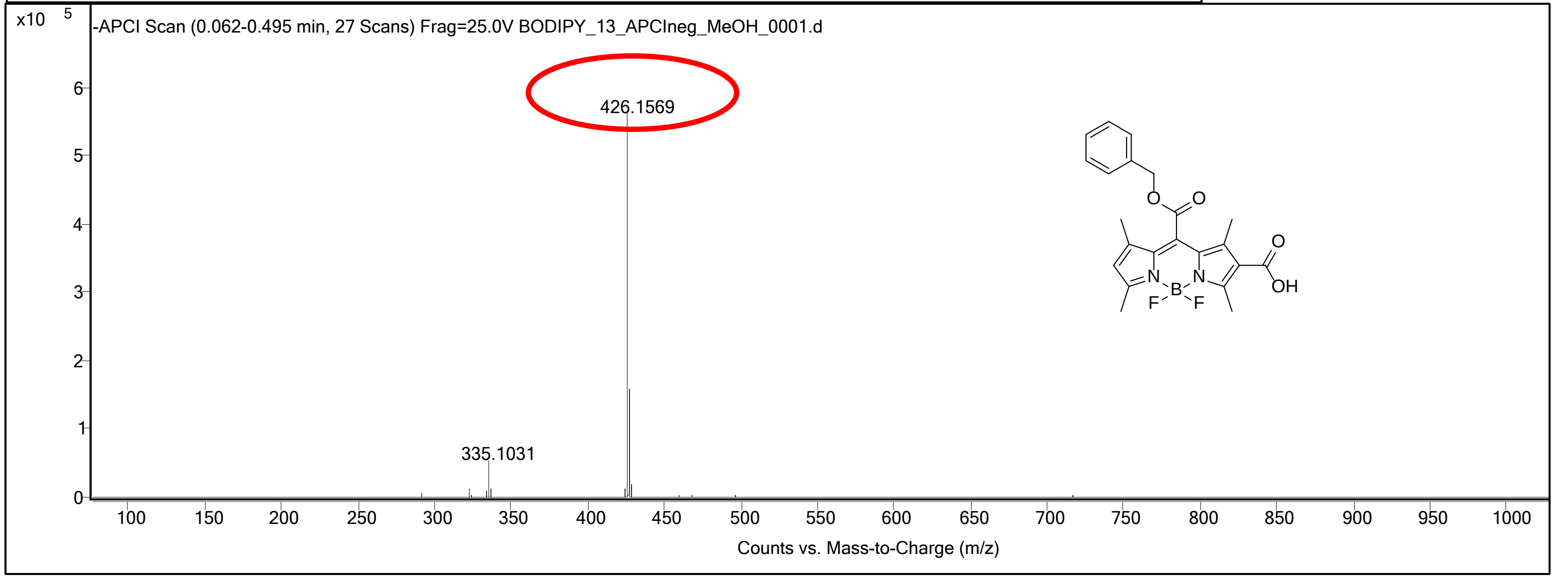

Figure S43: HRMS (APCI+): **17**

APCI+ (MMI)
nitrogen flow 5 L/min, gas temperature 325°C, nebulizer 45 psi, skimmer 65 V, vaporizer 200°C, fragmentor 25 V, dissolved in CH_2Cl_2

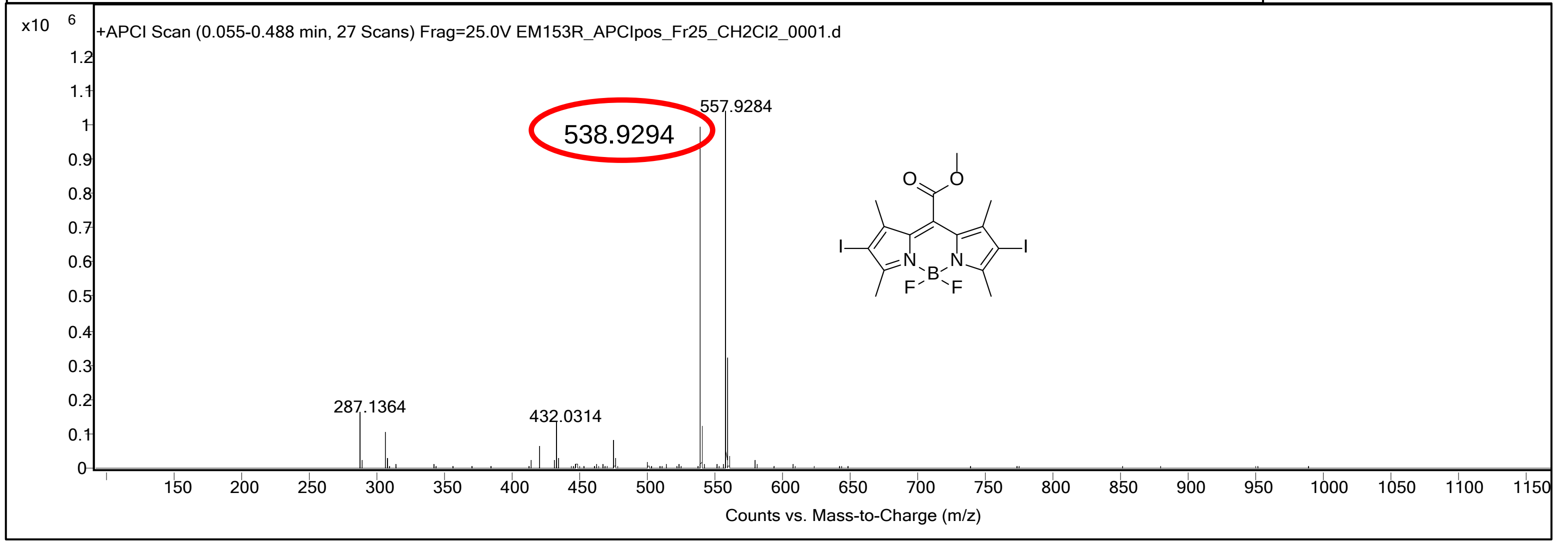

Figure S44: HRMS (APCI-): **18**

APCI - (MMI)
nitrogen flow 5 L/min, gas temperature 325°C, nebulizer 45 psig, skimmer -65 V, vaporizer 200°C, fragmentor -30 V, dissolved in DCM

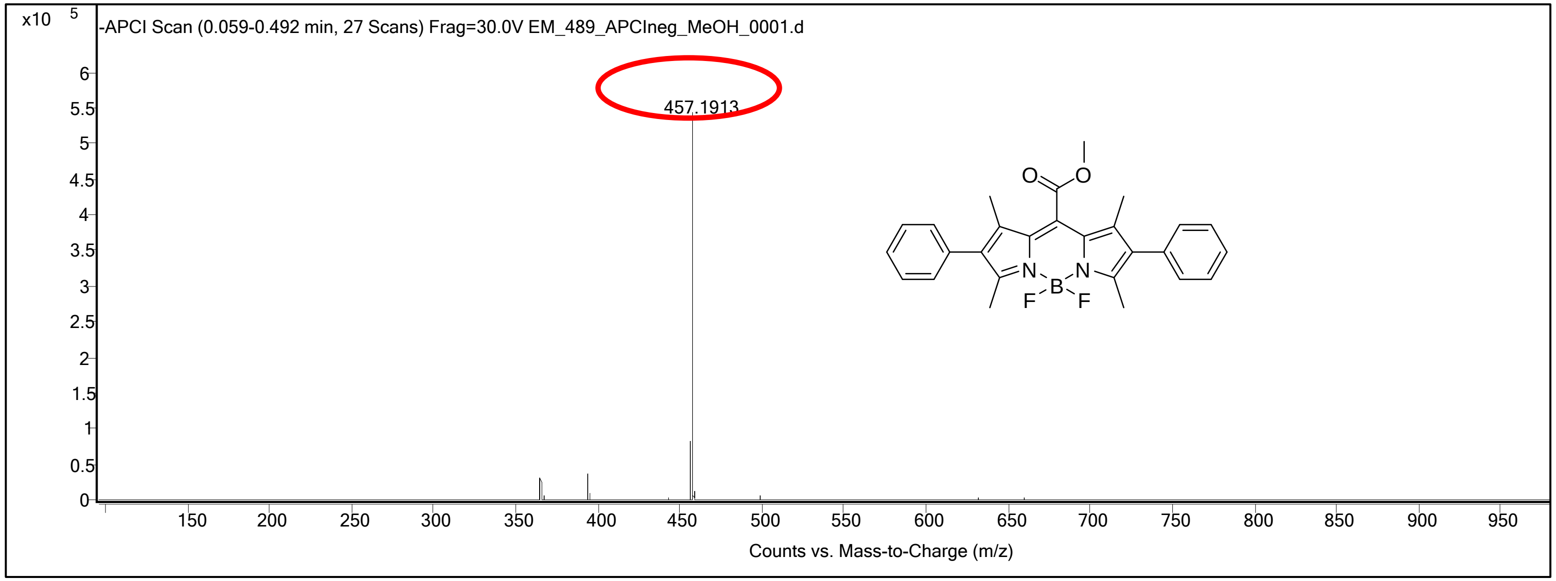

Figure S45: HRMS (APCI+): **19**

APCI + (MMI)
nitrogen flow 5 L/min, gas temperature 325°C, nebulizer 30 psi, skimmer 65 V, vaporizer 200°C, fragmentor 50 V, dissolved in $CHCl_3$

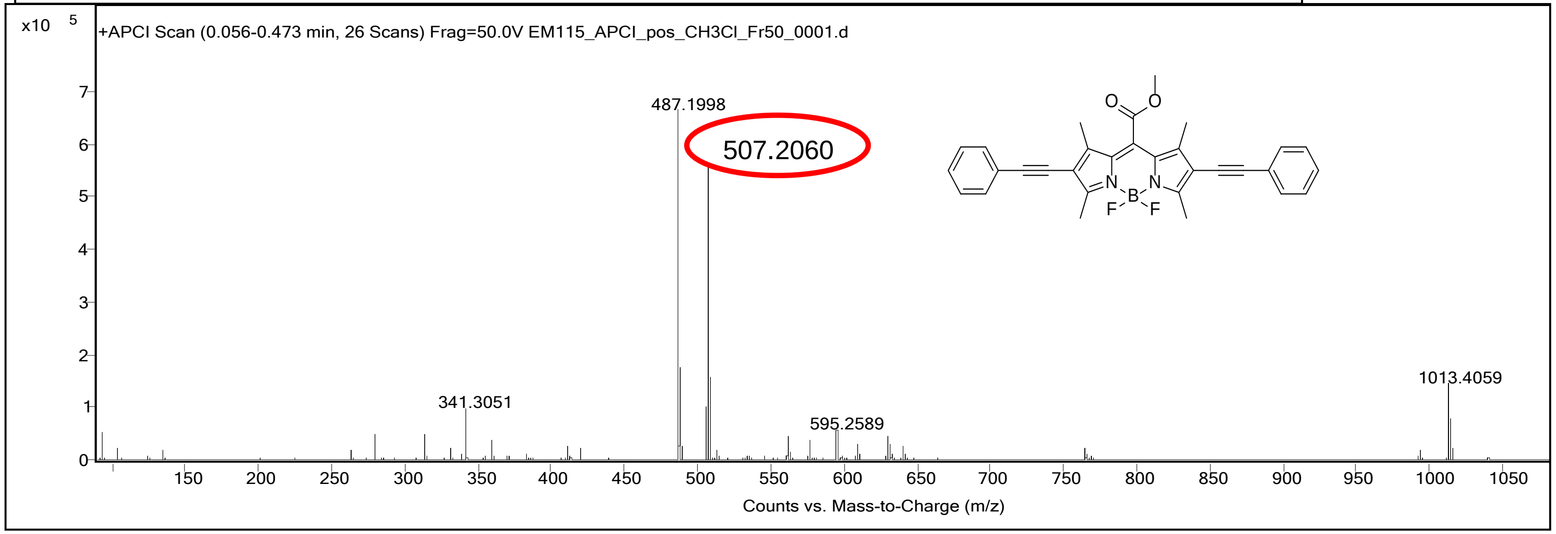

Figure S46: HRMS (APCI-): **20**

APCI - (MMI)
nitrogen flow 5 L/min, gas temperature 325°C, nebulizer 45 psig, skimmer -65 V, vaporizer 200°C, fragmentor -60 V, dissolved in DCM

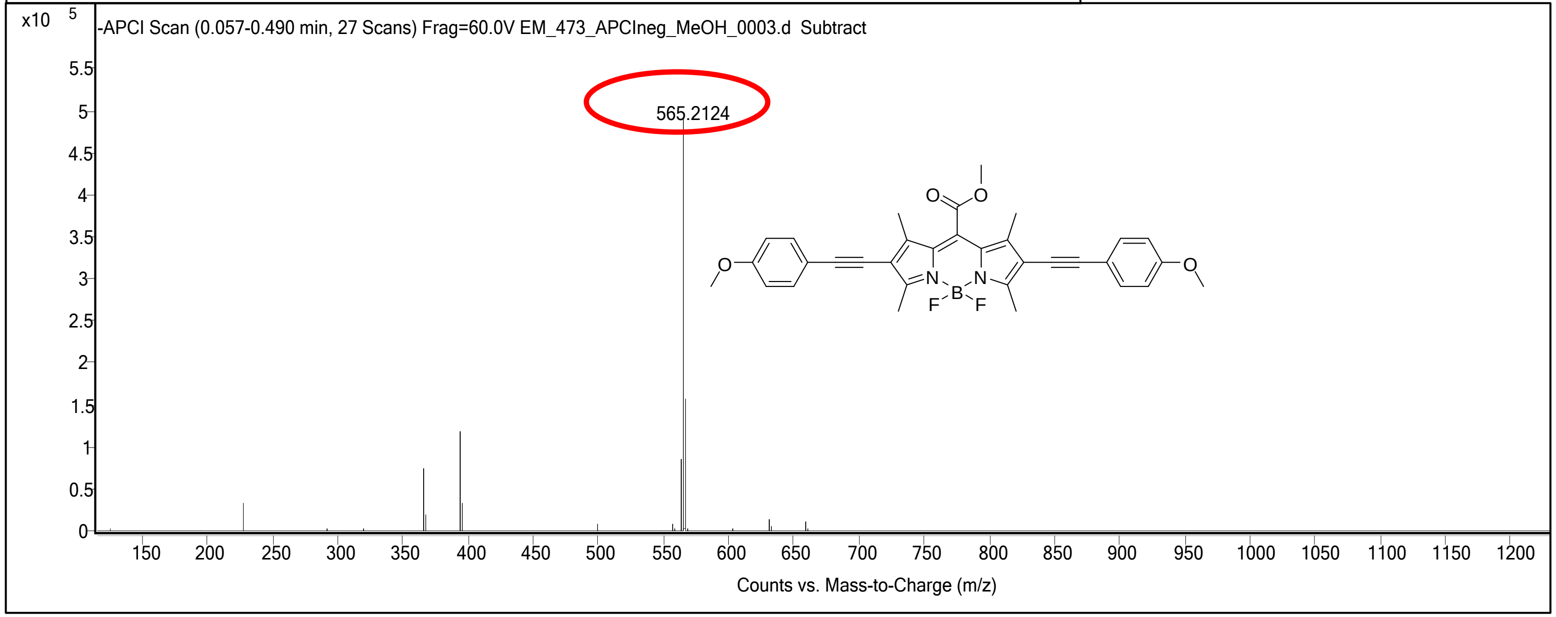

Figure S47: HRMS (APCI+): **21**

APCI+ (MMI)
nitrogen flow 5 L/min, gas temperature 325°C, nebulizer 45 psi, skimmer 65 V, vaporizer 200°C, fragmentor 30 V, dissolved in CH_2Cl_2

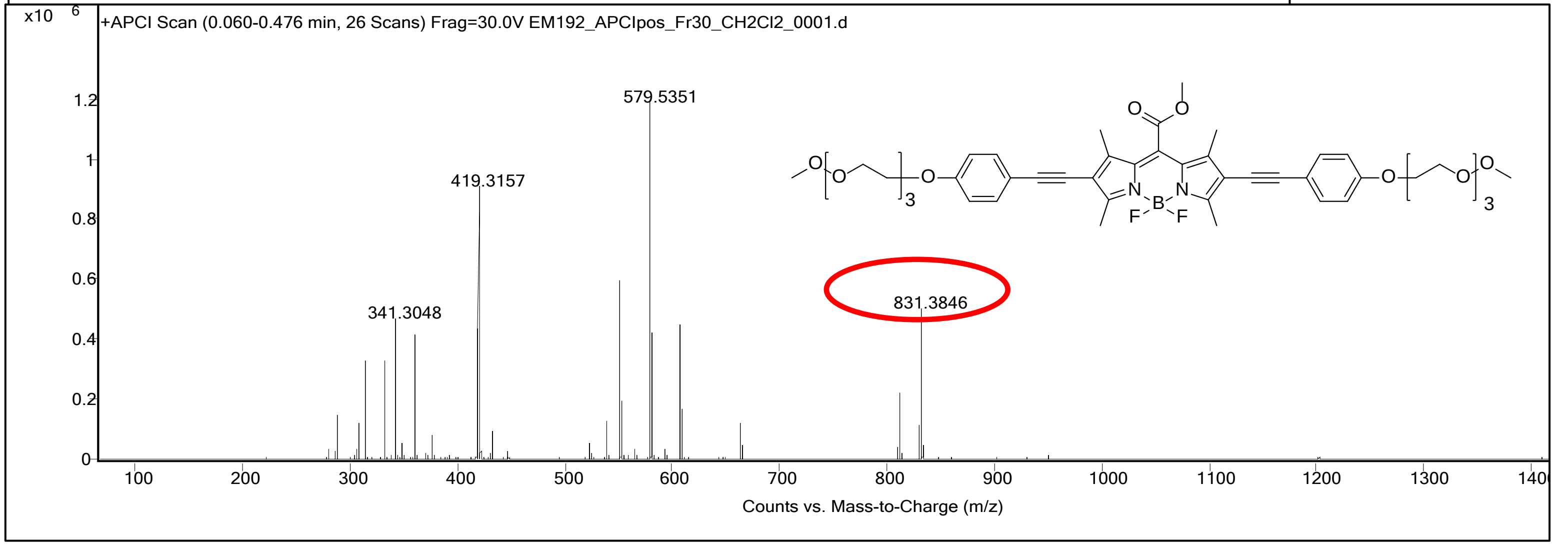

Figure S48: HRMS (ESI-): **2**

ESI- (MMI)
nitrogen flow 5 L/min, gas temperature 325°C, nebulizer 30 psi, skimmer 65 V, fragmentor 80 V, dissolved in methanol

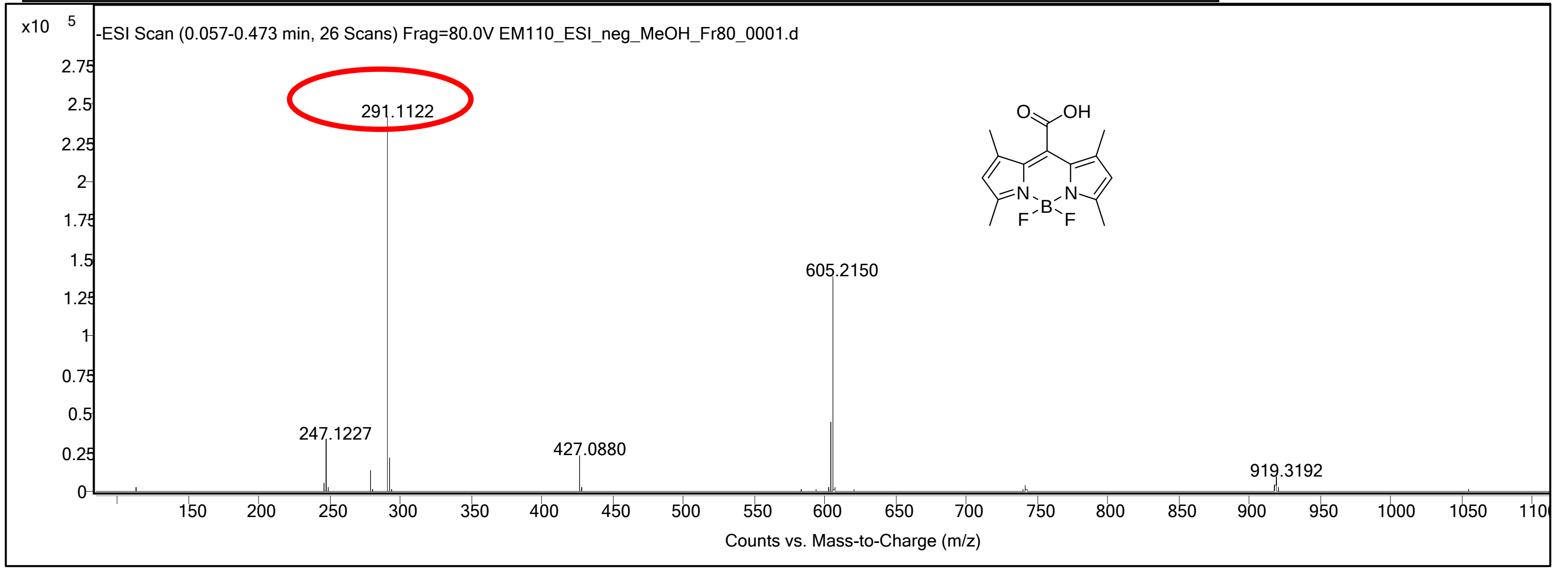

Figure S49: HRMS (ESI-): **3**

ESI - (MMI)
nitrogen flow 5 L/min, gas temperature 325°C, nebulizer 45 psig, skimmer -65 V, Vcap 2200 V, fragmentor -100 V, dissolved in methanol

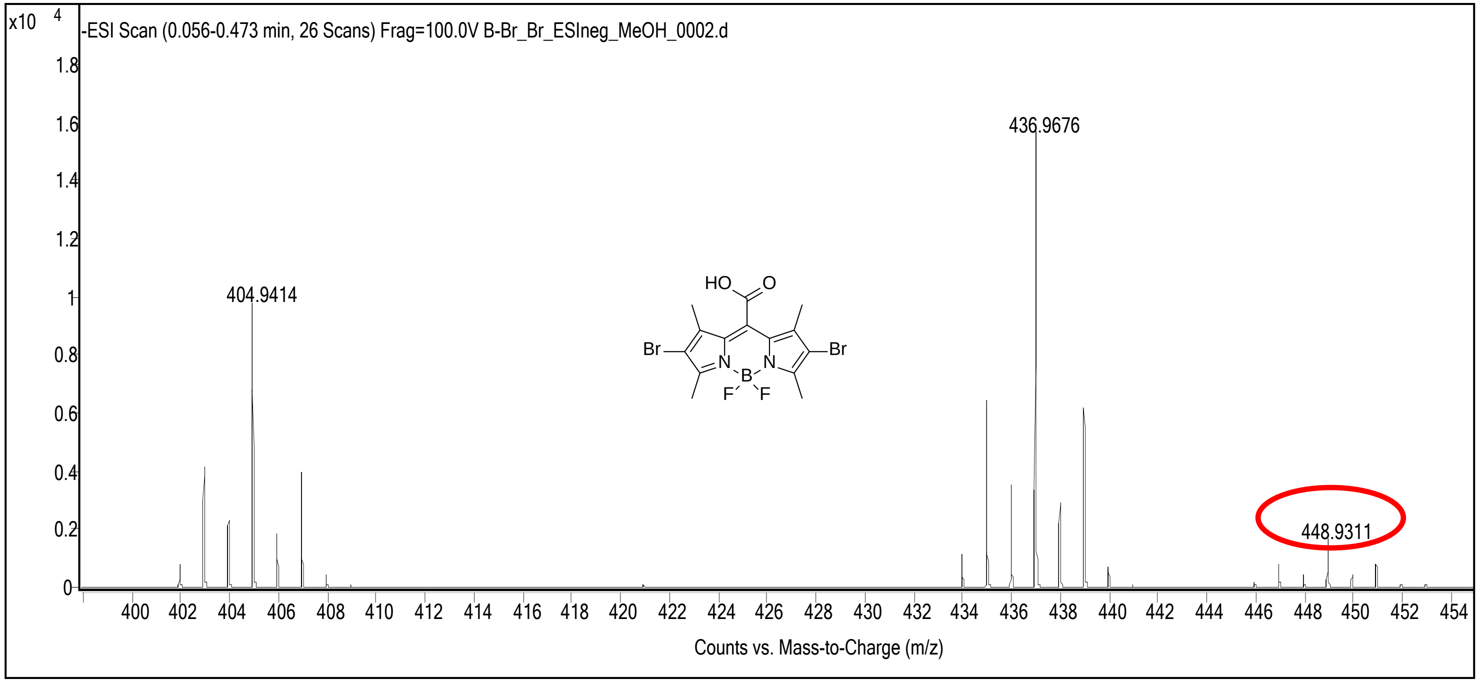

Figure S50: HRMS (APCI-): **4**

APCI - (MMI)
nitrogen flow 5 L/min, gas temperature 325°C, nebulizer 45 psig, skimmer -65 V, vaporizer 200°C, fragmentor -25 V, dissolved in methanol

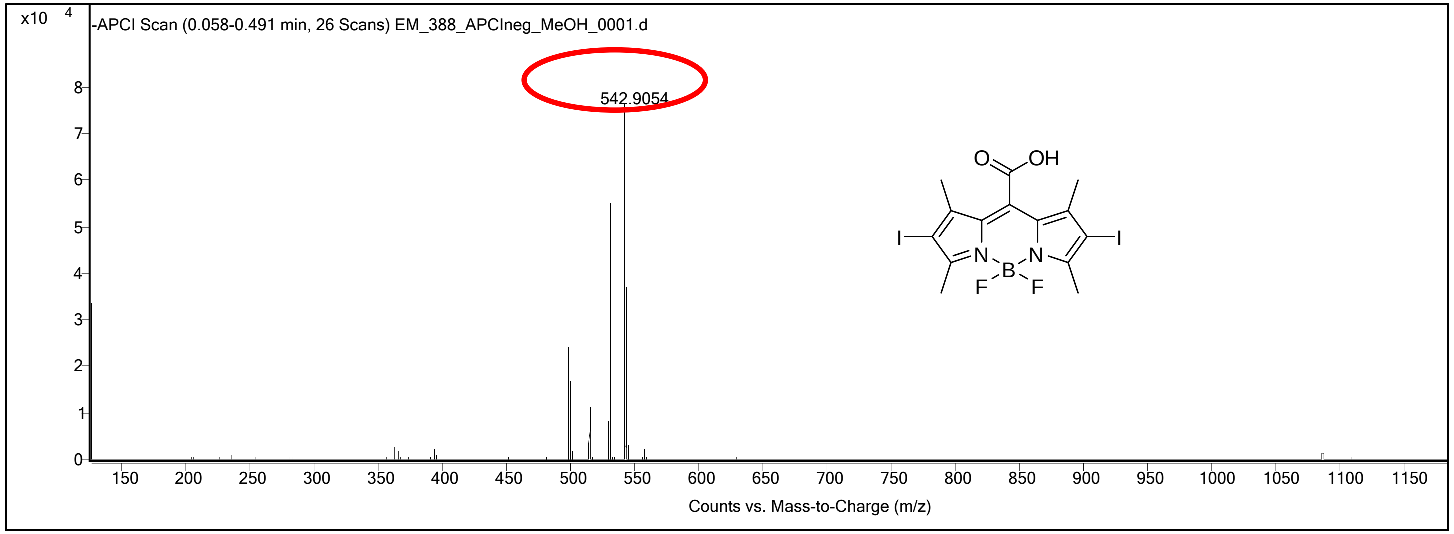

Figure S51: HRMS (ESI-): **5**

ESI - (MMI)
nitrogen flow 5 L/min, gas temperature 325°C, nebulizer 45 psig, skimmer -65 V, Vcap 2200 V, fragmentor -110 V, dissolved in methanol

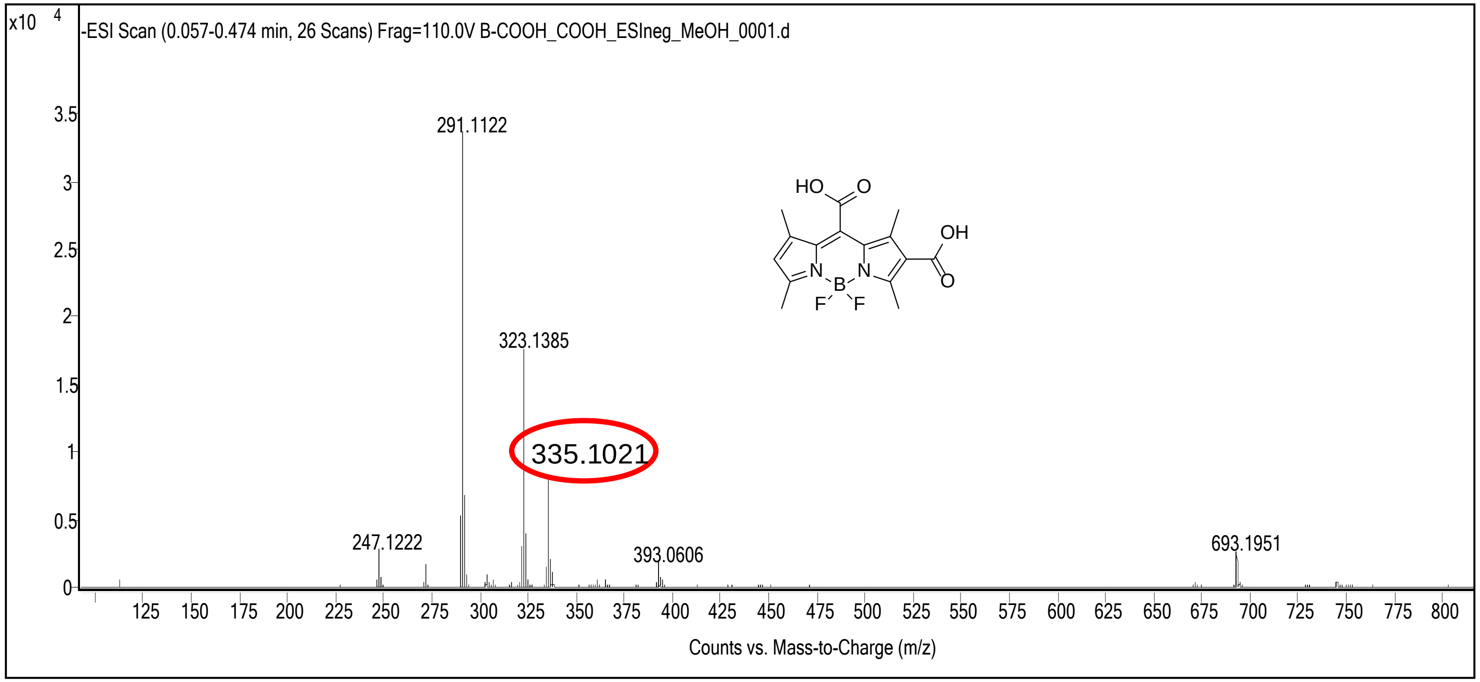

Figure S52: HRMS (ESI-): **6**

ESI - (MMI)
nitrogen flow 5 L/min, gas temperature 325°C, nebulizer 45 psig, skimmer -65 V, Vcap 2200 V, fragmentor -80 V, dissolved in methanol

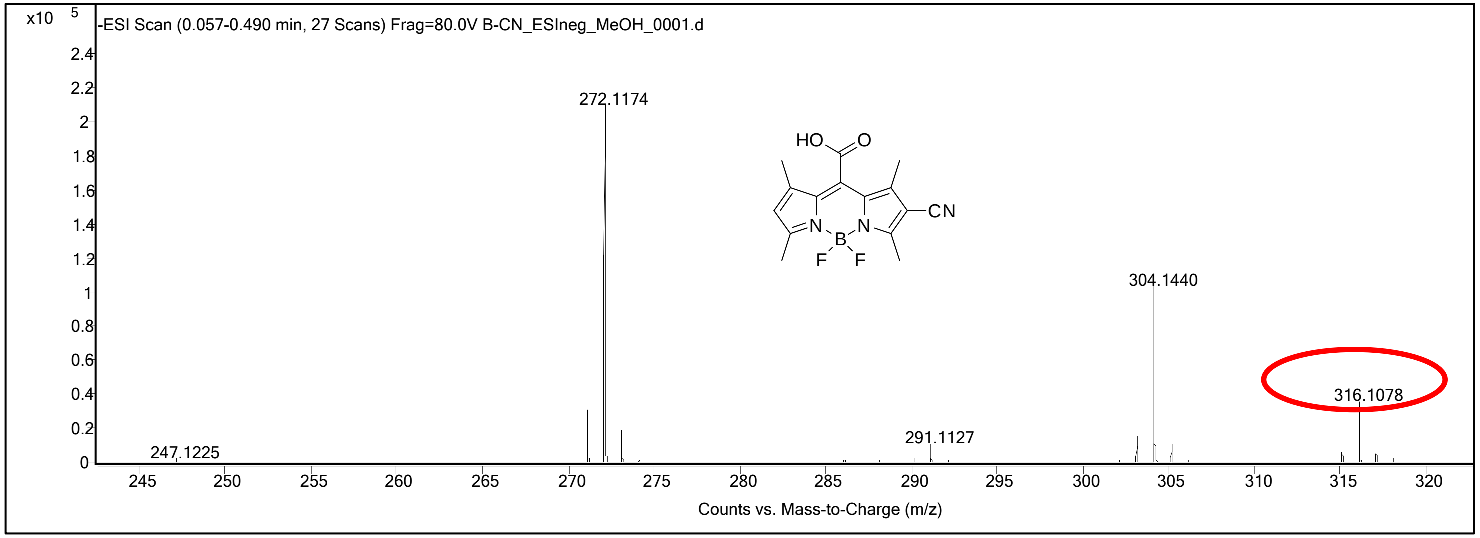

Figure S53: HRMS (ESI-): **7**

ESI- (MMI)
nitrogen flow 5 L/min, gas temperature 325°C, nebulizer 30 psi, skimmer 65 V, fragmentor 70 V, dissolved in methanol

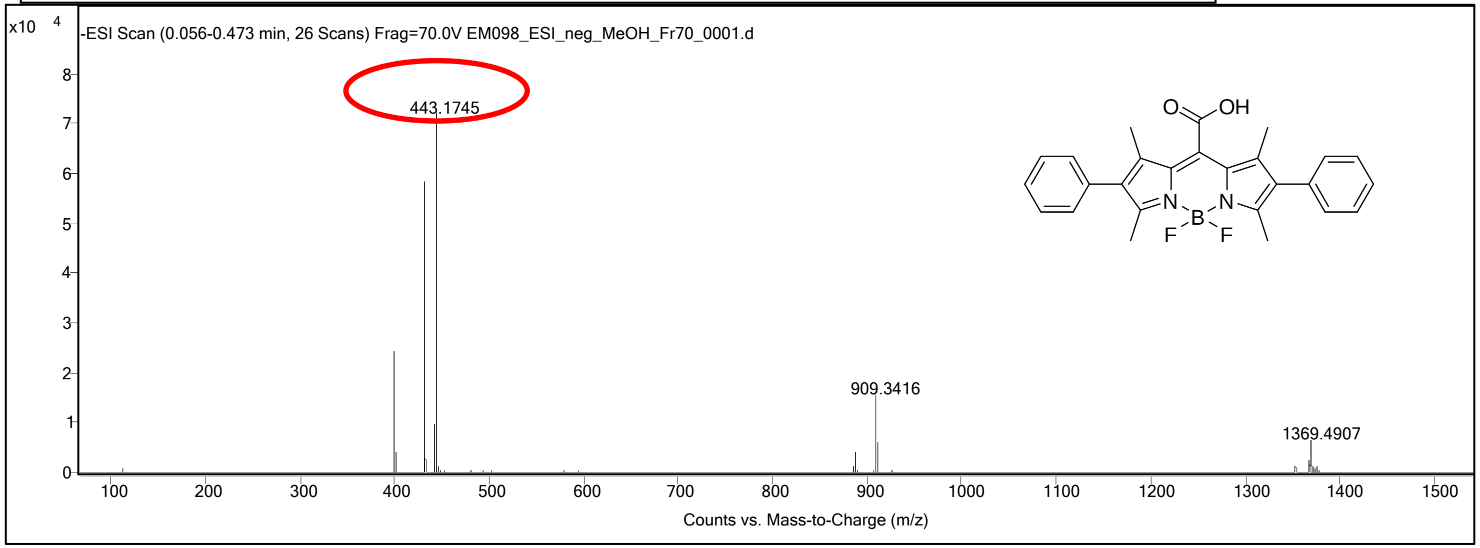

Figure S54: HRMS (ESI-): **8**

ESI- (MMI)
nitrogen flow 5 L/min, gas temperature 325°C, nebulizer 30 psi, skimmer 65 V, fragmentor 60 V, dissolved in methanol

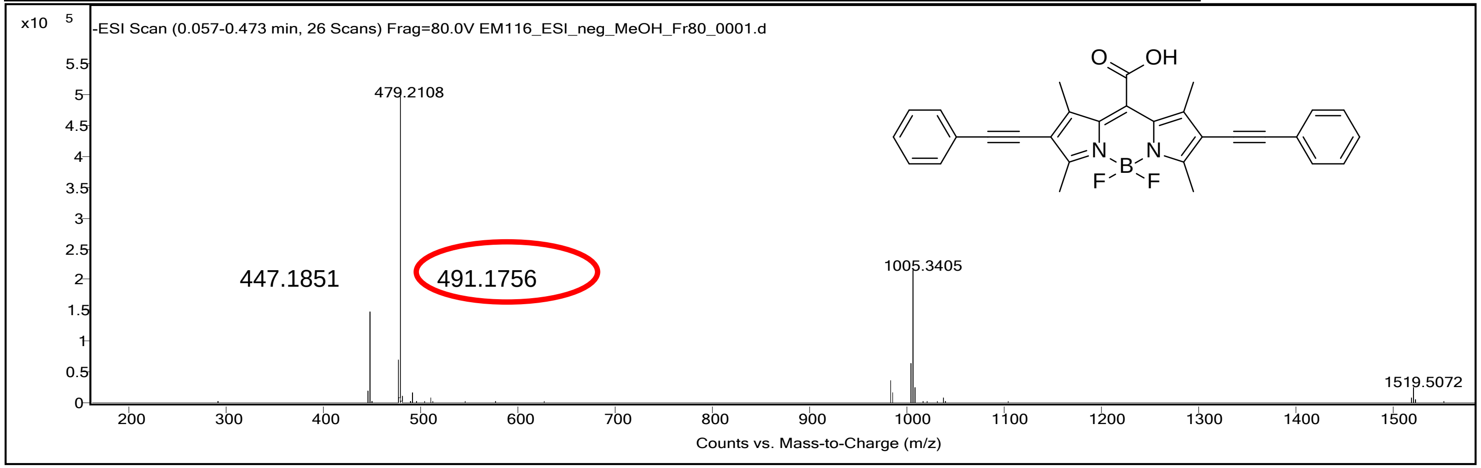

Figure S55: HRMS (ESI-): **9**

ESI- (MMI)
nitrogen flow 5 L/min, gas temperature 325°C, nebulizer 45 psi, skimmer 65 V, fragmentor 100 V, dissolved in MeOH/H_2O 1:1

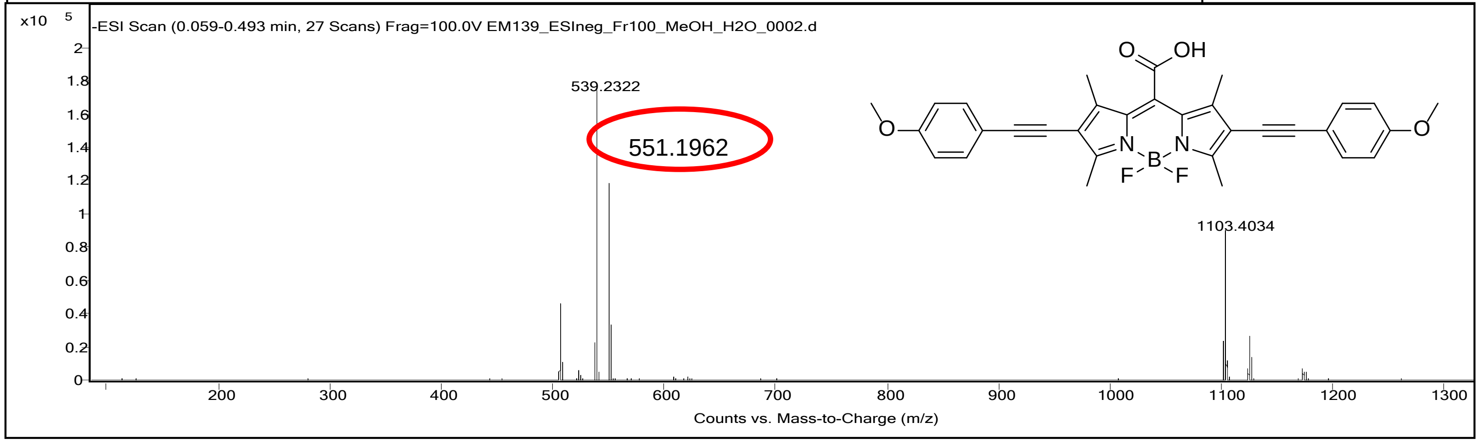

Figure S56: HRMS (ESI-): **10**

ESI- (MMI)
nitrogen flow 5 L/min, gas temperature 325°C, nebulizer 45 psi, skimmer 65 V, fragmentor 120 V, dissolved in MeOH/H_2O 1:1

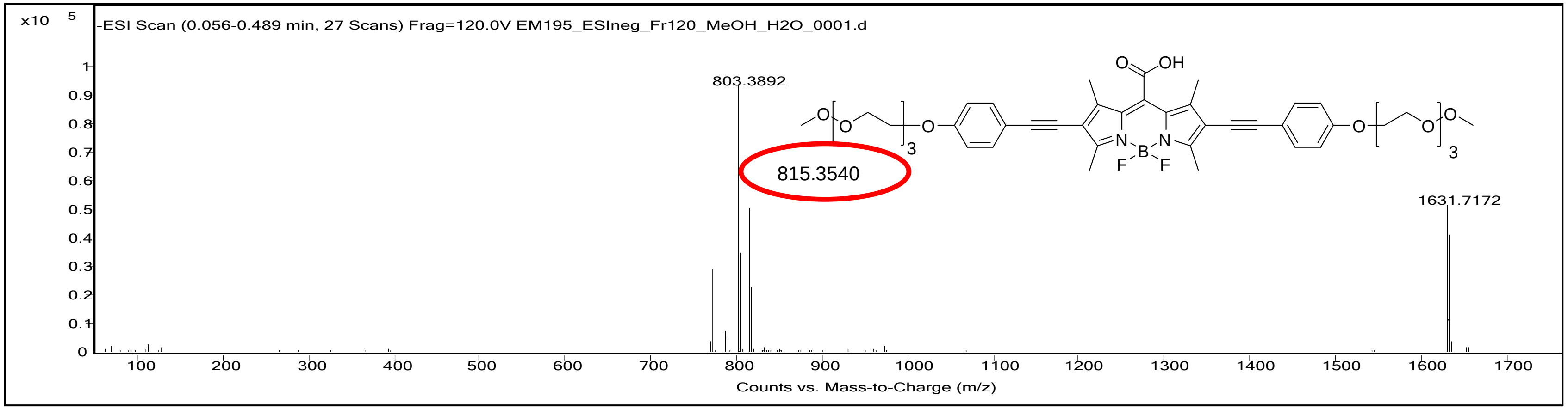

Absorption and Emission Spectra

Figure S57: Normalized absorption (solid line) and normalized emission spectra (dashed line, λ_{exc} = 450 nm) of **2** (c ≈ 10^{-6} M in MeOH).

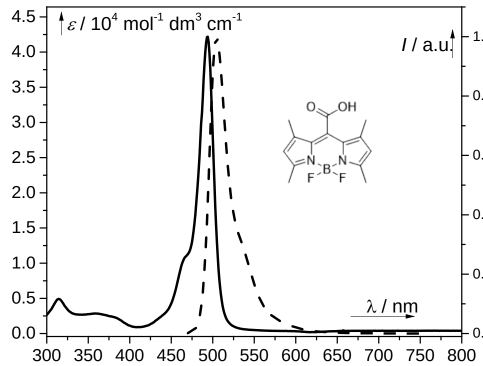

Figure S58: Normalized absorption (solid line) and normalized emission spectra (dashed line, λ_{exc} = 485 nm) of **3** (c ≈ 10^{-6} M in MeOH).

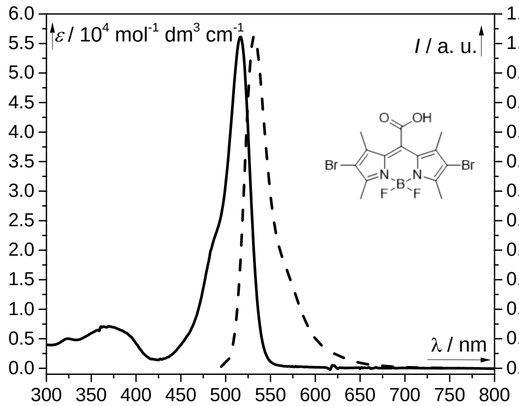

Figure S59: Normalized absorption (solid line) and normalized emission spectra (dashed line, λ_{exc} = 490 nm) of **3** (c ≈ 10^{-6} M in a PBS /DMSO mixture).

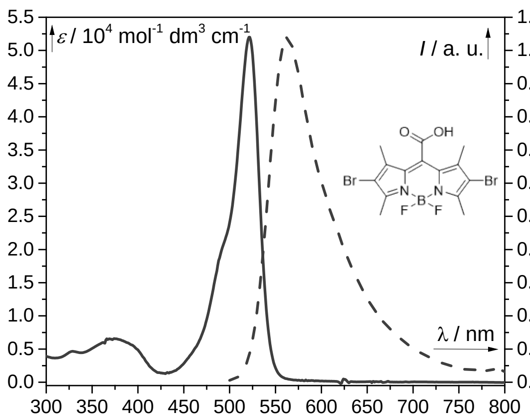

Figure S60: Normalized absorption (solid line) and normalized emission spectra (dashed line, λ_{exc} = 490 nm) of **4** (c ≈ 10^{-6} M in MeOH).

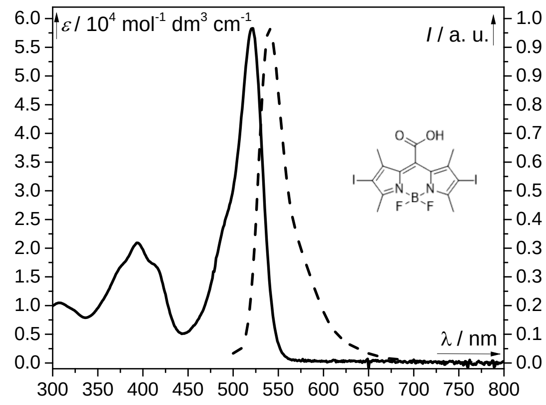

Figure S61: Normalized absorption (solid line) and normalized emission spectra (dashed line, λ_{exc} = 510 nm) of **4** (c ≈ 10^{-6} M in a PBS /DMSO mixture).

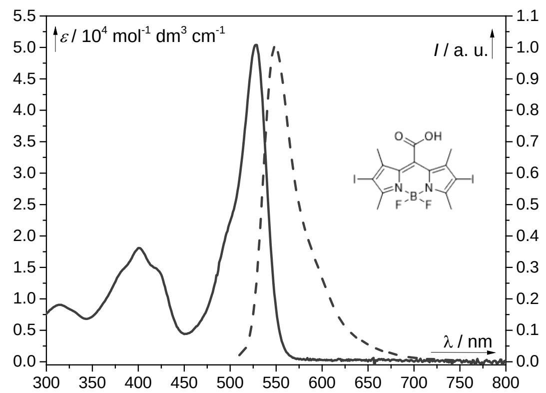

Figure S62: Normalized absorption (solid line) and normalized emission spectra (dashed line, λ_{exc} = 490 nm) of **5** (c ≈ 10^{-6} M in MeOH).

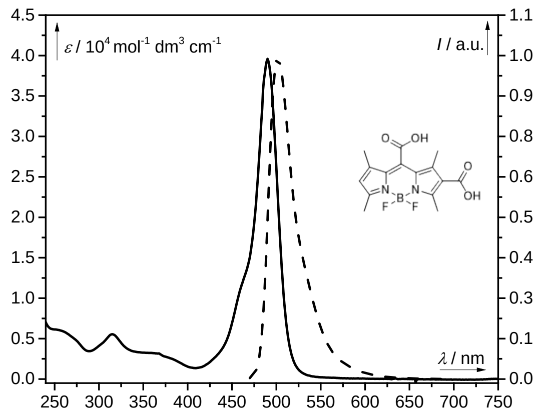

Figure S63: Normalized absorption (solid line) and normalized emission spectra (dashed line, λ_{exc} = 480 nm) of **5** (c ≈ 10^{-6} M in a PBS/DMSO mixture).

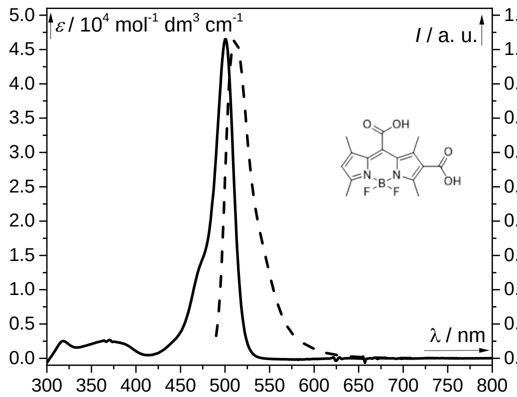

Figure S64: Normalized absorption (solid line) and normalized emission spectra (dashed line, λ_{exc} = 450 nm) of **6** (c ≈ 10^{-6} M in MeOH).

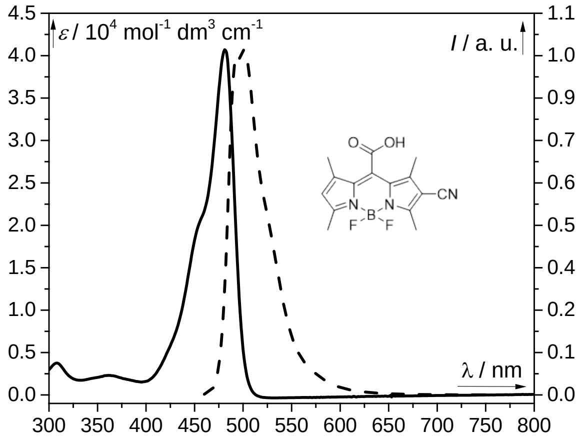

Figure S65: Normalized absorption (solid line) and normalized emission spectra (dashed line, λ_{exc} = 450 nm) of **6** (c ≈ 10^{-6} M in a PBS/DMSO mixture).

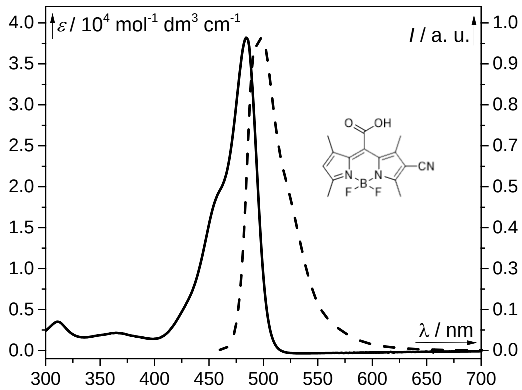

Figure S66: Normalized absorption (solid line) and normalized emission spectra (dashed line, λ_{exc} = 490 nm) of **7** (c ≈ 10^{-6} M in MeOH).

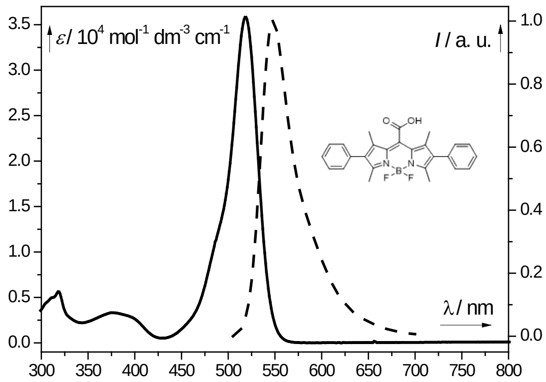

Figure S67: Normalized absorption (solid line) and normalized emission spectra (dashed line, λ_{exc} = 480 nm) of **7** (c ≈ 10^{-6} M in a PBS/DMSO mixture).

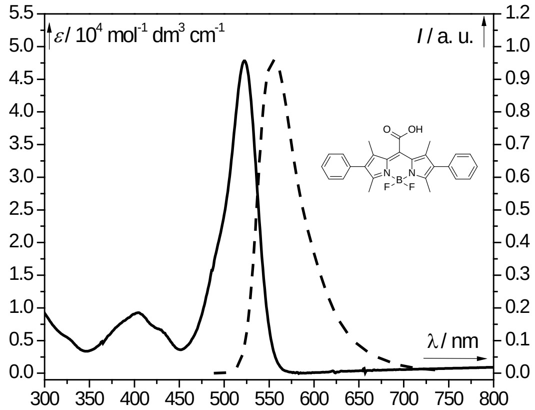

Figure S68: Normalized absorption (solid line) and normalized emission spectra (dashed line, λ_{exc} = 510 nm) of **8** (c ≈ 10^{-6} M in MeOH).

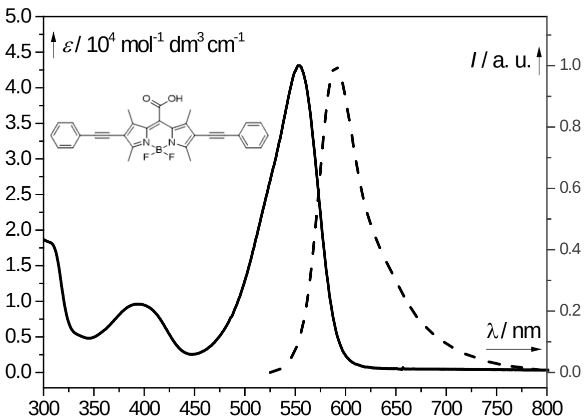

Figure S69: Normalized absorption (solid line) and normalized emission spectra (dashed line, λ_{exc} = 520 nm) of **8** (c ≈ 10^{-6} M in a PBS/DMSO mixture (80:20, v/v).

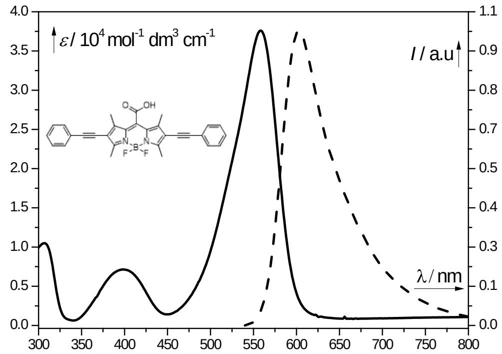

Figure S70: Normalized absorption (solid line) and normalized emission spectra (dashed line, λ_{exc} = 510 nm) of **9** (c ≈ 10^{-6} M in MeOH).

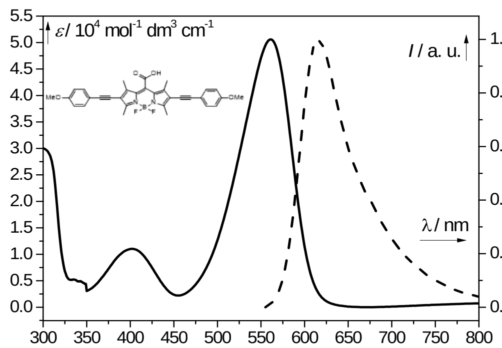

Figure S71: Normalized absorption (solid line) and normalized emission spectra (dashed line, λ_{exc} = 540 nm) of **9** (c ≈ 10^{-6} M in a PBS/DMSO mixture (80:20, v/v).

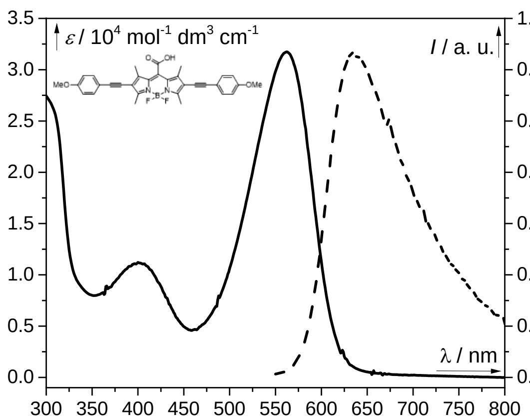

Figure S72: Normalized absorption (solid line) and normalized emission spectra (dashed line, λ_{exc} = 530 nm) of **10** (c ≈ 10^{-6} M in MeOH).

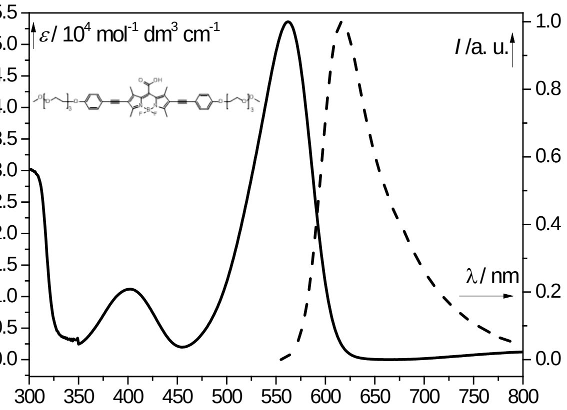

Figure S73: Normalized absorption (solid line) and normalized emission spectra (dashed line, λ_{exc} = 530 nm) of **10** (c ≈ 10^{-6} M in a PBS/DMSO mixture (80:20, v/v).

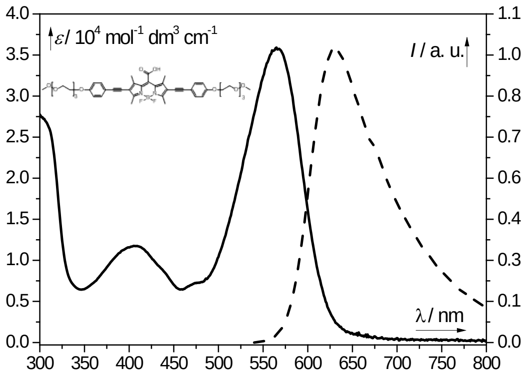

Stability in the Dark

Figure S74: Stability of **22** in aerated phosphate buffer solution (pH = 7.4) for 48 h in the dark (red line: the initial spectrum; blue line: the end spectrum).

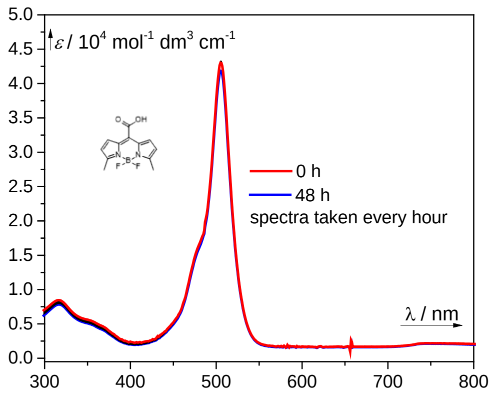

Figure S75: Stability of **2** in aerated PBS/DMSO mixture (99:1) for 48 h in the dark (red line: the initial spectrum; blue line: the end spectrum).

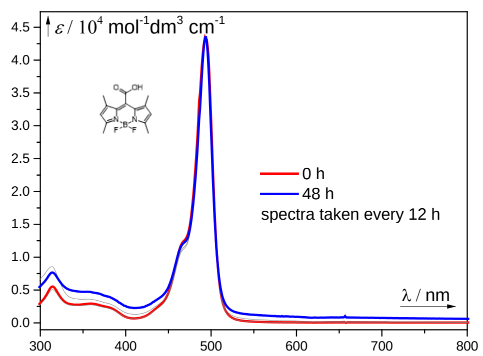

Figure S76: Stability of **8** in aerated PBS/DMSO mixture (90:10) for 48 h in the dark (red line: the initial spectrum; blue line: the end spectrum).

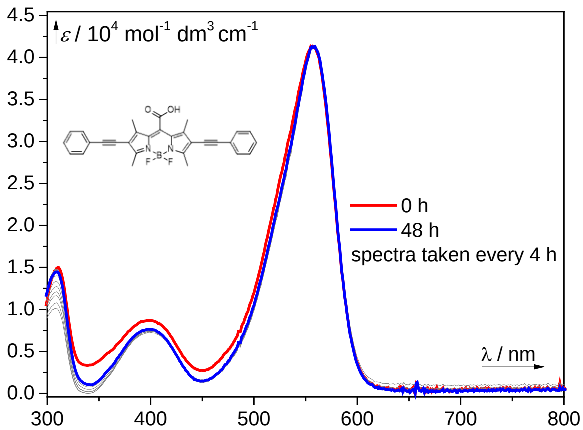

Photochemical Experiments

Figure S77. Irradiation of **2** in a non-degassed PBS/DMSO mixture (99:1, v/v) at λ_{max} = 490 nm for 3 h (red line: the initial spectrum; blue line: the end spectrum).

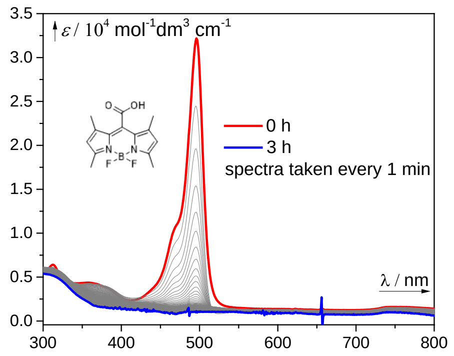

Figure S78. Irradiation of **2** in a degassed PBS/DMSO mixture (99:1, v/v) at λ_{max} = 490 nm for 4 h (red line: the initial spectrum; blue line: the end spectrum).

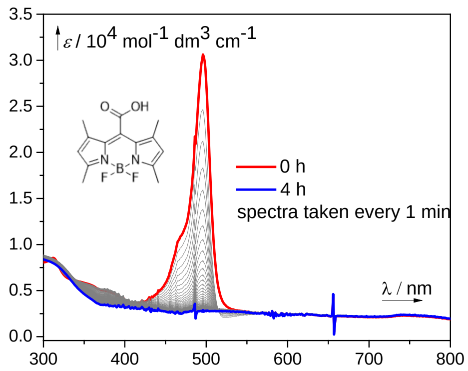

Figure S79. Irradiation of **3** in a non-degassed PBS/DMSO mixture (90:10, v/v) at λ_{max} = 525 nm for 5 minutes (red line: the initial spectrum; blue line: the end spectrum).

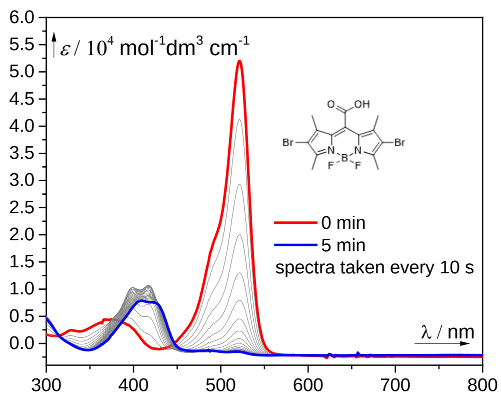

Figure S80. Irradiation of **3** in a degassed PBS/DMSO mixture (90:10, v/v) at λ_{max} = 525 nm for 2 h (red line: the initial spectrum; blue line: the end spectrum).

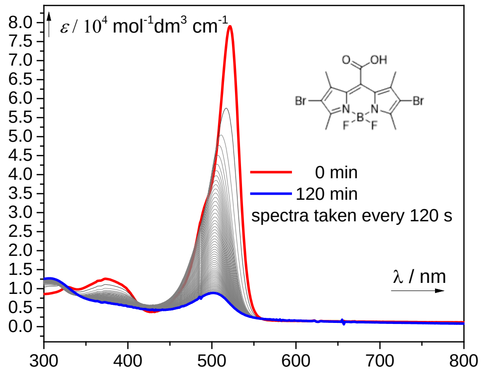

Figure S81. Irradiation of **4** in a non-degassed PBS/DMSO mixture (90:10, v/v) at λ_{max} = 525 nm for 5 min (red line: the initial spectrum; blue line: the end spectrum).

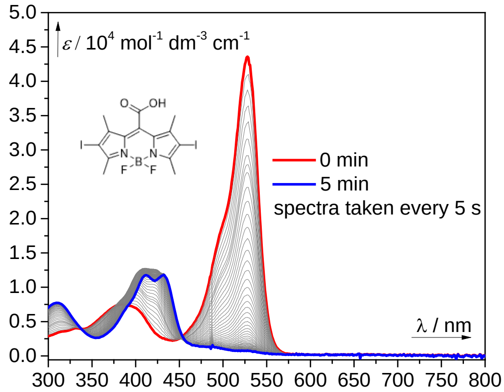

Figure S82. Irradiation of **4** in a degassed PBS/DMSO mixture (90:10, v/v) at λ_{max} = 525 nm for 1 h (red line: the initial spectrum; blue line: the end spectrum).

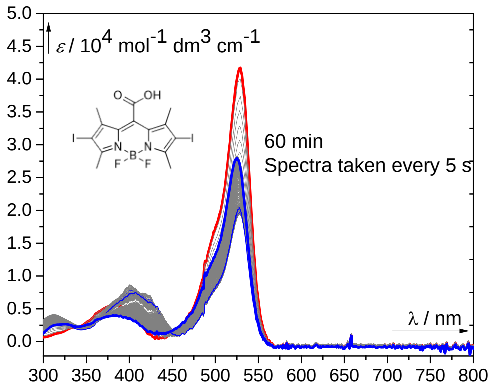

Figure S83. Irradiation of **5** in a non-degassed PBS/DMSO mixture (90:10, v/v) at λ_{max} = 490 nm for 12 h (red line: the initial spectrum; blue line: the end spectrum).

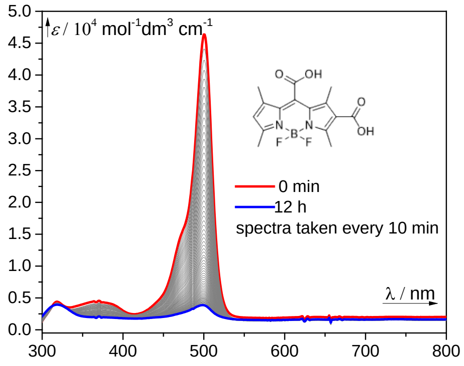

Figure S84. Irradiation of **5** in a degassed PBS/DMSO mixture (90:10, v/v) at λ_{max} = 490 nm for 12 h (red line: the initial spectrum; blue line: the end spectrum).

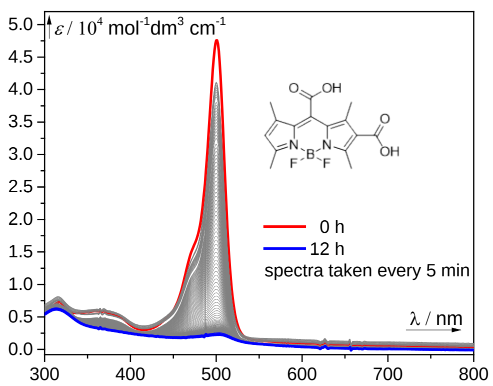

Figure S85. Irradiation of **6** in a non-degassed PBS/DMSO mixture (90:10, v/v) at λ_{max} = 490 nm for 12 h (red line: the initial spectrum; blue line: the end spectrum).

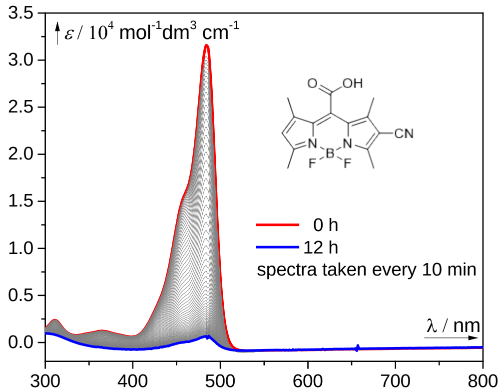

Figure S86. Irradiation of **6** in a degassed PBS/DMSO mixture (90:10, v/v) at λ_{max} = 490 nm for 12 h (red line: the initial spectrum; blue line: the end spectrum).

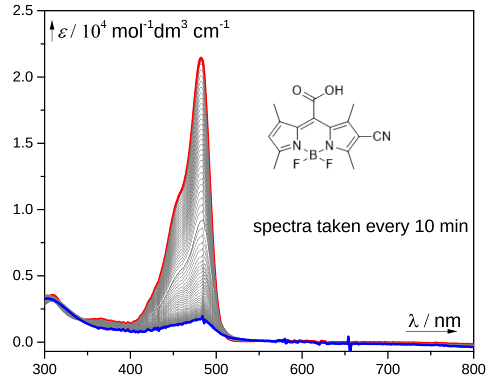

Figure S87. Irradiation of **7** in a non-degassed PBS/DMSO mixture (90:10, v/v) at λ_{max} = 525 nm for 30 min (red line: the initial spectrum; blue line: the end spectrum).

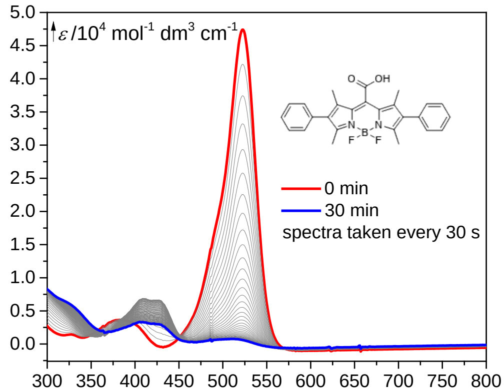

Figure S88. Irradiation of **7** in a degassed PBS/DMSO mixture (90:10, v/v) at λ_{max} = 525 nm for 30 min (red line: the initial spectrum; blue line: the end spectrum).

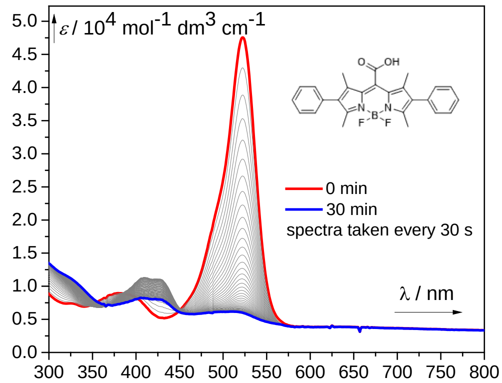

Figure S89. Irradiation of **8** in a non-degassed PBS/DMSO mixture (80:20, v/v) at λ_{max} = 545 nm for 12 h (red line: the initial spectrum; blue line: the end spectrum).

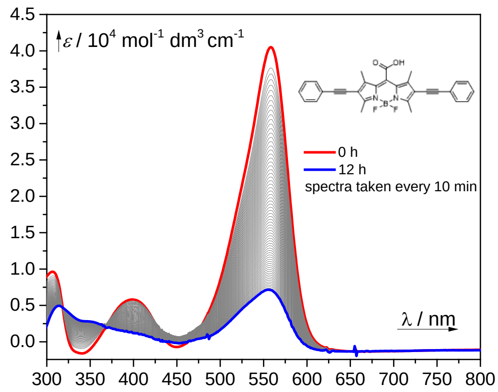

Figure S90. Irradiation of **8** in a degassed PBS/DMSO mixture (80:20, v/v) at λ_{max} = 545 nm for 12 h (red line: the initial spectrum; blue line: the end spectrum).

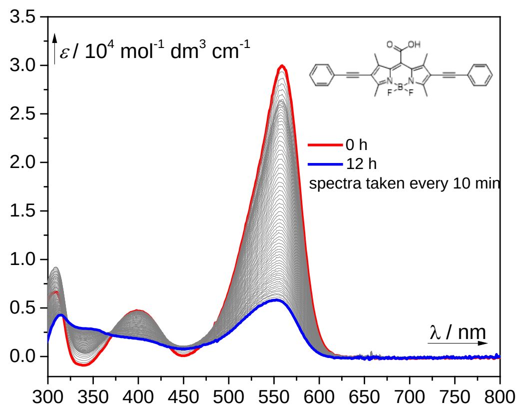

Figure S91. Irradiation of **9** in a non-degassed PBS/DMSO mixture (80:20, v/v) at λ_{max} = 545 nm for 12 h (red line: the initial spectrum; blue line: the end spectrum).

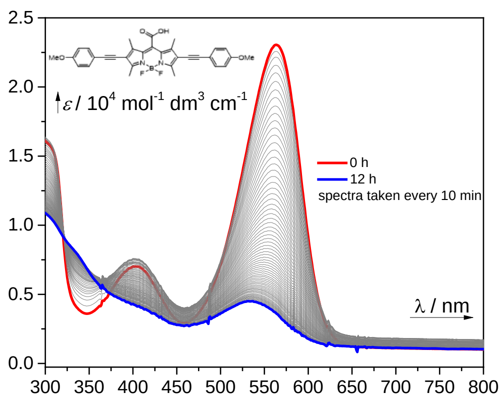

Figure S92. Irradiation of **9** in a degassed PBS/DMSO mixture (80:20, v/v) at λ_{max} = 545 nm for 12 h (red line: the initial spectrum; blue line: the end spectrum).

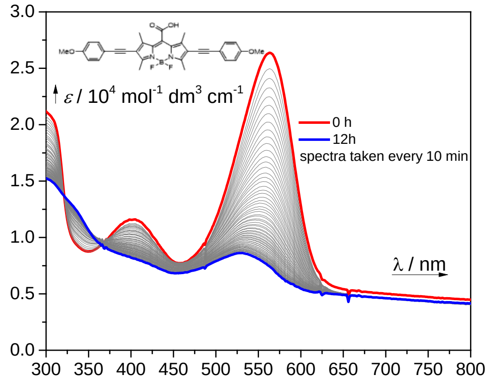

Figure S93. Irradiation of **10** in a non-degassed PBS/DMSO mixture (80:20, v/v) at λ_{max} = 545 nm for 12 h (red line: the initial spectrum; blue line: the end spectrum).

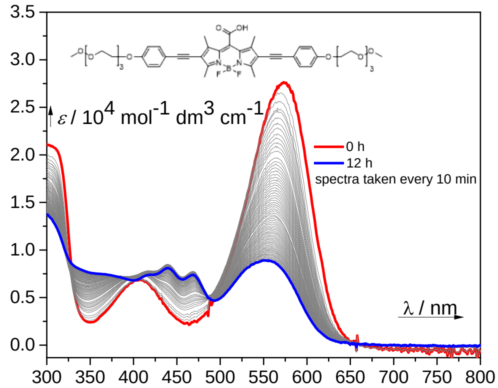

Figure S94. Irradiation of **10** in a degassed PBS/DMSO mixture (80:20, v/v) at λ_{max} = 545 nm for 12 h (red line: the initial spectrum; blue line: the end spectrum).

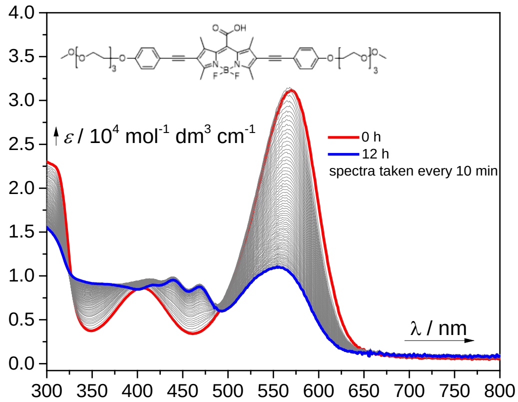

Singlet Oxygen Experiments

Figure S95: Reaction of the singlet oxygen generated by photosensitization in the presence of 1,3-diphenyl-isobenzofuran (DPBF) and compound **3** in methanol under irradiation at λ_{max} = 525 nm.

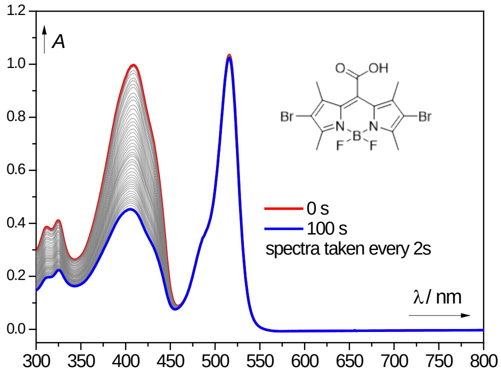

Figure S96: Reaction of the singlet oxygen generated by photosensitization in the presence of 1,3-diphenyl-isobenzofuran (DPBF) and compound **4** in methanol under irradiation at λ_{max} = 525 nm

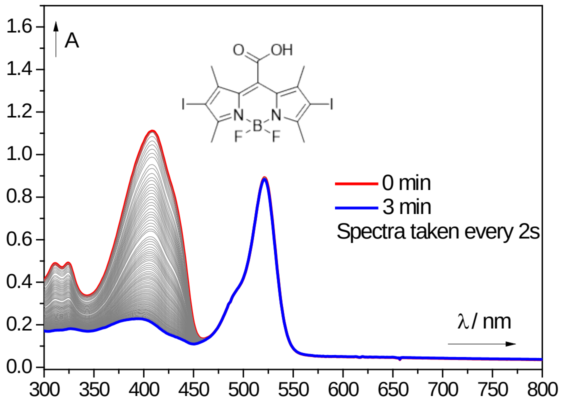

Figure S97: Reaction of the singlet oxygen generated by photosensitization in the presence of 1,3-diphenyl-isobenzofuran (DPBF) and compound **6** in methanol under irradiation at λ_{max} = 490 nm.

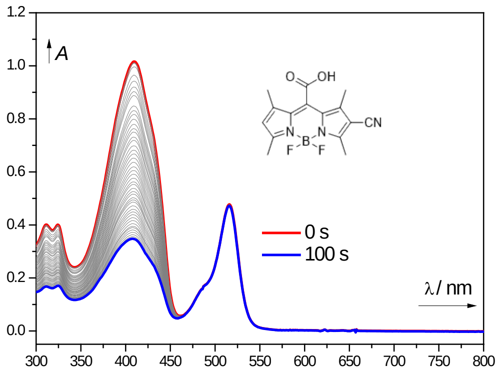

Figure S98: Reaction of the singlet oxygen generated by photosensitization in the presence of 1,3-diphenyl-isobenzofuran (DPBF) and compound **8** in methanol under irradiation at λ_{max} = 545 nm.

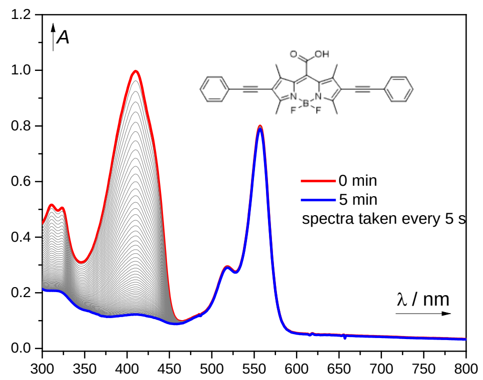

Figure S99: The pH titration of **9** in a PBS/methanol (95:5, v,v) solution.

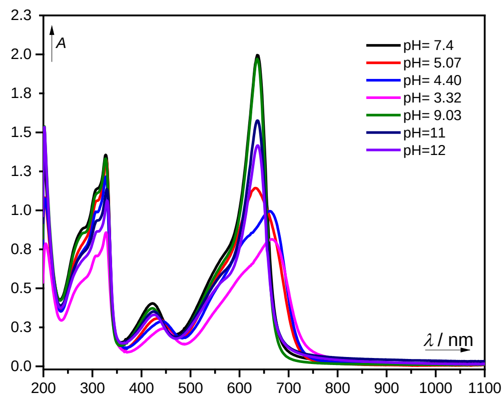

Transient Spectroscopy

Figure S100. The ns transient absorption spectra of **2** (*c* ~ 1.0 × 10^{-5} M; DMSO/ PBS (1:9); aerated); excited by a 532 nm laser pulse measured 10 ns – 20 ns after excitation.

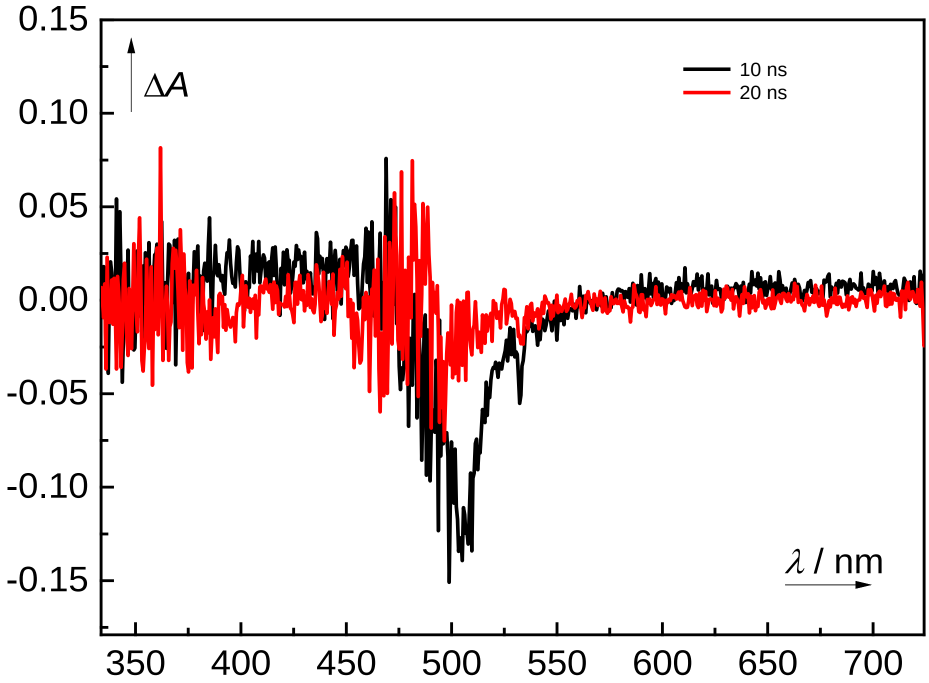

Figure S101. The ns transient absorption spectra of **2** (c ~ 1.0 × 10^{-5} M; DMSO/ PBS (1:9); degassed); excited by a 532 nm laser pulse measured 5 ns – 20 ns after excitation.

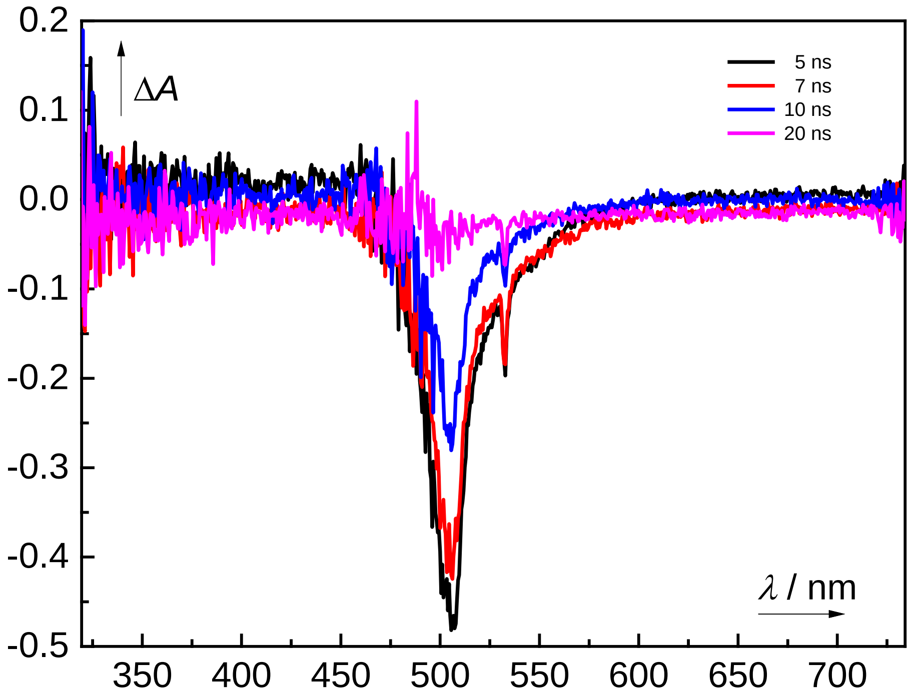

Figure S102. The ns transient absorption spectra of **3** (c ~ 1.0 × 10^{-5} M; DMSO/ PBS (1:9); aerated); excited by a 532 nm laser pulse measured 7 ns – 5 μs after excitation.

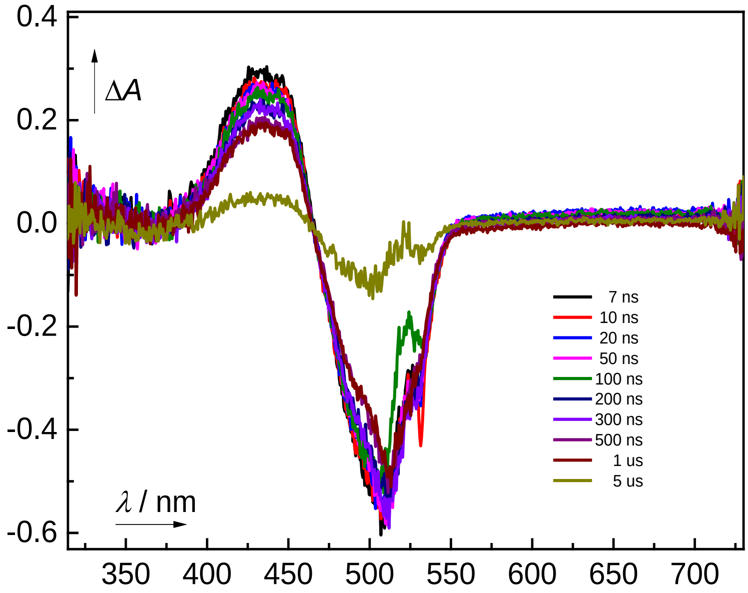

Figure S103. The ns transient absorption spectra of **3** (c ~ 1.0 × 10^{-5} M; DMSO/ PBS (1:9); degassed); excited by a 532 nm laser pulse measured 7 ns – 5 μs after excitation.

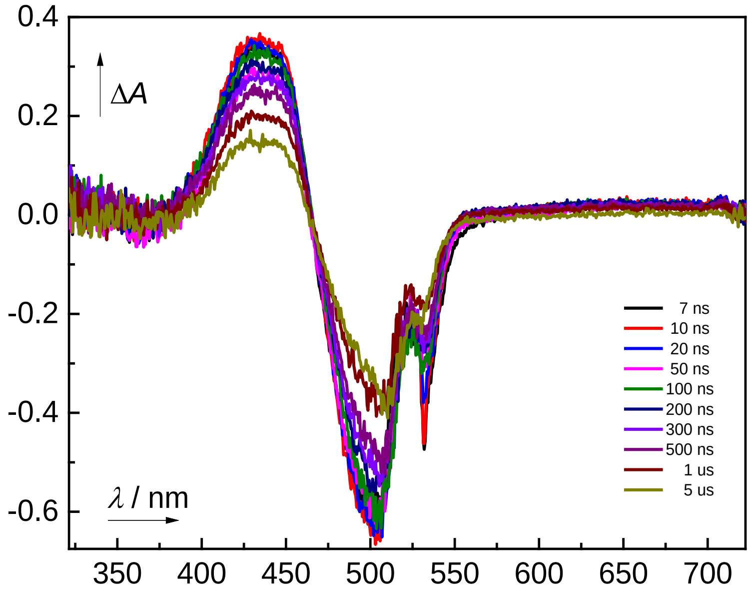

Figure S104. Kinetic decay of a transient formed from **3** (c ~ 1.0 × 10^{-5} M; DMSO/ PBS (1:9); aerated) by excitation with a 532 nm laser pulse and measured at 435 nm (top); the sum of residuals of the mono-exponential fitting is at the bottom.

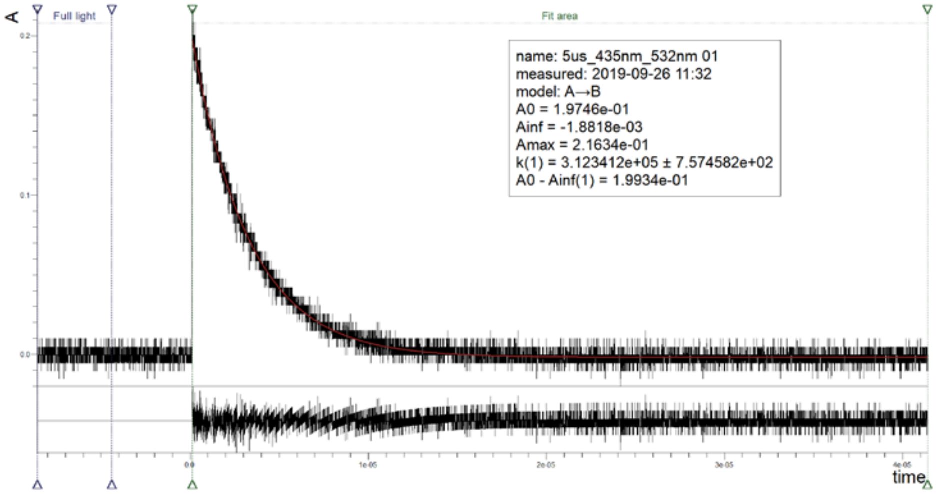

Figure S105. Kinetic decay of a transient formed from **3** (c ~ 1.0 × 10^{-5} M; DMSO/ PBS (1:9); degassed) by excitation with a 532 nm laser pulse and measured at 435 nm (top); the sum of residuals of the mono-exponential fitting is at the bottom.

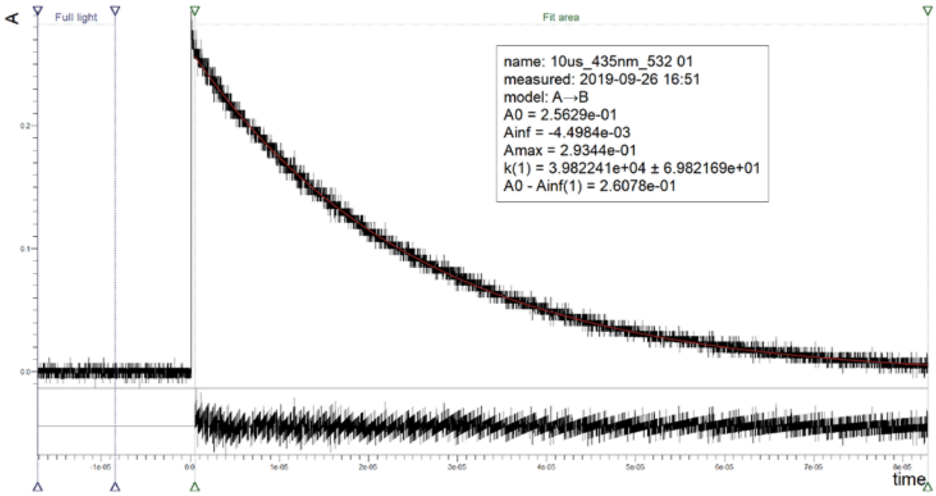

Figure S106. The kinetic trace of a transient formed from **3** (c ~ 1.0×10^{-5} M; DMSO/ PBS (1:9); degassed) by excitation with a 532 nm laser pulse and measured at 450 nm (top); the sum of residuals of the mono-exponential fitting is at the bottom. The estimated rate constant of triplet formation is $k = 5.52 \times 10^{8}$.

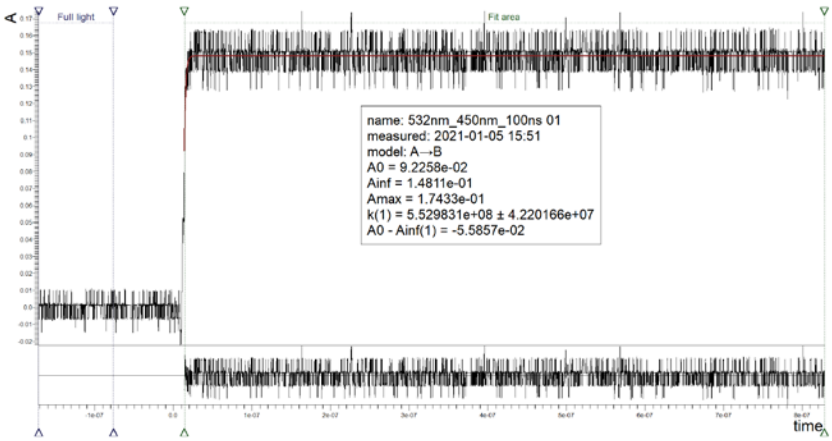

Figure S107. The ns transient absorption spectra of **4** (c ~ 1.0×10^{-5} M; DMSO/ PBS (1:9); aerated); excited by a 532 nm laser pulse measured 7 ns – 5 μs after excitation.

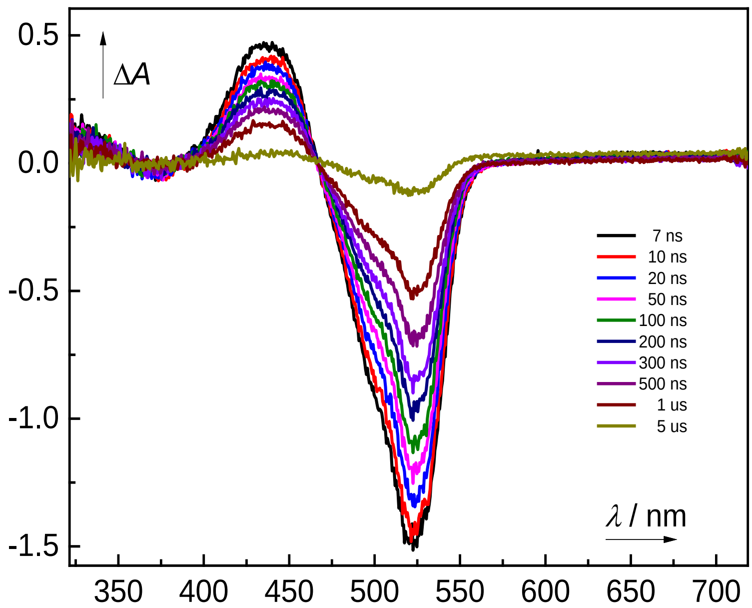

Figure S108. The ns transient absorption spectra of **4** (c ~ 1.0 × 10^{-5} M; DMSO/ PBSr (1:9); degassed); excited by a 532 nm laser pulse measured 7 ns – 5 μs after excitation.

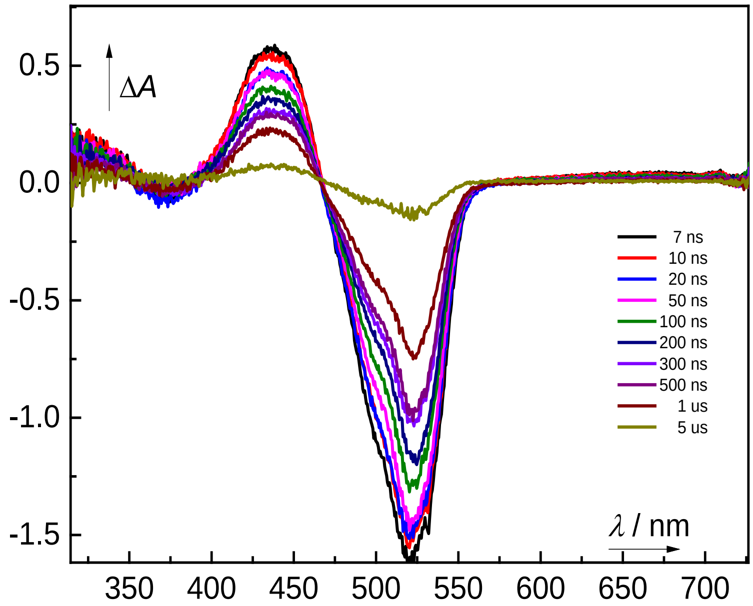

Figure S109. Kinetic decay of a transient formed from **4** (c ~ 1.0 × 10^{-5} M; DMSO/ PBS (1:9); naturally aerated) by excitation with a 532 nm laser pulse and measured at 440 nm (top); the sum of residuals of the mono-exponential fitting is at the bottom.

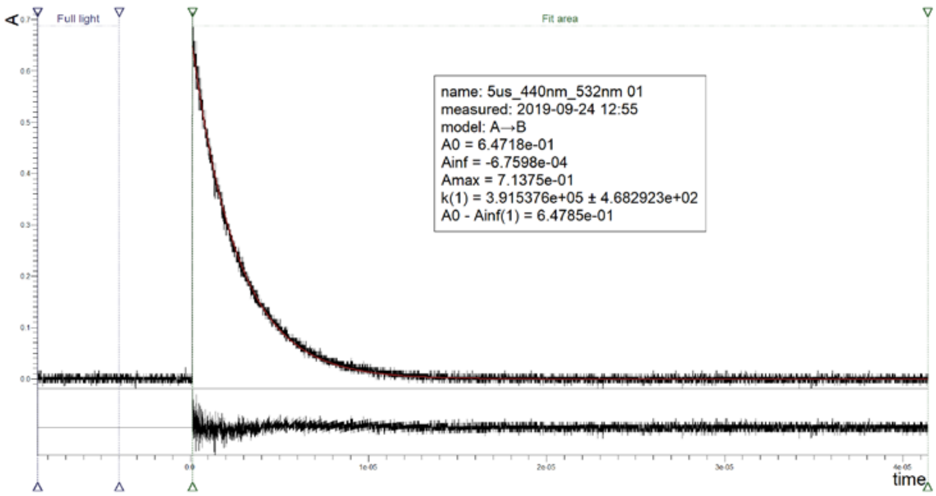

Figure S110. Kinetic decay of a transient formed from **4** (c ~ 1.0 × 10^{-5} M; DMSO/ PBS (1:9); degassed) by excitation with a 532 nm laser pulse and measured at 440 nm (top); the sum of residuals of the mono-exponential fitting is at the bottom.

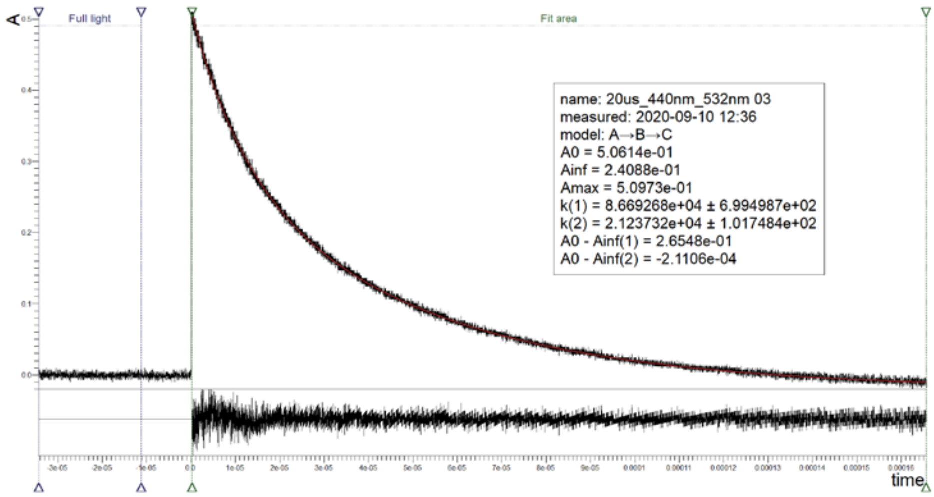

Figure S111. The kinetic trace of a transient formed from **4** (c ~ 1.0 × 10^{-5} M; DMSO/ PBS (1:9); degassed) by excitation with a 532 nm laser pulse and measured at 450 nm (top); the sum of residuals of the mono-exponential fitting is at the bottom. The estimation of the rate constant of triplet formation is $k = 5.74 \times 10^8$.

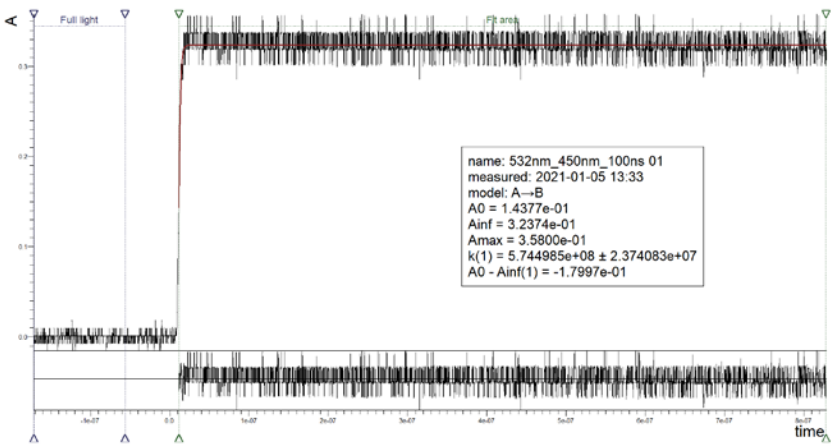

Figure S112. The ns transient absorption spectra of **7** (c ~ 1.0 × 10^{-5} M; DMSO/ PBS (1:9); aerated); excited by a 532 nm laser pulse measured 5 ns – 50 ns after excitation.

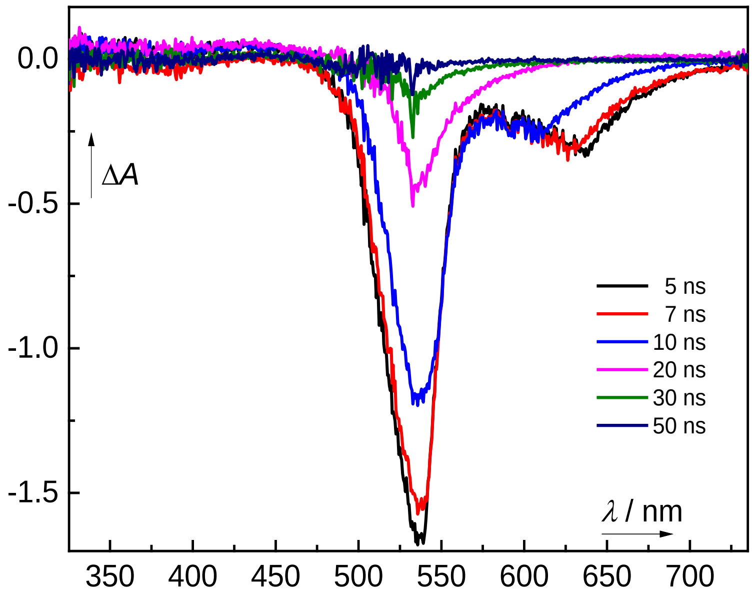

Figure S113. The ns transient absorption spectra of **7** (c ~ 1.0 × 10^{-5} M; DMSO/ PBS (1:9); degassed); excited by a 532 nm laser pulse measured 5 ns – 50 ns after excitation.

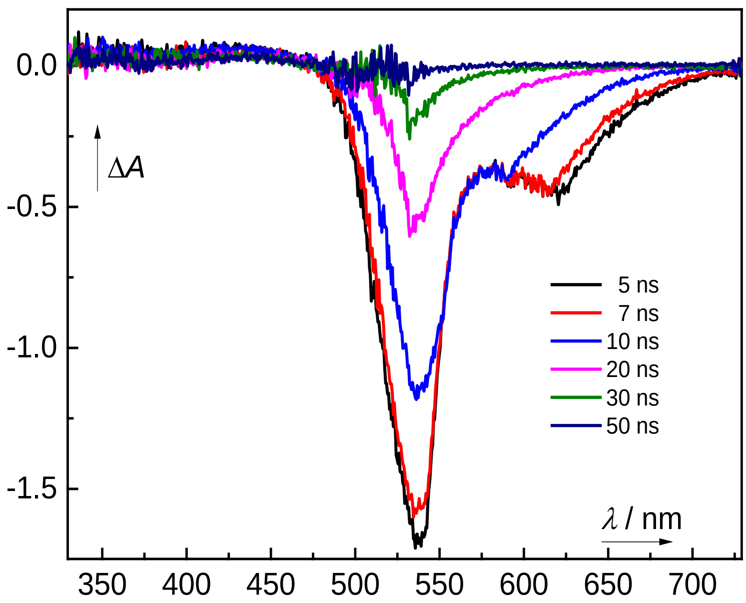

Figure S114. The ns transient absorption spectra of **10** (c ~ 1.0 × 10^{-5} M; DMSO/ PBS (1:9); aerated); excited by a 532 nm laser pulse measured 7 ns – 100 ns after excitation.

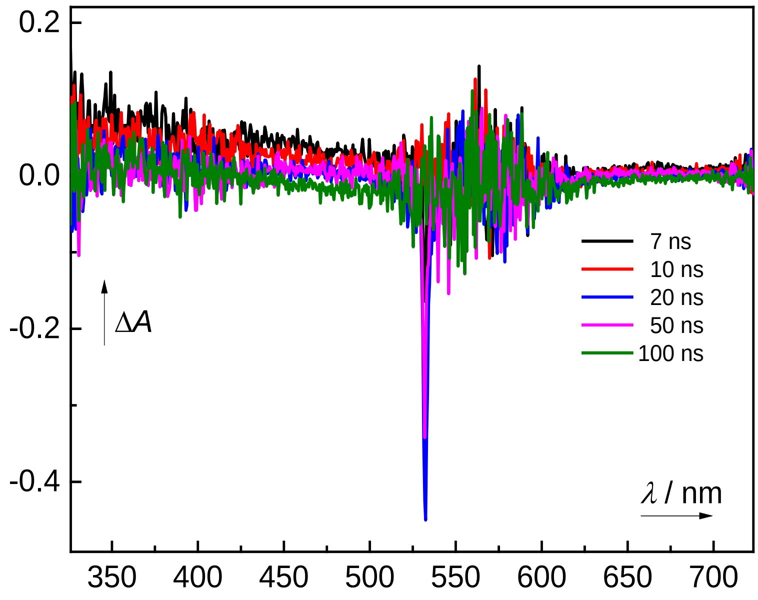

Figure S115. The ns transient absorption spectra of **10** (c ~ 1.0 × 10^{-5} M; DMSO/ PBS (1:9); degassed); excited by a 532 nm laser pulse measured 7 ns – 100 ns after excitation.

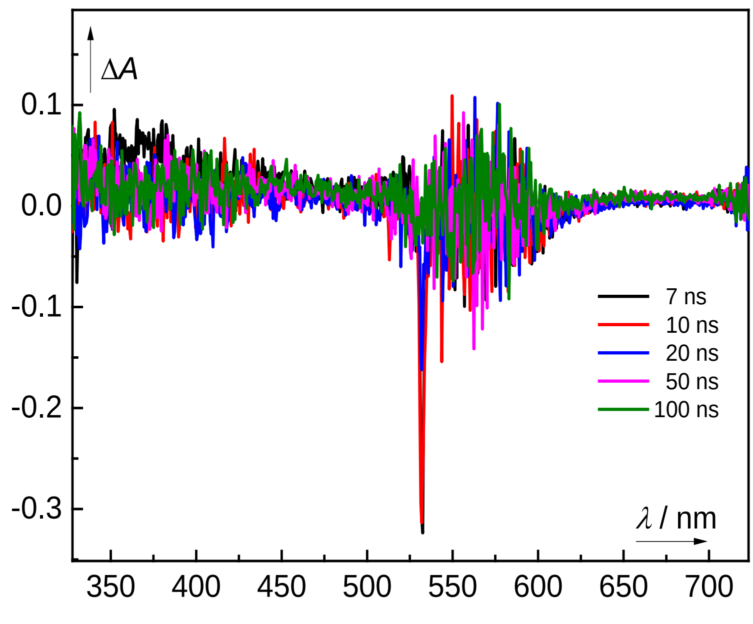

Table S1. Lifetimes of transient species of compounds **3-4**, (c ~1.0 × 10^{-5} M; DMSO/ PBS (1:9); in aerated (aer) and (deg) degassed solutions.

compound	lifetime / µs
3	3.20 ± 0.06 (aer)
	25.10 ± 0.08 (deg)
4	2.56 ± 0.06 (aer)
	11.40 ± 0.05 (deg)

Intersystem Crossing Quantum Yield Determination

The intersystem crossing quantum yields were determined using a previously published method [1] using nanosecond transient absorption spectroscopy. The absorbance ΔA of the solution at a certain wavelength λ before and after excitation is given by the equations Eq. 1 and Eq 2.:

$$\Delta A\ (\lambda) = \varepsilon_g\ (\lambda) \times C_0 \times l \qquad \text{Eq (1)}$$

$$\Delta A\ (\lambda) = [\varepsilon^*\ (\lambda) \times C^* + \varepsilon_g\ (\lambda) \times C_g]\ l \qquad \text{Eq (2)}$$

where ε^* (λ) and ε_g (λ) are the molecular absorption coefficients of the ground and excited state, respectively, at the given wavelengths, and C^* and C_g are the concentrations of the remaining ground-state molecules and the excited molecules; *l* is the optical path of the sample.
$C_0 = C^* + C_g$ is constant, but the relative values of C^* and C_g depend on the intensity *I* of the excitation:

$$\Delta A\ (\lambda) = [\varepsilon^*\ (\lambda) - \varepsilon_g\ (\lambda)]\ C^* \times I \times l \qquad \text{Eq (3)}$$

It has been demonstrated [2] that C^* may be written as a function of the excitation energy:

$$C^*\ (I) = C_0\ \{1\exp[-2.3 \times \Phi \times \varepsilon_g\ (\lambda') \times I]\} \qquad \text{Eq (4)}$$

Where Φ = quantum yield of the formation of the excited state analyzed, *I* = intensity of excitation (Einstein /dm^2) and ε_g (λ') = molecular absorption coefficient of the ground state at the wavelength of excitation.
The parameters ε^* and Φ may be obtained by combining the Eq. (3) and (4):

$$\Delta A\ (\lambda, I) = a(1-e^{b \times I}) \qquad \text{Eq (5)}$$

Where $a = [\varepsilon^*\ (\lambda) - \varepsilon_g\ (\lambda)]\ C^* \times l$ and $b = 2.3 \times \Phi \times \varepsilon_g\ (\lambda')$ and may be determined by fitting an experimental set of values of ΔA (*I*).

In this specific case, the Φ_{ISC} was evaluated in a degassed MeOH solution (three freeze−pump−thaw cycles) at three different concentrations (*c* ~3.0×10^{-6}, ~6.0×10^{-6} M, and ~1.0×10^{-5} M) and three different intensities (30, 50, and 70 mJ) to give $\Phi_{ISC} = 0.66$ and $\Phi_{ISC} = 0.83$ for **3** and **4**, respectively.

Cell Viability

Figure S116. Effect of **8** and its photoproducts on viability of HepG2 cells

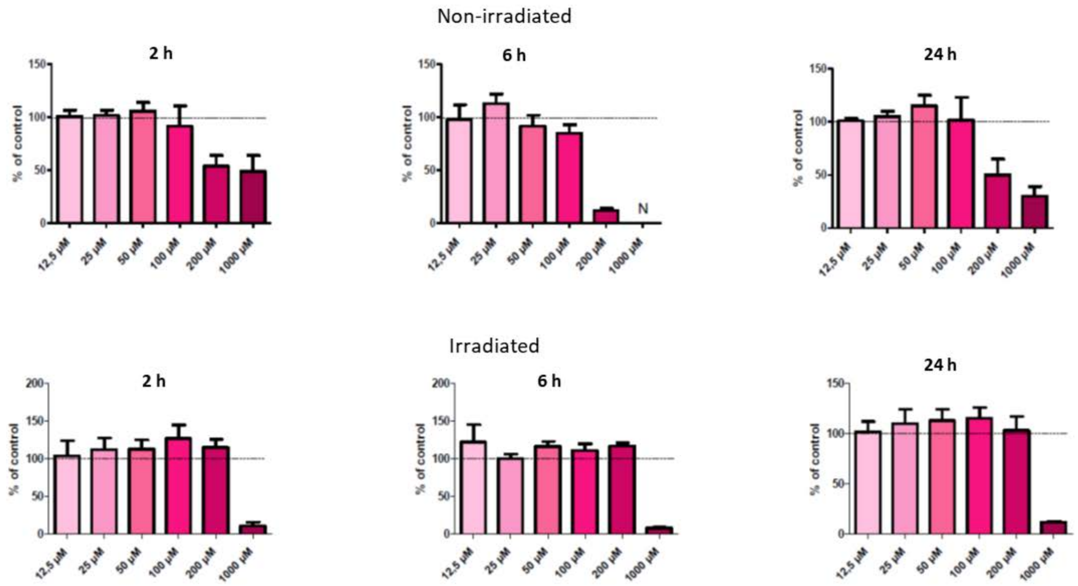

HepG2 cells were incubated with compound **8** (top panel) and its photoproduct (bottom panel) were obtained upon exhaustive irradiation of the compounds at λ_{irr} = 505 nm for 24 h. Cell viability was measured using an MTT assay. The experiments were performed at least in triplicates.

Figure S117. Effect of **10** and its photoproducts on viability of HepG2 cells

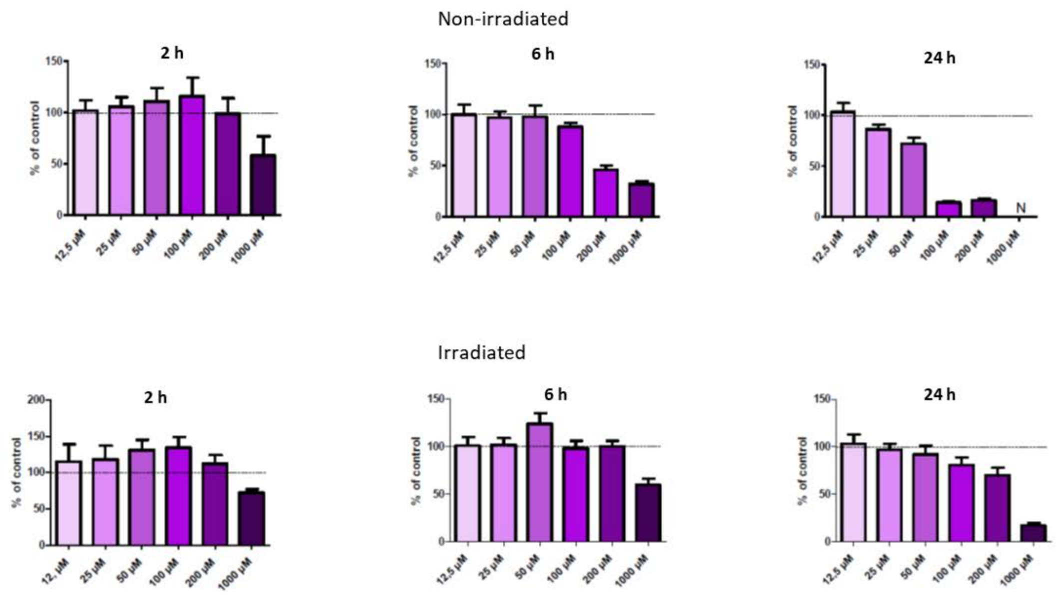

HepG2 cells were incubated with compound **10** (top panel) and its photoproduct (bottom panel) were obtained upon exhaustive irradiation of the compounds at λ_{irr} = 505 nm for 24 h. Cell viability was measured using an MTT assay. The experiments were performed at least in triplicates.

MS Analysis of Photoproducts Formed upon Irradiation of 10 in a PBS/DMSO Mixture

Before irradiation:

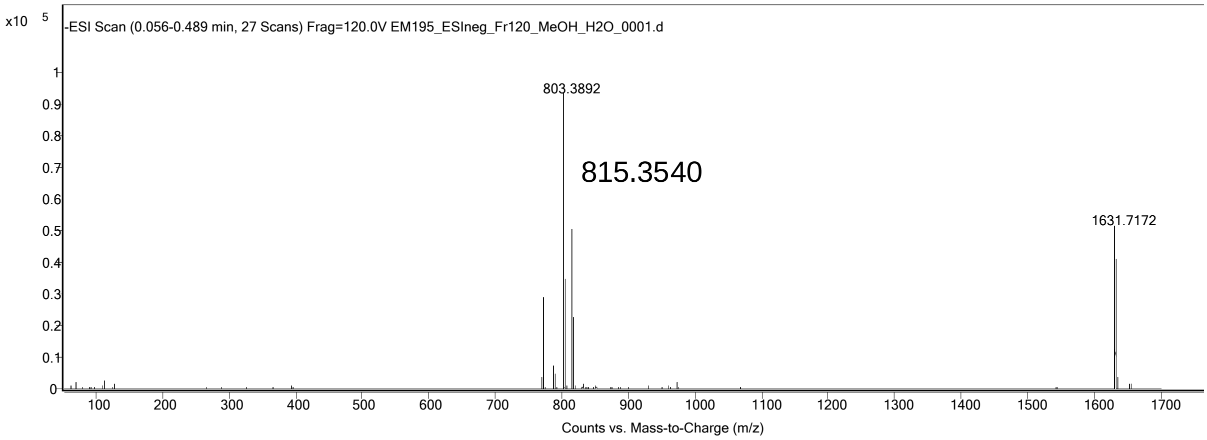

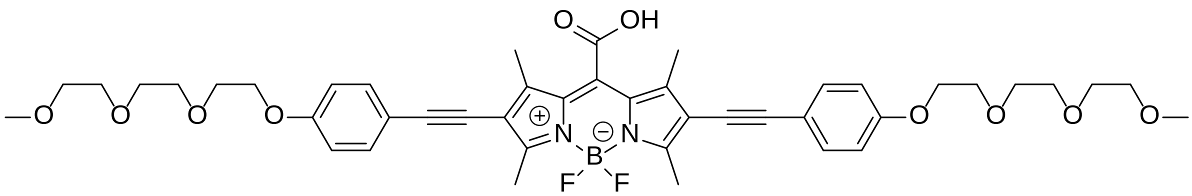

HRMS-ESI$^-$ *m/z*: [M–1]$^-$ calcd for $C_{44}H_{50}BF_2N_2O_{10}$ 815.3540, found **815.3540** (starting compound **10**)

After irradiation:

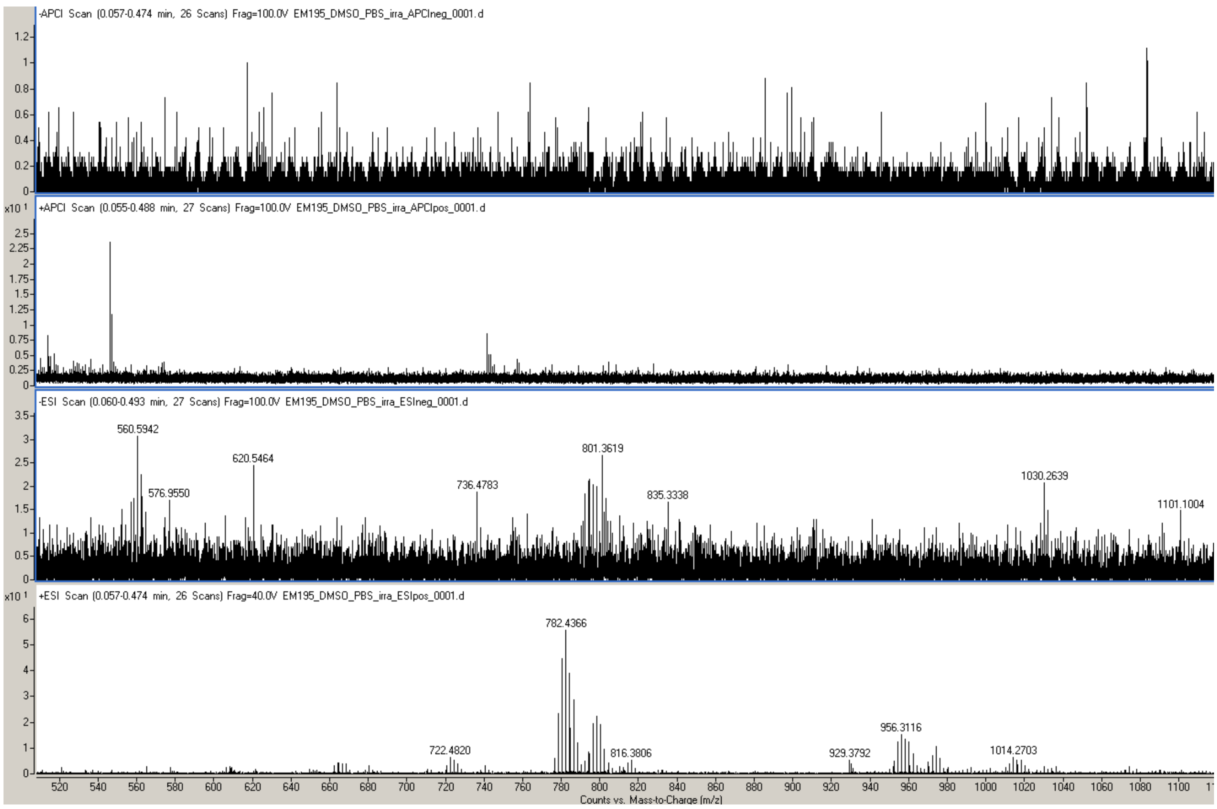

Plausible structures of some photoproducts proposed based on the MS spectra shown above:

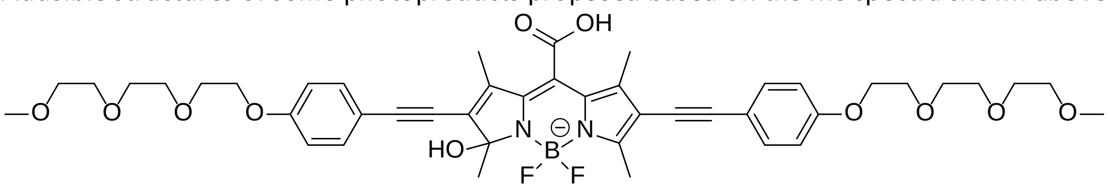

Chemical Formula: $C_{44}H_{52}BF_2N_2O_{11}^-$
Exact Mass: 833.7104

Addition of a nucleophile (water) according to *Chem. Commun*. **2010**, *46*, 4908-4910.

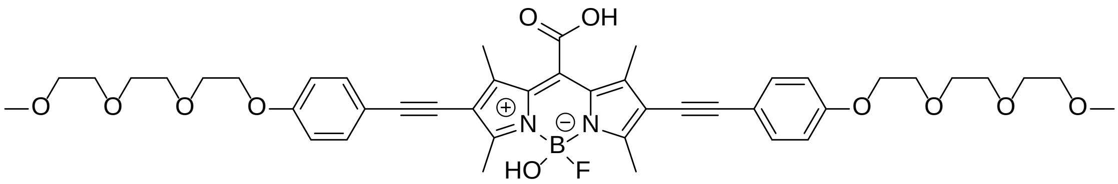

Chemical Formula: $C_{44}H_{52}BFN_2O_{11}$
Exact Mass: 814.3648

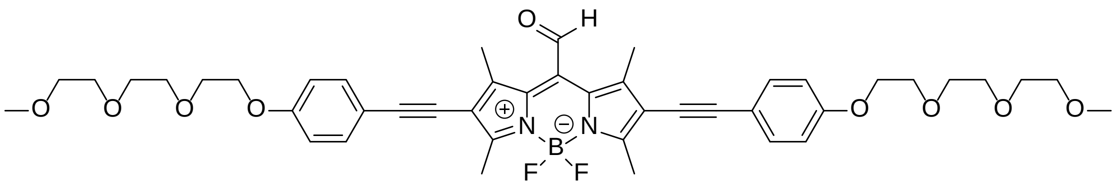

Chemical Formula: $C_{44}H_{51}BF_2N_2O_9$
Exact Mass: 800.3656

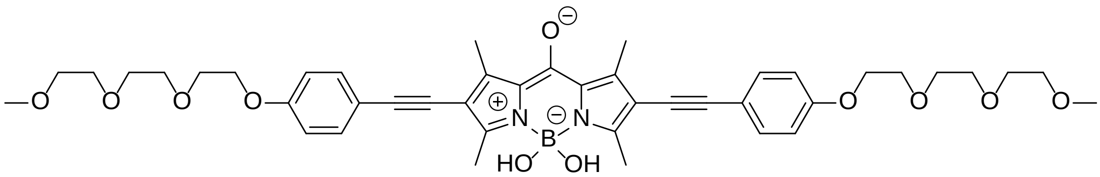

Chemical Formula: $C_{43}H_{52}BN_2O_{11}^-$
Exact Mass: 783.3670

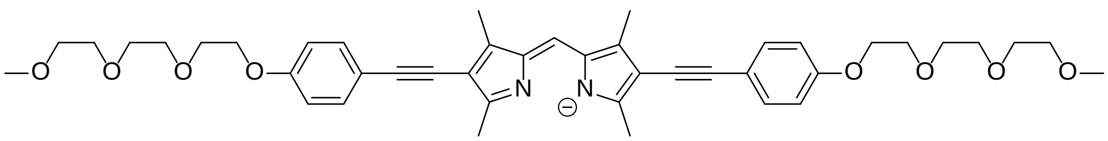

Chemical Formula: $C_{43}H_{51}N_2O_8^-$
Exact Mass: 723.3651

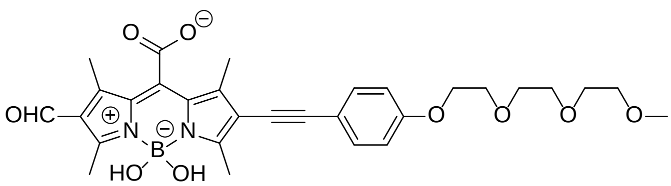

Chemical Formula: $C_{30}H_{34}BN_2O_9^-$
Exact Mass: 577.2363

References

1. Jacques, P.; Braun, A. M. Laser Flash Photolysis of Phthalocyanines in Solution and Microemulsion. *Helv. Chim. Acta* **1981,** 64, 1800-1806.
2. Lachish, U.; Shafferman, A.; Stein, G. Intensity Dependence in Laser Flash Photolysis Experiments: Hydrated Electron Formation from Ferrocyanide, Tyrosine, and Tryptophan. *J. Chem. Phys.* **1976,** 64, 4205-4211.